Visualization of the Smad direct signaling response to Bone Morphogenetic Protein 4 activation with FRET-based biosensors

Dissertation zur Erlangung des

naturwissenschaftlichen Doktorgrades

der Bayerischen Julius-Maximilians-Universität Würzburg

vorgelegt von

Kira V. Gromova

aus Samara, Russland

Würzburg, Oktober 2007.

Eingereicht am:

Mitglieder der Promotionskommission:

Vorsitzender:	Prof. Dr. Martin J. Müller
1. Gutachter :	Prof. Dr. G S Harms
2. Gutachter :	Prof. Dr. T. Müller

Tag des Promotionskolloquiums:

Doktorurkunde ausgehändigt am:

Table of Contents

Summary

The Transforming Growth Factor (TGF) superfamily of cytokines and their serine/threonine kinase receptors play an important role in the regulation of cell division, differentiation, adhesion, migration, organization, and death. Smad proteins are the major intracellular signal transducers for the TGF receptor superfamily that mediate the signal from the membrane into the nucleus. Bone Morphogenetic Protein-4 (BMP-4) is a representative of the TGF superfamily, which regulates the formation of teeth, limbs and bone, and also plays a role in fracture repair. Binding of BMP-4 to its receptor stimulates phosphorylation of Smad1, which subsequently recruits Smad4. A hetero-oligomeric complex consisting of Smad1 and Smad4 then translocates into the nucleus and regulates transcription of target genes by interacting with transcription factors.

Although the individual steps of the signaling cascade from the receptor to the nucleus have been identified, the exact kinetics and the rate limiting step(s) have remained elusive. Standard biochemical techniques are not suitable for resolving these issues, as they do not offer sufficiently high sensitivity and temporal resolution. In this study, advanced optical techniques were used for direct visualization of Smad signaling in live mammalian cells. Novel fluorescent biosensors were developed by fusing cyan and yellow fluorescent proteins to the signaling molecules Smad1 and Smad4. By measuring Fluorescence Resonance Energy Transfer (FRET) between the two fluorescent proteins, the kinetics of BMP/Smad signaling was unraveled. A rate-limiting delay of 2 - 5 minutes occurred between BMP receptor stimulation and Smad1 activation. A similar delay was observed in the complex formation between Smad1 and Smad4. Further experimentation indicated that the delay is dependent on the Mad homology 1 (MH1) domain of Smad1. These results give new insights into the dynamics of the BMP receptor – Smad1/4 signaling process and provide a new tool for studying Smads and for testing inhibitory drugs.

Zusammenfassung

Die Transforming Growth Factor" (TGF)-Superfamilie der Cytokine und ihrer Serin/Threonin-Kinase-Rezeptoren spielt eine bedeutende Rolle bei der Regulierung der Zellteilung, -differenzierung, -adhäsion, -migration, -organisation, und beim Zelltod. Die Smad-Proteine sind die wichtigsten intrazellulären Signalüberträger für die TGF-Rezeptor-Familie, da sie das Signal von der Zellmembran zum Kern übermitteln. Das „Bone Morphogenetic Protein4" (BMP-4) ist ein Vertreter der TGF-Familie, der die Bildung von Zähnen, Gliedmaßen und Knochen reguliert und darüber hinaus eine Rolle bei der Frakturheilung spielt. Das Binden von BMP-4 an seinen Rezeptor stimuliert die Phosphorylierung von Smad1, welches in der Folge Smad4 rekrutiert. Ein hetero-oligomerer Komplex bestehend aus Smad1 und Smad4 verlagert sich dann in den Zellkern, wo er durch Interaktion mit Transkriptionsfaktoren die Transkription von Zielgenen reguliert. Obwohl die einzelnen Schritte der Signalkaskade vom Rezeptor bis in den Zellkern bereits identifiziert wurden, blieben die Kinetik und die geschwindigkeitsbegrenzenden Schritte bisher unbekannt. Gängige biochemische Methoden eignen sich nicht um diese Fragen zu lösen, da sie nicht über ausreichende Empfindlichkeit und zeitliches Auflösungsvermögen verfügen. In der vorliegenden Arbeit wurden hochentwickelte optische Techniken angewandt, um die Smad-vermittelte Signaltransduktion direkt in lebenden Zellen sichtbar zu machen. Neue fluoreszierende Biosensoren wurden konstruiert, indem gelb- und cyan-fluoreszierende Proteine mit den Signalmoleküle Smad1 und Smad4 fusioniert wurden. Durch Messung des „Fluorescent Resonance Energy Transfer" (FRET) zwischen den zwei fluoreszierenden Proteinen konnte die Kinetik der BMP-Smad-Signalkaskade bestimmt werden. Zwischen der Stimulation des Rezeptors und der Aktivierung von Smad1 trat eine geschwindigkeitsbegrenzende Verzögerung von 2-5 Minuten auf. Eine ähnliche Verzögerung wurde bei der Bildung des Komplexes aus Smad1 und Smad4 beobachtet. Weitere Experimente zeigten, dass die Verzögerung von der Mad-Homologie-Domäne 1 (MH1) von Smad1 abhängt. Die Ergebnisse dieser Arbeit geben neue Einblicke in die Dynamik der BMP-Rezeptor-Smad1/4 Signaltransduktion und stellen neue Werkzeuge zur Untersuchung von Smads und zur Austestung inhibitorischer Wirkstoffe zur Verfügung.

"Alice : "Would you tell me, please, which way I ought to go
from here?"
"That depends a good deal on where you want to get to," said the
Cat.
"I don't much care where –" said Alice.
"Then it doesn't matter which way you go," said the Cat.
"– so long as I get *somewhere*," Alice added as an explanation.
"Oh, you're sure to do that," said the Cat, "if you only walk
long enough."

(From Alice in Wonderland by Lewis Carroll.)

Abbreviations

ACP	acyl-carrier protein
AGTM	O6-alkylguanine-DNA alkyltransferase
ActR-IA	activin receptor type 1a
ALK-2	activin receptor type 2
AMH	anti-Muellerian hormone
AR-Smad	activated by activin and TGF-β type I receptors
BISC	BMP induced signaling complexe
BMP	Bone morphogenetic protein
BRI	bone morphogenetic receptor type 1
BRII	bone morphogenetic receptor type 2
BSA	bovine Serum Albumin
BR-Smad	activated by BMP type I receptor
CCP	clathrin-coated pits
CD44	cytoplasmic domain
CFP	cyan fluorescent protein
Co-Smad	common-partner Smad
COS-1	African green monkey kidney cell line
C2C12	mouse myoblast cell line
DMEM	Dulbecco's modified Eagle's Medium
DRM	detergent-resistant membrane fraction
Dpp	Decapentaplegic
E.coli	Escherichia coli
EDTA	Ethylenediaminetetraacetic acid
EGF	epidermal growth factor
FCS	fluorescence correlation spectroscopy
FBS	Fetal Bovine Serum
FLIM	Fluorescence lifetime imaging microscopy
FLIP	Fluorescence Loss In Photobleaching
Fig.	Figure
FRAP	Fluorescence Recovery after Photobleaching

FRET	Fluorescence resonance energy transfer
GDF	growth/differentiation factors
HEK 293	human embryonic kidney cell line
HeLa	human cervix carcinoma cell line
I-Smad	inhibitory Smad
LMB	leptomycin B
LSM	Laser scanning confocal microscopy
Mad	mothers against dpp
MDA-MB468	human Adenocarcinoma breast cancer
MH1	Mad homolog N-terminal domain
MH2	Mad homolog C-terminal domain
NES	nuclear export signal
NLS	nuclear localization signal
PCR	polymerase chain reaction
PFC	preformed hetero-oligomeric complexes
R-Smad	receptor-regulated Smad
SARA	Smad anchor for receptor activation
SPIM	Selective Plane Illumination Microscopy
TGF-β	transforming growth factor
TβR-I	type I TGF-β receptor
TβR-II	type II TGF-β receptor
YFP	yellow fluorescent protein

1. Introduction

1.1 Bone morphogenetic signaling pathway

1.1. 1 Overview

As multicellular organisms appeared, control was needed over the ability of individual cells to divide, differentiate, move, and organize. Complicated intercellular communication systems between cells developed to ensure the proper behavior of individual cells in the context of the whole organism. One of the forms of communication between cells is mediated by secretory polypeptides that are recognized by membrane receptors coupled to transcriptional regulatory mechanism. With its about 40 members in the human genome the transforming growth factor-β (TGF-β) family is one of the most famous representatives of this class of polypeptides. TGF-β and its family members: the bone morphogenetic proteins (BMPs), myostatins, nodals, anti-Muellerian hormone (AMH), activins, and others — exert profound effects on cell division, differentiation, migration, adhesion, and death. Many cell types may produce these factors, and they may be active from the earliest stages of embryo development through adulthood, as in the case of the BMPs. The quest to understand how cells read these signals started as soon as these factors were identified in the 1980s and is ongoing until now.

Smad proteins are the major signal transducers for the TGF-β superfamily of cytokines and their serine/threonine kinase receptors. Smads mediate the signal from the membrane receptors into the nucleus. One of the members of the TGF-β superfamily is Bone Morphogenetic Protein-4 (BMP-4). BMP-4 stimulates two types of transmembrane serin-threonine kinases: BMP receptors type I and type II (BRI and BRII). BMP binding initiates a downstream signal primarily mediated by a receptor-regulated Smad (R-Smad), Smad1, and a common-partner Smad (Co-Smad), Smad4 (61), that transmit the signal into the nucleus. After BMP binds and activates the BRII receptor, BRII activates the kinase activity of BRI, and BRI phosphorylates Smad1. Smad1 becomes phosphorylated and dissociates from the BRI receptor because of the conformation change of Smad1. After dissociation from the receptor, Smad1 binds to

other Smad1 proteins and first forms a homotrimeric complex, and ultimately upon Smad4 exchange with Smad1 forms a heterotrimeric complex.

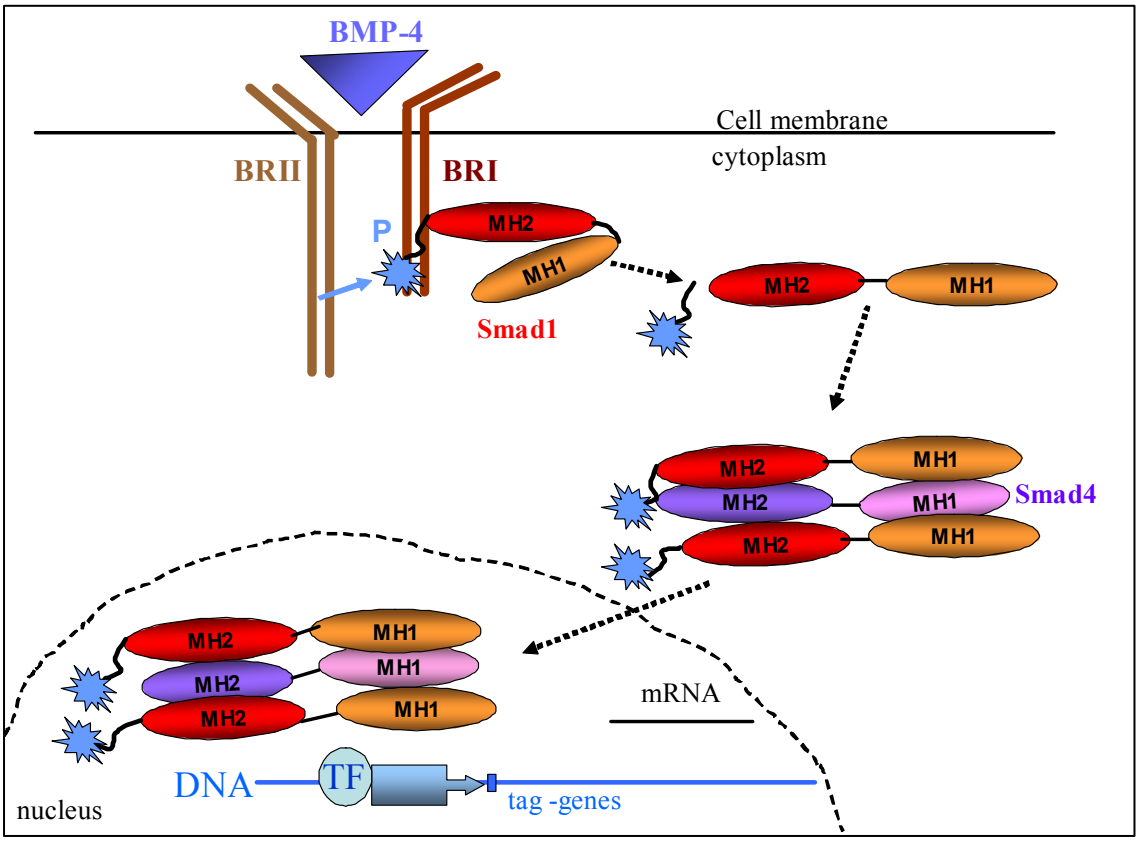

Fig. 1.1 *Schematic outline of the basic mechanism of BMP signaling through Smad proteins. First, the BMP-4 ligand binds to its corresponding preformed BMP receptors complex. Then, constitutively active type II receptor phosphorylates the type I receptor at the GS domain. Next, Smad1 is phosphorylated by the type I receptor and dissociates from the receptor complex due to conformational change. After dissociation, Smad1 forms homo-oligomeric complexes with Smad1, and then hetero-oligomeric complexes with Smad4. Smad1/Smad4 complexes accumulate in the nucleus, where they bind directly or indirectly to specific promoter regions of target genes together with transcription factors (TF)s and/or co-activators/repressors.*

The Smad complexes translocate into the nucleus. There, they regulate transcription of target genes by interacting with various transcription factors, transcriptional co-activators or co-repressors, and DNA sequences (Fig. 1.1). In this work, the initial steps

of the BMP signaling before and upon binding the BMP-4 ligand was studied by fluorescence resonance energy transfer (FRET) (Fig. 1.2).

The activation and phosphorylation of Smad1 and Smad1/Smad4 complex formation was observed with specific Smad1 biosensors. Fluorescence resonance energy transfer between cyan and yellow fluorescent proteins fused to Smad1 and Smad4 proteins was used to unravel the temporal aspects of BMP/Smad signaling. A rate-limiting delay of 2 - 5 minutes occurred between BMP activation and Smad1 activity. A similar delay was observed in the Smad1/Smad4 complexation. Further experimentation indicated that the delay is dependent on the MH1 domain and linker of Smad1. These results give new insights into the dynamics of the BMP receptor – Smad1/4 signaling process and provide a new tool for studying Smads.

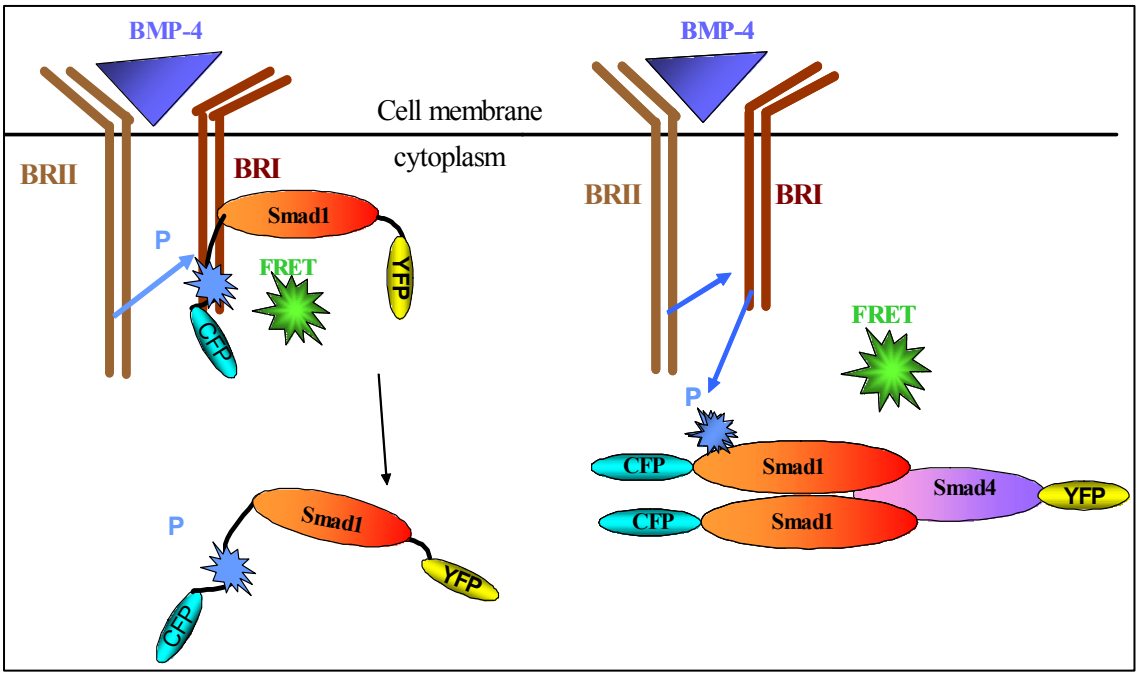

Fig. 1.2 *General outline of the aims of the work. The goal is to observe by FRET microscopy the kinetics of the Smad-dependent BMP signaling. The first goal is to study the kinetics of Smad1 phosphorylation with a specific Smad1 biosensor (left). The second goal is the observation of the Smad1/Smad4 complex formation with fluorescent biosensors (rite).*

1. 1. 2 TGF-beta and Smads in human disease

Germline mutations or misregulations in the TGF-β signaling pathway cause various developmental disorders and other diseases. The pathologies associated with aberrant TGF-β signaling generally affect the muscular, skeletal, and cardiovascular systems, as well as some types of cancer predisposition. Disease-related mutations have been identified at every level of TGF-β signaling, including the TGF ligands, type I and II receptor kinases, cytoplasmic and nuclear co-factors, and the Smad proteins (38, 124, 125, 244). Deregulation of TGF signaling has been implicated in autoimmune disorders, fibrosis, and vascular diseases such as atherosclerosis, but the majority of pathogenic mutations within the TGF-β signaling pathway have been identified in the context of human cancers (28). Mutations and dysregulation of the TGF-β signaling pathway result in different cancers and also cardiovascular, musculoskeletal and urogenital diseases. For example, mutations were found in human hereditary disease like pulmonary arterial hypertension (155). The biological effects of TGF-β is the inhibition of proliferation of most normal epithelial cells using an autocrine mechanism of action, and this suggests a tumor suppressor role for TGF-β. Dysregulation in autocrine TGF-β activity and loss in responsivess to exogenous ligands appears to provide some epithelial cells with a growth advantage leading to malignant progression. This suggests a pro-oncogenic role for TGF-β in addition to its tumor suppressor role (4, 29). The TGF-β signaling pathway inhibits tumor growth by inducing cell cycle arrest and apoptosis in the early stage of epithelial cancer. But, in late stages of this cancer, tumor cells become resistant to growth inhibition by TGF-β. The tumor cells are able to inactivate the TGF-β signaling pathway and to regulate the cell cycle in an aberrant way. In this case the role of TGF-β becomes one of tumor promotion (146). Mutations in the Smad proteins have been found in many cancers (58, 59). Smad4 was identified as a possible tumor suppressor gene (52). Mutations in Smad4 are associated with approximately 50% of pancreatic cancers and 30% of colorectal cancers (26, 181, 197-199). Smad4 has also been found to be the target of inactivating mutations, albeit less frequently, in prostate (114), ovarian (170), in breast (236), lung (209), and skin cancers (40, 235). Juvenile polyposis syndrome (8, 9) is caused by germline mutations in either Smad4 (25%) (86) and, to a lesser extent, BRIa (17%–40%), and is characterized specifically by a high risk of colorectal and gastric

cancer. Smad2 has likewise been found to be mutated in colorectal cancer (40). Smad2 and Smad4 may have tumor suppressive functions; Smad3 is likely a mediator of oncogenic TGF-β signaling. Loss of Smad3 expression in gastric cancer tissues and cell lines promotes tumor genesis (27). Study of missense mutations in Smads have been particularly fruitful in yielding information about the mechanism of Smad-dependent signaling (58, 178). Mutations that occur in Smad2 and Smad4 proteins in tumors occur most frequently in the MH2 domain, with only a small number mapping to the MH1 (DNA-binding) domain (118). The most important tumor-derived MH1 domain mutation is the exchange of a arginine to cysteine in Smad2 (R133C) causing colon carcinoma and, in the equivalent position of Smad4 (R100T), causing pancreatic carcinoma (40, 49, 170). These mutations increase the affinity of the MH1 domain to the MH2 domain of Smad2 or Smad4 proteins that make complex formation of Smad2 and Smad4 after activation with ligand difficult (56). It is still not completely clear how TGF-β can have a dual role as a tumor suppressor and a pro-oncogenic factor. Now, the TGF-β signaling pathway is considered as a biomarker for prediction of progressive tumorigenesis. Also, the TGF-β signaling pathway is considered as a molecular target for prevention and treatment of cancer (146).

1. 1. 3 TGF-β superfamily of cytokines

The TGF-β system is highly conserved throughout the animal kingdom. Its basic pathway provides for a number of signals from the extracellular environments via receptors at the cell membrane to the cytoplasm and the nucleus. .

The proteins with conserved structures have pleiotropic functions *in vitro* and *in vivo* (88, 211). The TGF-β family signaling molecules (i.e., TGF-βs, inhibins, activins, nodal, BMPs, myostatin, AMH, and growth/differentiation factors (GDFs)) exert a wide range of biological effects on a large variety of cell types. For example, they regulate cell differentiation, growth, and apoptosis. All of these effects play an important role in patterning during embryonal development. During the postnatal development they are important for modulation of the immune system and tissue repair. As was explained before, they act as inhibitors of growth for most types of cells. The TGF-β family members induce apoptosis of epithelial cells. They are able to stimulate the production of

extracellular matrix proteins, inducing fibrosis in various tissues. AMH induces Müllerian duct regression during embryogenesis and inhibits the transcription of gonadal steroidogenic enzymes. Activins play important roles in the induction of dorsal mesoderm during early embryogenesis. Nodal plays critical roles in the induction of dorsal mesoderm, anterior patterning, and formation of left–right asymmetry. Myostatin or GDF-8 is produced by skeletal muscle cell lineages, and it inhibits their growth. GDF-5 is structurally related to BMPs. It induces cartilage-like tissue. All these TGF-β superfamily proteins have different biological effects *in vivo*. However, they transmit similar, but not identical, intracellular signals in different target cells (31, 117).

1. 1. 4 BMP

The activity of BMPs was first identified in the 1960s (210) as cytokines that induce bone and cartilage tissues *in vivo* (229), but already in the 1930 Levander discovered that simple alcohol extracts of bone induced new bone formation when injected into muscle tissue.

The proteins responsible for bone generation were identified after purification and sequencing of bovine BMP-3 and cloning of human BMP-2 and -4 in the 1980s (113, 216, 226, 229). More than 20 BMP-related proteins have meanwhile been identified, and these polypeptides can be subdivided into several groups based on their structures and functions (83, 84). BMPs were shown to have diverse effects on various cells, bone and cartilage formation and healing, and induction of the ventral mesoderm during early embryogenesis (62). BMP-2, 4, and the Drosophila decapentaplegic (dpp) gene product form one subgroup (BMP-2/4 group). BMP-5, 6, 7 (also termed osteogenic protein-1), BMP-8 (termed osteogenic protein-2), and the Drosophila gbb-60A gene product form another subgroup (osteogenic protein-1, OP-1 group). GDF-5, 6 (CDMP-2 or BMP-13), and GDF-7 (BMP-12) are from a third group (GDF-5 group). Members of the BMP family have distinct spatiotemporal expression profiles. Furthermore, the biological activities of BMPs are not identical among members, because they bind to their receptors with different affinities. *In vitro* and *in vivo* functions of BMP regulatory molecules and signaling crosstalk with other pathways have led to a better understanding of the roles of BMPs under various physiological and pathological

conditions (15-19, 39, 45, 46, 53, 68-70, 77-79, 83-86, 108, 109, 129, 130, 136, 156-160, 180, 190, 191, 200, 216, 225, 227-229, 238-240, 245, 246).

1. 1. 5 TGF-β superfamily serine/threonine kinase receptors.

The initial step in the cellular action of many growth factors is the interaction with specific receptors at the plasma membrane. It is generally assumed that, upon binding to the appropriate ligand, receptors generate secondary intracellular signals carrying necessary information to selectively affect cellular functions. The TGF-β family members initiate their cellular action by binding to receptors with intrinsic serine/threonine kinase activity (44). First some TGF-βs have been shown to interact strongly with epidermal growth factor (EGF) receptors (142, 182). The specific receptor structures for the TGF-βs in target cell membranes were identified in 1982 (145, 154, 202). This receptor family consists of two subfamilies, type I and type II receptors, which are structurally similar, with small cysteine-rich extracellular regions and intracellular parts consisting mainly of the kinase domains. Phosphorylation sites in the type II TGF-β receptor (TβR-II) and the type I TGF-β receptor (TβR-I) have been mapped using wild-type and chimeric receptors (100, 110, 186). All members of the TGF-β superfamily bind to a characteristic combination of type I and type II receptors, both of which are important for signaling. Analyses of ^{125}I-labelled TGF-β crosslinked to its receptors have shown that the signaling complex is a heterotetramer consisting of two TβR-I and two TβR-II molecules. Thus an important step in receptor activation is phosphorylation of the tetrameric receptor complex (127, 143, 193, 195, 196, 242). Given the large number of ligands within this family (about 30), it is surprising that there are only seven type I and only five type II receptors to mediate these signals. It is known, that only a few of the theoretically possible receptor combinations can occur. Therefore, each receptor combination mediates the downstream cellular signaling of multiple grow factors. Only type I receptors have a region rich in glycine and serine residues (GS domain) in the juxtamembrane domain. The type II receptors do not have this region. Initially, it was shown that the TGF-β1,2,3 ligands bind the TβRII, which then activates one of the TβRI's (ALK1, ALK2, or ALK5) with multiple

phosphorylations in the GS domain. In the receptor-activation model, TβRI determines of the intracellular signals (14, 30, 41, 100, 222). The TβRI phosphorylations are proposed to alter the conformation of the TβRI such that the L45 loop is available for binding to R-Smads. Studies of the receptors for the TGF-β ligand have provided two models for the activation of these serine/threonine kinase receptor complexes (230). In the first model, TGF-β binds to the type II receptor (TβR-II). The TβR-II is present at the cell surface in an oligomeric form with activated kinase (23, 63). The TβR-I is in an oligomeric form (111) and cannot bind TGF-β in the absence of TβRII. Then, the TβR-I is recruited into the complex with the TβRII. Then, TβR-II phosphorylates and activates TβR-I. The assembly of the receptor complex is triggered by ligand binding, but the complex is also stabilized by the direct interaction between the cytoplasmic parts of the receptors (42). The second model (230) predicts that the type II and type I receptors act in sequence. This model is supported by the finding that a constitutively active TβR-I is able to exert TGF-β signals in the absence of TβR-II (222). It is likely that some other serine/threonine kinase receptor complexes are also activated by a similar mechanism (6, 224).

1. 1. 6 BMP serine/threonine kinase receptors and their signaling pathways

BMPs also signal through serine/threonine kinase receptors, composed of type I and II subtypes. BMP first binds to the type I receptor, and subsequently forms an oligomer with the type II receptor. There are three type I receptors and three type II receptors have been shown to bind BMPs. The type IA and IB BMP receptors (BMPR-IA or ALK-3 and BMPR-IB or ALK-6) and type IA activin receptor (ActR-IA or ALK-2) (93, 116, 193, 195, 196). The type II BMP receptor (BMPR-II) and type II and IIB activin receptors (ActR-II and ActR-IIB) (82, 85, 161, 243). The BMPR-IA, IB and II are specific to BMPs, ActR-IA, II and IIB and also for activins. The type I BMP receptor activates different intracellular mediators like R-Smads and p38 MAP kinase. R-Smads such as Smad1, 5 and 8 bind the BMPR type I and get phosphorylated in a ligand-dependent manner (21, 66, 101, 115, 137, 189). It is also known that the BMPs bind with different affinity to type-I and type-II receptors and its subtypes (89-91, 132,

161, 196). This observation supports the idea that the affinity of the BMPs to the receptors is important for the activation of the signal transduction cascade. It leads to the theory that some BMP ligands prefer to bind specific receptors for their signaling (39, 116, 196) The BMP receptors type I and type II can exist on the cell surface as preformed hetero-oligomeric complexes or as homo-oligomeric complexes only (49). Initially, it was shown receptors form a heterotetrameric-activated receptor complex after BMP binding. These complexes are consisting of two pairs of a type I and II receptors (129, 186). Presently, there is ample evidence suggesting that the oligomerization mode of the receptors at the cell surface determines the activation of the downstream signaling. The ligand, BMP-2 or BMP-4, has two options for binding to the BMP receptors. First, it can bind to the high-affinity receptor Alk3 or Alk6 and then recruit BRII into a hetero-oligomeric complex (BMP induced signaling complexes: BISC). This process leads to activation of the p38 pathway. The second alternative is that BMPs bind simultaneously to the preformed hetero-oligomeric complexes (PFC) consisting of one Alk3 or Alk6 and one BRII receptor protein. In this case the affinity of the BMP-receptors complex increases (172). This complex then activates the Smad signaling pathway (139). However, not only the oligomerization mode of the receptors can determine the downstream signaling, but also the endocytosis of the BMP receptor modulates signaling. After binding of BMP, the BMP receptors can be internalized into early endosomes where signal transduction occurs. Then, receptors can be recycled to the plasma membrane or transported to lysosomes or targeted to proteosomes for degradation (81). One of the internalization routes is clathrin-coated pits (CCP)-mediated endocytosis that was proposed to be required for the signaling of several transmembrane receptors (20, 32, 121). Another route is clathrin-independent through caveolae. The caveolae are membrane invaginations considered to be a subset of lipid rafts containing the integral membrane protein caveolin (96, 164).

Lipid rafts are specialized membrane domains enriched in certain lipids cholesterol and proteins. The existence of lipid rafts was first hypothesized in 1988 (185, 214). Several authors postulated the existence of micro domains, which are enriched with many kinds of lipids such as cholesterol, glycolipids, and sphingolipids. Later, these micro domains were called "lipid rafts". First, the concept of lipid rafts was

used for explanation of the transport of cholesterol from the trans-Golgi network to the cell surface membrane. The present idea was developed in 1997 (184). The authors showed that lipid rafts differ from the rest of the plasma membrane and can be extracted. The extraction takes advantage of lipid raft resistance to non-ionic detergents. The most common of them are Triton X-100 and Brij-98, which should be used at low temperatures (e.g., 4°C). After one of these detergents is added to cells, the fluid membrane will dissolve. The lipid rafts may remain intact under these conditions and can be extracted. Due to their capacity to resist detergents, lipid rafts are also called Detergent Resistant Membranes (DRMs). Also, because it was shown that lipid rafts consist primarily of glycosphingolipids, lipid rafts are called detergent-insoluble glycolipid-enriched complexes (GEMs) (12). A protein which has glycosylphosphatidyl inositol (GPI) anchor can be collected from lysates of some cells in detergent-insoluble form. In this case, the protein is associated with DRM that contain other GPI-anchored proteins and are enriched in glycosphingolipids (12).

The dependence of BMP signaling from raft domain has been shown (168). First, it was shown that cav-1 isoforms (route through caveolae) bind to overexpressed BRII causing BRII to be internalized. Subsequently, BRII is translocated into the cytosol and degraded by proteasomes. This degradation process mediated by cav-1 influences Smad signaling by reducing the BRII level (141, 168). However, BRI and BRII, as hetero-oligomeric or homo-oligomeric complexes, are constantly internalized via clathrin-mediated endocytosis. BMP binding to PFCs induces R-Smad phosphorylation at the plasma membrane. A continuation of Smad signaling requires receptor endocytosis into CCPs because inhibition of clathrin-mediated endocytosis reduces the continuation of Smad signaling (Fig. 1.3). A second population of BMP receptors (BISC) resides in DRMs and activates the p38 MAPK through a Smad-independent pathway. Cholesterol depletion specifically inhibits BMP-mediated p38 signaling, leaving the Smad signaling pathway unaffected (56). These results demonstrated distinct membrane localizations of BMP receptors for specific signaling properties and a tight regulation of signaling by different endocytic routes. How the membrane machinery together with different endocytic routes of the BMP receptors influences downstream signaling mechanisms still remains to be analyzed (56).

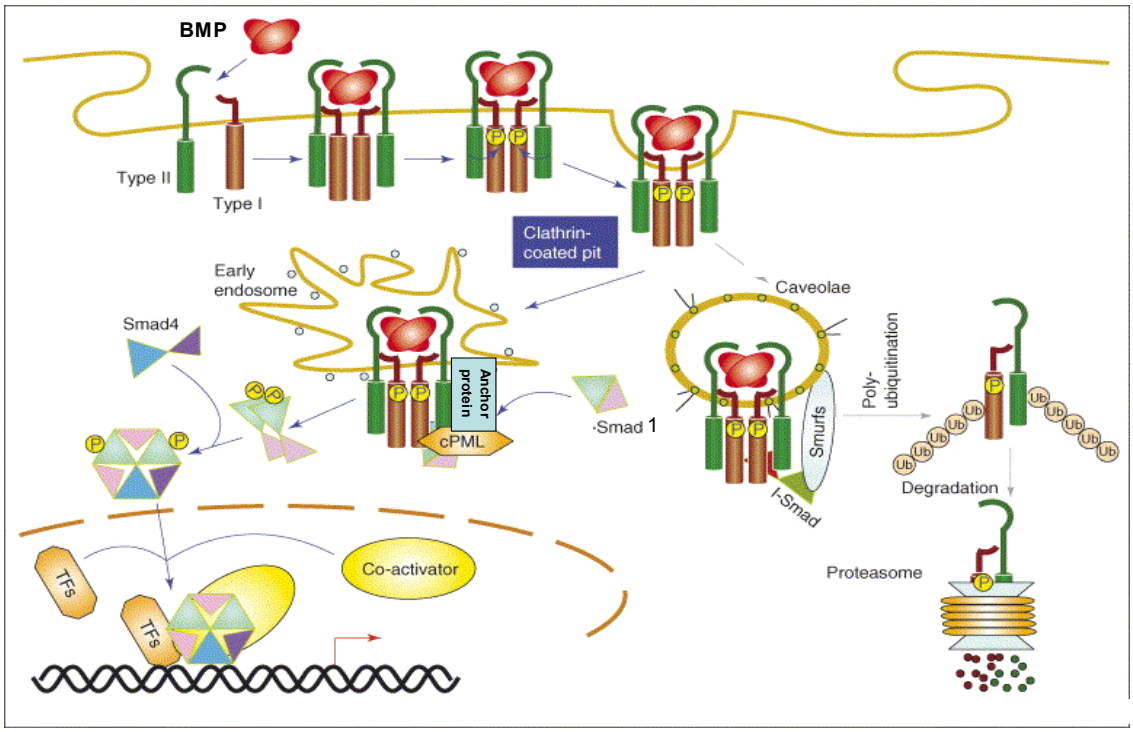

Fig. 1.3 *General outline of the BMP receptor/Smad signal transduction pathway. BMP binding to the heteromeric complex consisting of BMP type I and type II receptors. One way of the internalization of these receptors after activation with BMP can occur via clathrin-coated pits. This way of the internalization increases the duration of Smad signaling. Early endosomes bind anchor proteins, which can recruit more R-Smads to the activated receptor. Another way of internalization is clathrin-independent through caveolae. In this case, receptors are transported to proteosomes for degradation (taken from Susumu Itoh and Peter ten Dijke, 2007 (73)).*

1. 1. 7 Downstream signaling mechanisms

Smad proteins

Studies in the genetically accessible *Drosophila* and *Caenorhabditis elegans* have led to a breakthrough in our understanding of how signals are transduced from serine/threonine kinase receptors to the nucleus. In *Drosophila*, the BMP-2/4 homologue Decapentaplegic (Dpp) acts by binding to the type II and the type I receptors. In a genetic screen for dominant enhancers of weak *dpp* alleles, *mothers*

against dpp (*Mad*) and *Medea* were discovered (153, 174). Homozygous *Mad* mutants were found to have a phenotype similar to *dpp* mutants. These mutants have defects in embryonic dorsal–ventral patterning, midgut morphogenesis, and imaginal disc development (174).

Evidence that Mad is a downstream component in the Dpp pathway came from the finding that *Mad* partially rescued the eye phenotype of *dpp*blk (222), that Mad is required for the response to Dpp of the visceral mesoderm or endoderm (132), and that *Mad* mutations suppress dominant *thick veins* alleles (41, 116). There is also biochemical evidence that Mad functions downstream of Dpp receptors in *Drosophila* (132). In *C. elegans*, *daf-1* and *daf-4* encode serine/threonine kinase receptors. *Daf-4* mutants are dauer-constitutive and smaller than wild type. Moreover, females are defective in egg laying, and males have fused tail rays. Screening for mutants with similar phenotypes revealed three genes, *sma-2*, *sma-3* and *sma-4*, which proved to be homologous to *Mad* of *Drosophila* (169). Because Sma-2 acts in the same cell as Daf-4, and *daf-4* is unable to rescue *sma-2* mutations, it was concluded that Sma molecules are involved in downstream signaling from the Daf-4 receptor. At least nine genes homologous to *Mad* and *sma* have been identified in *Xenopus*, mouse, and man, and have been shown to be components in signal transduction pathways downstream of serine/threonine kinase receptors. To simplify the nomenclature, the name *Smad* has been proposed for vertebrate homologues of *Sma* and *Mad* (169). In mammals, eight Smad proteins were identified. Smad1, Smad5, and Smad8 are BR-Smads. They are activated by BMPs and BMP type I receptors. Smad2 and Smad3 are AR-Smads that are activated by TGF-β and activin and its type I receptors. There is only one Co-Smad, Smad4, in mammals that are shared by BMP and TGF-β/activin signaling pathways. Smad4 was originally identified as a possible tumor suppressor gene, which is frequently deleted or otherwise mutated in pancreatic carcinomas (118). The third class of Smads, inhibitory Smads (I-Smads), represented by Smad6 and Smad7, negatively regulate signaling.

Structure of Smads

R-Smads and Co-Smad, but not I-Smads, contain two structurally conserved domains. The N-terminal MH1 domain is responsible for binding to DNA, transcription factors, and also to the cytoskeletal scaffold (113). The C-terminal MH2 domain is responsible for phosphorylation and complex formation between Smad proteins and for interaction with type I receptors, transcriptional activation, and degradation by ubiquitination. All R-Smads have a specific sequence at their C-terminal ends (Ser-Ser-Val/Met-Ser or SSXS motif). Two distal Ser of this motif are phosphorylated by type I receptors upon ligand binding. The linker region between the MH1 and MH2 domains of R-Smads has consensus sequences phosphorylated by MAP kinases (Fig. 1.4). In addition, the PPXY sequence (known as the PY motif), which interacts with proteins containing WW domains (250), is present in the linker regions of most R-Smads and I-Smads (66, 69, 127).

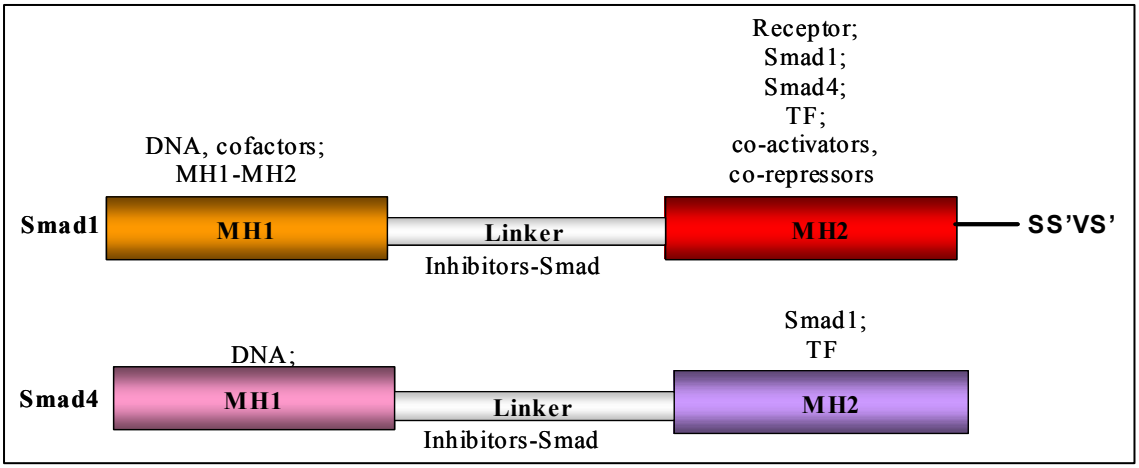

Fig. 1.4 *Structure of Smads. R-Smads and Co-Smad contain two structurally conserved domains. In the basal (unphosphorylated) state, the MH1 and MH2 domains inhibit each other though interaction. The N-terminal MH1 domain is responsible for binding to DNA and transcription factors. The C-terminal MH2 domain is responsible for interaction with type I receptors and phosphorylation by it and for complex formation between Smad proteins. The R-Smads have a characteristic Ser-Ser-Val/Met-Ser sequence (SSXS motif) at their C-terminal, which is phosphorylated. Once activated, R-Smads associate with Smad4 and DNA-binding proteins via the MH2 domains, and the MH1 domain is able to mediate DNA binding.*

Activation of Smads

The phosphorylation of R-Smad is an energetic driver for the Smad-dependent signaling pathway. An important question regarding Smad-dependent signaling is the mechanism of phosphorylation-induced activation of the R-Smads. One part of the mechanism of phosphorylation-induced activation of R-Smads at the MH2 domain is through relieving the inhibition of the MH2 domain by MH1. It leads to a dissociation of the R-Smad from BRI and complex formation with Co-Smads and subsequent binding to DNA and transcription factors (57). Upon BMP stimulation, BRII initiates the kinase activity of BRI leading to the phosphorylation of R-Smad (reviewed in (58, 62, 127, 221)).

R-Smads have the structurally important L3 loop in the MH2 domain, which interacts with the type I receptor. Upon this interaction, the type I receptor kinases directly phosphorylate two distal serines in the C-terminus within the SSXS motif (1, 209). The specific phosphorylation of the R-Smads is controlled by two mechanisms of the receptor kinase complexes. First, a loop structure in the receptor kinase domain, the L45 loop, interacts with the L3 loop of an R-Smad protein (30, 42, 107, 149). Second, R-Smads, such as Smad2 and Smad3, are anchored at the cell membrane by interacting with various cytoplasmic proteins, like SARA and cytoplasmic PML or some other proteins. In contrast, the molecules that interact with Smad1, -5, or -8 in the cytoplasm have not been fully determined until now (208). Recently, it was shown, that Smad1 interacts with the cytoplasmic domain of CD44. CD44 is a receptor for the extracellular matrix macromolecule hyaluronan in chondrocytes. CD44 anchors Smad1 at the plasma membrane in resting cells, and helps to present Smad1 to the BMP receptor type I for phosphorylation. Disruption of the interaction between Smad1 and CD44 results in inhibition of BMPRI-mediated Smad1 phosphorylation. This indicates an important role of the CD44-Smad1 interaction in the regulation of BMP signaling (150, 208). Also, it was recently shown that the endosome-associated FYVE-domain protein, endofin, is a Smad1 anchor protein for receptor activation in the BMP signaling pathway (177). Endofin binds Smad1 and enhances Smad1 activation by phosphorylation upon BMPRI and nuclear localization after BMP stimulation. Endofin also contains a protein

phosphatase-binding motif, which can negatively regulate Smad-dependent signaling by dephosphorylation of the BMP receptors. Thus, it plays an important role in both positive and negative feedback regulation of the BMP signaling pathway (177). To summarize, these evidences demonstrated that the scaffolding proteins contribute to the interaction between Smad proteins and receptors, and that this is also a very important regulatory mechanism in Smad-dependent signaling. It might also provide an explanation for the complicated cell context-dependent specificity of ligand responses.

Upon BMP stimulation Smad1 changes conformation. Thus, activation of Smad1 is dependent on a phosphorylation-induced concerted conformation switch of the Smad1-MH2 domain. These changes may serve as a trigger in Smad dissociation from the receptor and Smad-anchor proteins and make it available for complex formation. The L3 loop of R-Smads refolds after R-Smad phosphorylation. It helps to form and stabilize the trimeric interaction between R-Smads.

Phosphorylated R-Smads may initially have a slow rate of release from the receptor kinase complex for unclear reason. The released phosphorylated R-Smad protein can function as a catalyst to cooperatively induce dissociation of other phosphorylated R-Smad molecules from the type I receptor. The phosphorylated R-Smad can directly compete with the L45 loop from the receptor for the L3 loop interaction using the phosphorylated C-terminal tail. Thus, activation of R-Smad is considered to be complex cooperative process (152).

Regulation of Smad activity

There are many processes at the cell membrane and in the cytoplasm that can regulate Smad activation. Endocytosis of the TGF-β receptors also plays a key role in regulation of Smad activation. Ligands induce receptors internalization to early endosomes, which may be required for continuous TGF-β signaling through Smads (56, 61). It is known that composition of the heteromeric receptor complex including different co-receptors dictate TGF-β-ligand-binding specificity. These complexes can also confer differential intracellular routing. Accordingly, receptor-associated proteins may have a role in vesicular trafficking, as well as facilitating TGF-β-induced receptor internalization and Smad recruitment to the receptors (61). Multiple protein interactions

are likely to control subcellular receptor localization and cell-surface receptor availability. These parameters may in turn control the duration of Smad phosphorylation and activation. Smad activity differs among cell types and depends on the cell cycle, and also on genetic background. Also Smad activity is regulated by different proteins from others signaling pathways. Many Smad binding proteins remain to be analyzed (119). Smads interact with various proteins including the anchor proteins (see below), which play important roles in regulation of their activation. These proteins can directly interact with Smads or interact with receptors and modulate Smad signaling. Cytoskeletal proteins play an important role, too, in the localization and signaling of Smads. For example, unphosphorylated R-Smads bind microtubule filaments, and BMP stimulation induces their dissociation. Thus, if Disruption of microtubules increases this dissociation from R-Smads, and enhances Smad phosphorylation (33). R-Smads also can interact with filamin, a scaffold for intracellular signaling proteins that crosslinks actin. ELF, a β-spectrin, associates with R-Smads and induces phosphorylation of Smads (193) .

Smads can also be negative regulated. Smad6 and Smad7 regulate activation of R-Smads (1, 2, and 3). They inhibit Smad signaling through binding to the MH2 domains of R-Smads and also to the type I receptor. Thus, they prevent recruitment and phosphorylation of R-Smads. Smad6 also interferes with the heterooligomerization of BMP-activated Smads with Smad4, preventing the formation of an effector Smad complex.

When Smad7 is at the type I TGF-β receptor it forms a complex with Smurf1 or Smurf2. This results in receptor ubiquitination by the Smurf proteins and targets the receptor for degradation (38, 82) at caveolin-containing compartments (32), leading to inhibition of R-Smad activation. It was also shown that Smad7 is able to block the binding of the RSmad/Smad4 complex to DNA. There are a number of new phosphatases, which are able to inhibit Smad signaling. Pyruvate dehydrogenase phosphatase (PDP) inhibits Smad signaling. PDP physically interacts with R-Smad and dephosphorylates it (22). PPM1A is protein phosphatase that was identified as a nuclear phosphatase for R-Smad. It directly dephosphorylates C-terminal phosphorylated Smad1, -2 and -3. As was mentioned before, the linker region of R-Smads has

consensus sequences phosphorylated by MAP kinases that block Smad activity (48, 95). However, the small C-terminal domain phosphatases (SCP1, -2 and -3) were found to dephosphorylate the linker regions of Smad2 and 3, thereby enhancing the TGF-β signaling pathway by avoiding MAPK-induced blocking of Smad activity. Some of R-Smad C-terminal domain phosphatases dephosphorylate phosphorylation sites in the linker, which plays an inhibitory role for R-Smads by activating C-terminal phosphoserines in Smad1 (93, 166). R-Smads have been found to be ubiquitinated and targeted for proteasomal degradation by various classes of ubiquitin ligases (37, 73).

The eIF4A (translation initiation factor) limits the spatial distribution of Smad proteins and the duration of Smad signaling. It is directly interacting with Smad1 and Smad4 (104).

Smads also interact with p53 family proteins in the cytoplasm and in the nucleus. Recently, it was shown that the full transcriptional activation of the CDK inhibitor $p21^{WAF1}$ by TGF-β requires p53. The p53-deficient cells display an impaired cytostatic response to TGF-β signals. p53 and Smad proteins bind separate *cis* binding elements on a target promoter, but they are able to interact and synergistically activate TGF-β-induced transcription. The p53 protein can directly interact with Smad2 in a TGF-β-dependent fashion. The p53 protein binds to the MH1 domain of Smad2. The binding site includes the Smads DNA-binding element (SBE) as well as the binding domain for other transcription factors, like JunD, LEF-1 and FoxO. This opens the possibility that these proteins could modulate the interaction between p53 and Smad2. As was mentioned, p53 interacts with the MH1 domain of Smad2, the C-terminal MH2 domain of Smad2 is open to interact with FAST-1 and Smad4. This indicates that Smad2 can bridge the DNA-bound p53 and FAST-1. It is leading to the assembly of a more stable and specific DNA-p53 multifactorial complex (5, 36, 37, 219, 224). The TGF-β signaling pathway enhances an expression level of Maspin. This activation requires Smad2, which can interact with p53-binding elements in the Maspin promoter. Smad2 and p53 both cooperate to induce Maspin transcription. The well known promoters, PAI-1 and Mix.2, contain a p53-binding element in proximity of the TGF-β enhancer (219). The p53 protein can also directly induce the expression of the homeobox genes *Xhox3* and *Mix.1/2*. by physical interaction with Smad1.

The p53-related protein p73 or its antagonist, ΔNp73, also could interact with BMP-2 pathways and affect processes of development and tissue regeneration (68, 103).

Smad complex formation

After R-Smad phosphorylation and conformational change, it dissociates from the type I receptor (180), and interacts with other R-Smads to form a homodimer or homotrimer. Then, these complexes become a heterodimer or heterotrimer consisting of one or two R-Smads and one Co-Smad, Smad4 (Fig. 1.6) (116, 253, 254).

This heteromeric complex translocates to the nucleus where it is involved in transcriptional regulation (7, 98, 106, 254). The structure of the MH2 domain of the R-Smads, together with L3 loop and phosphorylation sequence, provides insight into the mechanism of phosphorylation-induced trimerization between R-Smads.

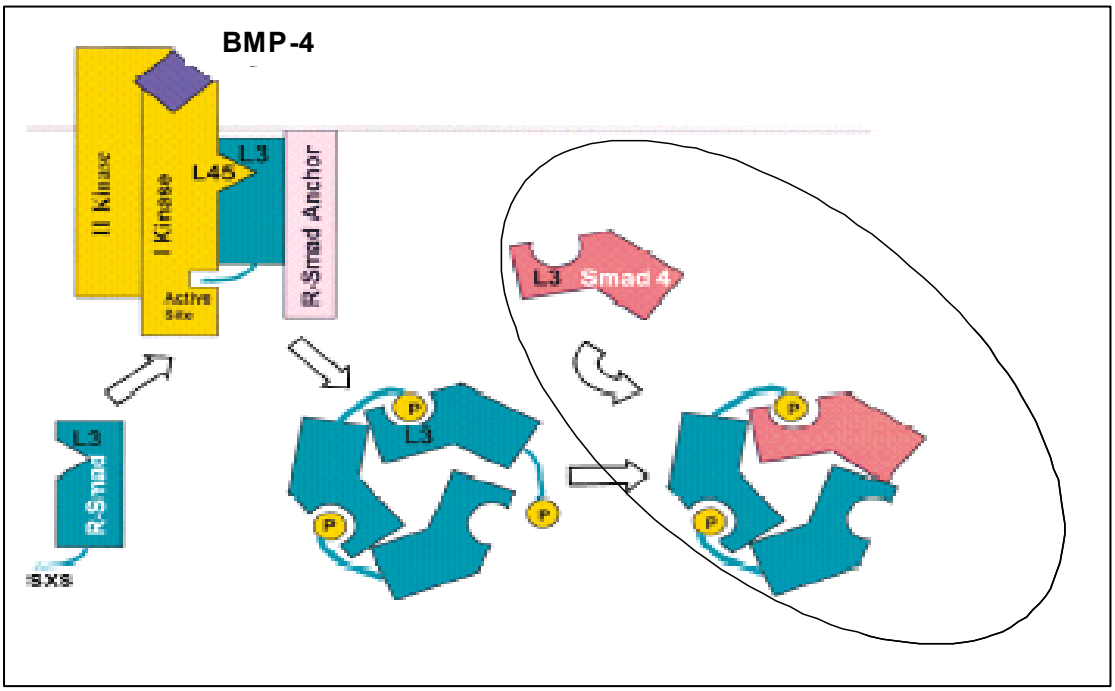

Fig. 1.6 *General mechanism of Smad1/Smad4 complexation. After activation of BMP receptors with BMP ligand, BRI phosphorylates Smad1. After this, Smad1 dissociates from BRI and forms a homotrimer with other Smad1 molecules. One of the Smad1 proteins is subsequently exchange with Smad4 (from Qin et. al, 2001(152))*

There are two distinct structural arrangements of C-terminal tails. The phosphorylated tails of R-Smad interact with Lys 418 and Arg 426 in the L3 loop regions of the neighboring Smad molecules. The interactions between the tail and the L3 loop provide additional intersubunit contact, and the L3 loop undergoes an open to closed conformational transition upon binding of the C-terminal tail. After the trimerization of R-Smads, Smad4 replaces one subunit of the R-Smad homotrimer via the conserved trimer interface. The L3 loop of Smad4 then functions in place of the R-Smad L3 loop, which accepts the phosphorylated C-terminal tail of the neighboring R-Smad due to the possible increase in the total subunit contact area in hererotrimer. Furthermore, phosphorylated R-Smads can acquire different stoichiometries of heterotrimers with one R-Smad molecule and one Smad4 or two with R-Smads and one Smad4. This makes it possible to form a heterodimer between R-Smad and Smad4. Smad heterodimers and heterotrimers may both exist in the cytoplasm and in the nucleus (152).

Smad nuclear translocation

The mechanisms of Smad nuclear import and export (120) have been extensively studied. The nuclear import of these proteins can occur without the intervention of nuclear transport factors (52). Smad proteins in the resting state realize passive nucleo-cytoplasmic shuttling (154), which is controlled by two opposing signals: the nuclear localization signal (NLS) in the MH1 domain and the nuclear export signal (NES) in the MH2 domain. After ligand activation of the receptors, the complexes form, and Smad hereterocomplexes translocate to the nucleus apparently due to slow diffusion of the Smad heterocomlexes in the nucleus and slow dynamic of the nuclear export. After activation of target genes, Smads become dephosphorylated by specific phosphatases. Then Smads realize export into the cytoplasm where they either can bind with receptors again to become re-phosphorylated and reactivated or can be translocated into the proteasome and degraded. These processes are regulated by different signaling mechanisms and depend on the stage within the cell cycle. Nuclear translocation of Smads in response to regulatory signals relies on importins. Importins are factors that mediate nuclear import by recognizing an NLS motif (76). This motif physically interact with importin and also with the nuclear pore components, nucleoporins

Nup153 and Nup214 (238). The presence of an NES in the MH2 domain of Smad4 and Smad1, but not Smad2 and Smad3, and the recognition of this sequence by the general nuclear export factor CRM1 (44) provides for nuclear export of these proteins. If CRM1 is inhibited by the specific inhibitor leptomycin B (LMB), the nuclear export of Smad1 and Smad4 is prevented (235).

Smads transcription factors

After Smad heterocomplexes translocate into the nucleus they regulate transcription of target genes by directly binding via their MH1 domain to specific DNA sequences. They can interact with other DNA-binding proteins, recruiting transcriptional co-activators or co-repressors (127, 195). Smad3 and Smad4 physically interact with Smad-binding elements (SBEs), such as AGAC or GTCT sequence. Smad2 does not bind to DNA directly; it forms a complex with Smad4, and the complex binds to SBEs. Thus, SBEs are important for activin and TGF-β signaling. In contrast, Smad1, -5, and -8 bind to the AGAC/GTCT sequence only weakly, and instead bind to the GCCGnCGC sequence of some target genes (88, 97). Some common genes that show similar expression profiles in different biological processes under control of Smads including Vent2, BAMBI, Mix2, Smad6, Smad7, Id proteins 1-3, OASIS, Prx2, TIEG, Snail, Hey1 (also termed HesR1 and Herp2), Tcf7, ITF-2, ICSBP and also in number of organisms BMP-4, BMP-7, BR-II, Tsg, Msx1 and 2, GATA2 and 3, Tlx2, and Tbx2 (77). In the nucleus, Smads are able to interact with different proteins and complexes and can participate in histone modifications and chromatin remodeling (163). Some transcription factors interacting with R-Smads in the nucleus play critical roles in mediating specific signals by regulating the transcription of target genes. Like the transcription factors Runx1, Runx2, and Runx3 (72), Smads also interact with other transcription factors such as MyoD (105), OAZ (58), Vent2 (65), homeobox proteins Hoxc-8 (178) and Msx1 (242), and transcriptional repressors SIP1 (215) and FoxG1/BF-1 (235). Menin is the product of the MEN1 (multiple endocrine neoplasia 1) gene. It can be required for mesenchymal stem cells to differentiate into the osteoblast lineage. Menin directly interacts with R-Smads and Runx2 in mesenchymal stem cells. It helps to facilitate transcriptional activity induced by R-Smads and Runx2 in the

earlier stage of osteoblast differentiation (188). YY1 is a transcription factor that can positively and negatively regulates the transcription of many genes. It is able to represses the induction of TGF-β- and BMP-early response genes, such as PAI-1 and Id1. YY1 interacts with R-Smads and Smad4, and inhibits the binding of the Smad heterocomplexes to their DNA in SBE. Smads interact with transcriptional co-activators and co-repressors. Transcriptional co-activators, including p300 and CBP (CREB binding protein), have histone acetyl transferase (HAT) domains. They induce transcription of target genes by opening of nucleosomal structures. This increases the accessibility to the general transcription machinery. CBP and p300 physically interact with various R-Smads upon TGF-β-ligand stimulation and enhance Smad-dependent transcription of target genes (127). Smads bind transcriptional co-repressors including c-Ski and SnoN. They recruit N-CoR/SMRT and histone deacetylases (HDACs), and repress transcription of target genes.

1.2 Fluorescence microscopy

1. 2. 1 Overview of used techniques

In recent time (in about 20 years) it has become possible to visualize biological events in single live cells using fluorescence microscopy by fusing proteins of interest to the green fluorescent protein (GFP) and its variants. With these techniques different molecules and their properties can be visualized and analyzed; their interactions and conformations change inside of a cell, organelles, tissue and organs.

In this work, a number of fluorescent microscopy techniques were used, and this chapter will explain all of them. Basically, most of the work was based on FRET (see 1.2.2), and others techniques were used for support and control experiments. Laser scanning confocal Microscopy (LSM) was used to observe the nuclear translocation of fluorescent fusion proteins. Total internal reflection (TIRF) microscopy was used to excite only molecules at the basolateral surface of the cellular membranes and measure FRET on them; Fluorescence Lifetime Imaging Microscopy (FLIM) was used to conduct FRET control experiments. All these techniques will be described and discussed in more detail below.

LSM

LSM is one of the most major advancement in optical microscopy during the past (from 1957). In fact, confocal technology has proved to be one of the most important advances ever achieved in optical microscopy.

With this technique it become possible to use also for visualization of genetically engineered proteins (fusions with GFP-like proteins), a wider spectrum of laser light sources attached to highly accurate acousto-optic tunable filter controls. Also the combination of more advanced software with modern computers (255).

Confocal microscopy has several advantages over conventional widefield optical microscopy: first, the ability to control depth of field, second, elimination or reduction of background information away from the focal plane, and, third, the capability to collect serial optical sections from thick specimens. The optical resolution of a confocal microscope is 250nm, which can be calculated by this formula: 0, 61 *λemn/NA. Images are taken point-by-point and reconstructed with a computer, not just projected through an eyepiece. In an LSM, a laser beam passes a light source aperture. Then, it is focused by an objective lens into a small focal volume within a fluorescent specimen. The emitted fluorescent light and reflected laser light from the illuminated spot are recollected by the objective lens. A beam splitter separates these lights and allows only the laser light to pass through and also reflects the fluorescent light into the detection apparatus. After passing a pinhole the fluorescent light is detected by a photo-detection device; photomultiplier tube (PMT) or avalanche photodiode. They transform the light signal into an electrical one, which is recorded by a computer. Thus, the out-of-focus points are suppressed. Most of their returning light is blocked by the pinhole. The detected light originating from an illuminated volume element within the specimen represents one pixel in the resulting image. Because the laser scans over the plane of interest, a whole image is obtained pixel by pixel and line by line, while the brightness of a resulting image pixel corresponds to the relative intensity of detected fluorescent light. Slower scans provide a better signal to noise ratio resulting in better contrast and higher resolution. Information can be collected from different focal planes. In this case it is necessary to raise or lower the microscope stage. Once images have been collected,

a computer can generate a three-dimensional picture. For this, the computer program needs to assemble a stack of these two-dimensional images from successive focal planes.

TIRF

The Total Internal Reflection Fluorescence (TIRF) microscopy or evanescent wave microscopy has opened the possibility to look at important cellular processes. These processes are taking place near the basolateral surface of the plasma membrane (189). TIRF microscopy typically illuminates a vertical slice of 100 to 200 nm. The cellular photodamage and photobleaching are minimal, and minimizing focal plane drift is also more crucial. TIRF images are captured frame-by-frame with charge-coupled device (CCD) cameras. These are sensitive and fast and can reach up to ~90% quantum efficiency and speeds of ~200 Hz (frames/s). Image intensifiers are required for single molecule sensitivity or can be used to minimize exposure times when imaging live cells. This technique can enable the direct observation of membranes and vesicles and the movement of single molecules during signal transduction and endocytosis. The principle of TIRF is based on a number of considerations. First, light travelling in a dense medium (high refractive index, n1) strikes a less dense medium (of lower refractive index, n2) beyond a certain 'critical angle', Ø, (n1*sinØ1=n2*sinØ2, for oil/glass the Øc is about 65°) the light will undergo total internal reflection. As you can see, this critical angle depends on the relative refractive indexes of the two media (189). For TIRF experiments, cells are grown on glass coverslips or transparent materials of high refractive index. A beam of light, usually from a laser or fluorescence lamp, is optically coupled into the coverslip by the objective or a prism. If light approaches the aqueous medium, it totally reflects into the glass. However, if the light 'rays' simply bounced off the interface like a mirror; this would not illuminate the cells. In this case, some of the energy slightly penetrates the aqueous medium as an 'evanescent wave'. It is propagating parallel to the interface due to 'near field' effects. The big advantage of TIRF lies in its combinations with other microscopy techniques, for example FRET which was used in this work (204).

FLIM

Fluorescence Lifetime Imaging Microscopy (FLIM) is a powerful application, which uses pulsed excitation to reveal fluorophore lifetime in cell imaging. By fluorescence lifetime we understand the mean time that a fluorophore spends in the excited state, usually a few nanoseconds. This state is strongly dependent on the microenvironment. Any energy transfer between an excited molecule and its surrounding molecules changes the fluorescence lifetime in a predictable way (99), independent of chromophore concentration. Thus, fluorescence lifetime can be used to quantify anything that involves energy transfer. Fluorescence Resonance Energy Transfer (FRET) shortens the fluorescence lifetime of a 'donor' fluorophore (100). FRET (see below) describes the non-radiative energy transfer from a donor to an acceptor fluorophore with overlapping emission and excitation spectra. Two excited-state dipoles have to come within a critical distance.

A difficulty in intensity-based FRET measurements in cells is that concentrations of the donor and acceptor are variable and unknown. The emission band of the donor extends into the absorption and emission band of the acceptor. Thus, the absorption band of the acceptor normally extends into the absorption band of the donor. Another complication is that only a part of the donor molecules interact with an acceptor molecule. These effects are difficult to differentiate in intensity-based FRET measurements. Nevertheless, a number of FRET techniques have been developed (34, 35, 51). They require several measurements, including images of cells containing only the donor and the acceptor. By contrast, FLIM-based FRET techniques have the advantage that the results are obtained from a single lifetime measurement of the donor. These approaches are nondestructive, and do not require calibration in different cells. Furthermore, FLIM can resolve the interacting and noninteracting donor fractions(34, 35, 51).

1. 2. 2 FRET

FRET is a distance-dependent physical process by which energy is transferred from an excited molecular fluorophore (the donor) to another fluorophore (the acceptor) by means of intermolecular long-range dipole–dipole coupling. FRET is typically measured as the ratio of acceptor emission to donor emission on excitation of the donor,

giving a value that is proportional to the degree of physical association between the two fluorophores.

FRET is a photophysical phenomenon that occurs between a fluorescent donor and an acceptor that are in molecular proximity of each other if the emission spectrum of the donor overlaps the majority of the excitation spectrum of the acceptor. By using two fluorescent proteins with appropriate spectra makes it possible to monitor distances between them in living cells based on FRET. These techniques are based on using special proteins with several qualities that make them suitable for *in vivo* imaging. The most common is green fluorescent protein (GFP) from the jellyfish *Aequorea victoria* (206). GFP is a 238 amino acid protein with a β-barrel structure, bearing an internal chromophore group consisting of several interacting amino acids (Fig. 1.7A). The chromophore of this protein is a hydroxybenzylidene-imidazolidinone derivative formed by an autocatalytic, posttranslational cyclization and oxidation of the polypeptide backbone, involving Ser-65, Tyr-66, and Gly-67 residues (25, 151). The GFP crystal structure has been characterized with 1.9 Å resolution as a monomer (11), as a dimer (178), and of several mutants (145, 216). For GFP it was shown that the chromophore is always located in the middle part of a central helix inside an 11-stranded *β*-barrel (Fig. 1.7A). It is thus totally embedded in the protein matrix and isolated from the bulk solvent. The chromophore of the wild type GFP possesses peculiar spectroscopic properties such as two absorption peaks at 395 and 475 nm, usually attributed to the neutral and anionic forms of the chromophore (220). GFP can be expressed in a variety of cells, where it becomes fluorescent without any cofactors. GFP can be used to tag signaling peptides or fused to other proteins targeted to specific organelles, such as the mitochondria, the nucleus, or the endoplasmic reticulum. Mutagenesis of GFP has generated many mutants with different spectral properties. Therefore, it is now possible to use several fluorescent proteins simultaneously (175, 207, 218, 251). GFP has been used as a marker for studying protein folding, trafficking, and localization, and also gene expression. Recently, various GFP-mutants were produced. They exhibited - compared to GFP - changed fluorescent spectrum properties, most importantly shifted excitation and emission spectra (Fig. 1.7 B). Examples for this are the enhanced cyan fluorescent protein (CFP) and the enhanced yellow fluorescent protein (YFP). Under

these conditions, energy is transferred non-radiatively from the donor to the acceptor with an efficiency E defined by the equation (Fig. 1.7A), where r is the distance between two fluorophores and R_0 (Förster distance) is the distance at which 50 % energy transfer takes place (30 Å) for CFP/YFP FRET. The latter is dependent on the extent of spectral overlap, the quantum yield of the donor and the distance and relative orientation of the donor and acceptor (251).

Once these proteins had been developed(122, 123, 251), many important applications have been developed by using several GFP-mutants to generate FRET-biosensors. These biosensors are capable of monitoring complex processes including intracellular protein-protein interactions and others (122, 123, 175, 218, 248, 251). Recently, modifications of GFP have provided several fluorophores that can serve as FRET donor/acceptor pairs. For example, red-shifted fluorescent proteins (RFPs) can be used as FRET acceptors in combination with a GFP donor and also: BFP/YFP, BFP/RFP, GFP/RHOD-2.

When fluorescent proteins are to be selected as workable FRET pairs, three spectroscopic properties of the donor and acceptor should be taken into consideration. First, there needs to be sufficient separation in excitation spectra to achieve a selective stimulation of the donor. Second, as was mentioned before, their needs to be an overlap between the emission spectrum of the donor and the excitation spectrum of the acceptor to obtain efficient energy transfer (Fig.1.7B). Third, a reasonable separation in emission spectra between donor and acceptor fluorophores is required to make sure that the fluorescence of each fluorophore can be measured independently (151). However, there are also limitations of using GFP-mutants for FRET: the fluorescent proteins (FPs) are relatively large, which can cause problems with misfolding or aggregation of the fusion protein.

To date, the most frequently and successfully used donor-acceptor pair is the CFP–YFP combination. In FRET experiments, the donor is excited by incident light, and, if an acceptor is in close proximity, the excited state energy from the donor can be transferred to the acceptor. According to the Förster equation, a doubling of the distance between the two fluorophores, for example from R_0 to $2R_0$, may decrease the efficiency of

transfer from 50 % to 1.5 %. Therefore, FRET provides a very sensitive measure of intermolecular distances and conformational changes. The FRET technique described above suffers from a contamination of the FRET images with bleedthrough components because of the incomplete separation of the donor and acceptor excitation and emission spectra. When using CFP/YFP, for example, excitation of CFP is associated with partial direct excitation of YFP, which therefore will emit independently of FRET.

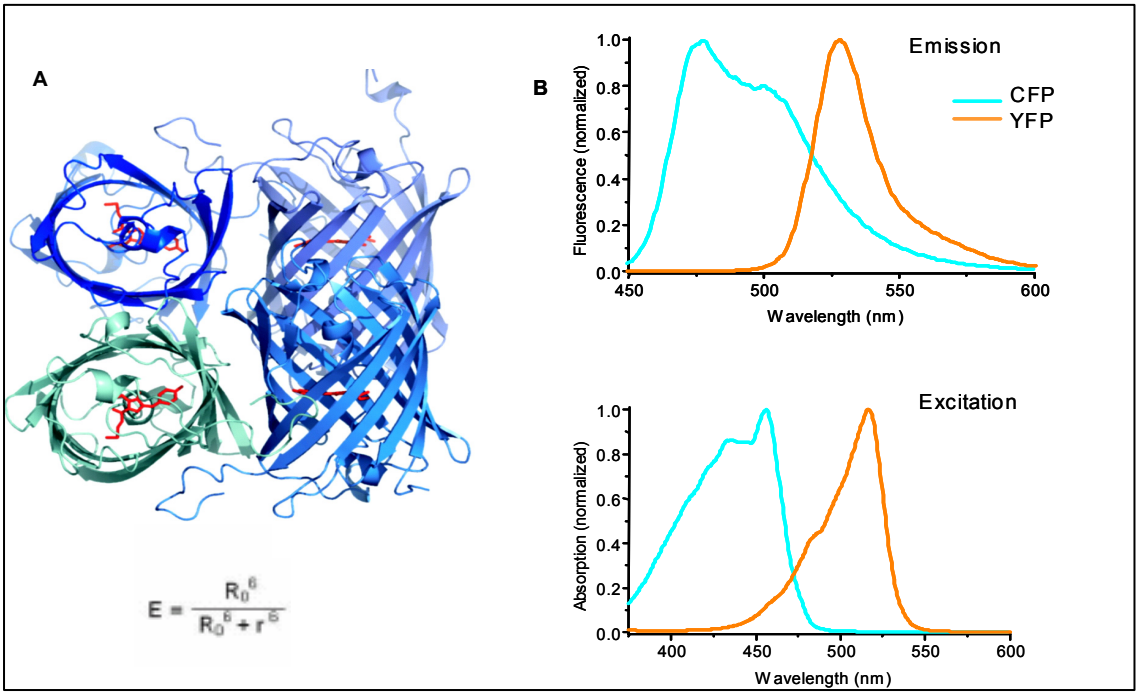

Fig. 1.7 *General properties of YFP and CFP when used for FRET . A, A crystal structure of GFP. It consists of numerous β-sheets forming the β-barrel. The chromophore is a group of amino acids interacting in the core of the barrel. Below – a general equation to calculate Förster resonance energy transfer efficiency (explained in text). B, Excitation and emission spectra of the fluorescent proteins CFP and YFP which were used as a FRET pair. Overlap of the CFP emission and YFP excitation spectra is the basis for FRET (Fig. 1.7A from (151).*

The amount of this bleedthrough of CFP emission in the YFP channel between fluorophores has to be analyzed for each individual FRET imaging system. To minimize the amount of crosstalk it needs careful choice of filter sets. Furthermore, the amount of crosstalk should be measured and be used for in the offline image processing phase

(233). It should include corrections for bleedthrough and direct YFP excitation (see example in materials and methods). Fluorophore crosstalk is a problem for using intermolecular FRET. In this case, the intracellular molar ratio between donor and acceptor is difficult to control. When different concentrations of the two fluorophores occur, it can be misinterpreted as FRET. This problem is overcome if the experimental setup for an intermolecular FRET allows monitoring of dynamic FRET. In this situation, it is possible to establish by monitoring donor and acceptor fluorescence intensity over time whether a change in donor to acceptor fluorescence is a true change in FRET. A true FRET change corresponds to a symmetric change of acceptor and donor intensity. If it is the case, we see an increase in FRET – simultaneous increase in the donor and decrease in acceptor fluorescence as evidence that the FRET signal is true. Another method for imaging intermolecular FRET consists in collecting the donor emission before and after acceptor photobleaching. In this case, elimination of the acceptor by photodestruction releases the energy transferred from donor to acceptor with consequent brighter emission from the donor.

1. 2. 3 GFP-based FRET biosensors

First way to create fluorescent biosensors is to fuse fluorophores to two independent domains or proteins whose interaction depends on induced activation (for example Smad1 and Smad4). In this case the *intermolecular FRET* (Fig. 1.8A) is measured. FRET increases when two proteins interact or decreases upon protein dissociation. Another way to create biosensors is based on *intramolecular FRET* (Fig. 1.8B) between CFP and YFP fused to a one-protein sequence interacting with a molecule of interest. Binding of the specific ligand to this sequence leads to a conformational change, which is monitored by FRET. The constructs for *intramolecular FRET* have an extra advantage. They are containing equimolar amounts of the acceptor and donor fluorophores. Thus they allow observing of the dynamic range of FRET changes and facilitating quantification. In the past, many biosensors have been developed to observe multiple intracellular processes (123). For example: sensors for phospholipase C activation (213) and phosphoinositides (24, 252), cameleons to monitor intracellular calcium (124, 151, 205), and reporters of activity of different protein

kinases (where a target sequence for a particular kinase is sandwiched between GFP variants) (167, 202, 252). Also, bimolecular biosensors have been developed as a tool to monitor interactions between proteins, for example between the regulatory catalytic subunit of the PKA(249) or subunits of trimetric G-proteins (13, 75).

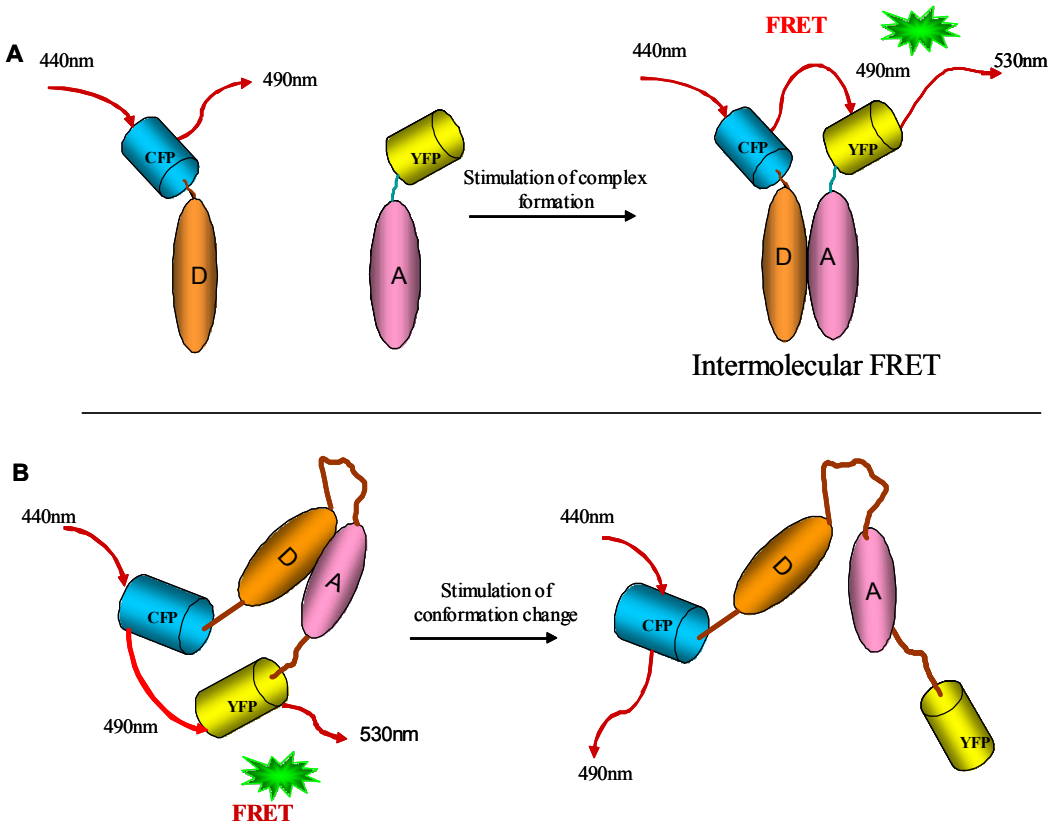

Fig. 1.8 *General principles of fluorescent biosensors. A, Principle of a bimolecular biosensor. It consists of two proteins, A and D, fused to YFP and CFP, respectively. Intermolecular FRET appears when the proteins are interacting. B, Monomolecular biosensor, where a protein sequence, containing two different domains D and A, is placed between CFP and YFP. Interaction between the domains leads to a conformational change monitored by a change in intramolecular FRET.*

Recently novel biosensors for cAMP (2, 3, 135, 165) and cGMP (136) were developed. cAMP and cGMP are second messengers of G protein-coupled receptors and regulate a wide variety of cellular processes. cAMP exerts its effects by a dependent protein kinase (PKA). cAMP-gated ion channels. Two isoforms of exchange protein

directly activated by cAMP (Epac).The cGMP binds specific domains from cGMP-dependent protein kinase I (GKI). Then it forms phosphodiesterases (PDEs). FRET between enhanced CFP and enhanced YFP fused directly to the cAMP-binding and cGMP-binding domains of Epac1/2 or GKI was used to analyze in more detail spatial and temporal aspects of cAMP/cGMP as well as its physiological role in different cells (135, 136).

1. 3 Smad and florescence microscopy

There are numerous methods and ways to study the activation and duration of Smad signaling, the most common being of course, biochemical techniques. But recently, with the development of advanced fluorescence microscopy and labeling technique, Smad signaling has been studied in more detail by a few microscopy-based methods: LSM, FLIP, FRAP. LSM was used to investigate the sub-cellular distributions of Smad proteins their sequences for NES was examined. A second and equally important aim was to thoroughly investigate the nucleocytoplasmic shuttling of the Smad1, Smad2, and Smad3 proteins. The study showed that continued nucleocytoplasmic shuttling is a common requisite for the active signaling of R-Smads (234, 235). Another example is the investigation of Smad nucleocytoplasmic shuttling in a quantitative manner in living cells. The fusions of Smad2 and Smad4 with enhanced GFP or photoactivatable green fluorescent protein was used. Direct evidence of the shuttling and the shuttling kinetics were determined by simple time-lapse fluorescence microscopy of translocation and by combined Fluorescence Loss In Photobleaching (FLIP) and Fluorescence Recovery After Photobleaching (FRAP) experiments. In these experiments, fluorescence labeled Smads were first observed to enter the nucleus upon stimulation and were then photobleached in the area of the nucleus to measure the diffusion rates in the nucleus and cytoplasm and ratios between them during stimulation (134, 170). The experiments showed that Smad2 and Smad4 shuttle between the cytoplasm and nucleus in both TGF-β- induced cells and in uninduced cells. In uninduced cells, GFPSmad2 is less mobile in the cytoplasm than is GFPSmad4, suggesting that it may be tethered there. However, GFPSmad2 and GFPSmad4 undergo a substantial decrease in mobility in the nucleus after stimulation

with TGF-β. Later on, the same authors have determined with the same technique rate constants for import and export of Smad2 and showed that the cytoplasmic localization of Smad2 in uninduced cells reflects its nuclear export being more rapid than import. A pronounced drop in the export rate of Smad2 caused by TGF-β-induced nuclear accumulation of Smad2 was apparently associated with a strong decrease in nuclear mobility of Smad2 and Smad4. Last, this data indicated that TGF-β-induced nuclear accumulation involves neither a release from cytoplasmic retention nor an increase in Smad2 import rate (134, 170).

1. 4 Aims of the work

The signaling through TGF-β family members, at first glance appears to be a simple process. TGF-β ligands bind to serine/threonine kinase transmembrane receptors, which then activate intracellular Smad proteins. Smads can control gene transcription in the nucleus. However, it has recently become evident that additional layers of complexity exist at each step in the TGF-β/Smad pathway from membrane all the way to the nucleus, involving processes of receptor activation through Smad activation and also translocation into the nucleus. The nature of the effect of each step depends on the cellular context. The question is not what the signal can do to the cellular processes but what the cell with all its communication systems can do to signal an effect? The dynamics of activation and inactivation, subcellular localization, and stability of TGF-β signaling components are tightly regulated and subject to input from other signaling pathways and specific cellular conditions. Smad signaling has remained to be more complicated with all cellular mechanisms at the membrane and in the cytoplasm during its activation, and communications due other signaling pathways that either work in conjunction to Smad signaling or interfere with the Smad pathway, appeared recently. In addition, the number of Smad partners is still rapidly increasing, indicating that this process and all of the binding partners of Smads still remain to be discovered. Moreover, the rate limiting steps of Smad signaling still needs to be investigated.

At present, the information from dynamic optical microscopic techniques indicates that Smad proteins are more mobile than as indicated from biochemical techniques. For

example, it is not clear why activation and complexation of R-Smads is relatively slow (118) when they are apparently freely mobile in the cytoplasm (170). The studies also indicate that the shuttling is reduced after Smads form complexes, Smads have their NES motif blocked after phosphorylation, and phosphorylated pools of Smads do not exist in the cytoplasm (170). In these experiments and results, only fluorescence measurements were performed to indirectly indicate the detailed events up to Smad signaling, including the dynamics of phosphorylation and complex formation. Up to now, the direct imaging analogies to Western blot analyses of Smad phosphorylation and to immunoprecipitations of Smad complexes are lacking. Direct imaging could provide the evidence to find the rate-limiting steps in the process of phosphorylation and complex formation. To better understand TGF/Smad signaling events, the BMP signaling pathway was investigated as an example. For the first time, fluorescent biosensors of Smad1 and Smad4 proteins fused with YFP or CFP were created. With these biosensors the activation of Smad1, the role of the Smad1 MH1 domain in this activation, and Smad1/Smad4 complex formation upon BMP-4 stimulation was observed and monitored with detailed time resolution by Fluorescence Resonance Energy Transfer (FRET) microscopy (Fig. 1.2).

Summary of the aims:

1. Create fluorescent Smad1 and Smad4 biosensors
2. Observe functional activity of these biosensors
3. Study the kinetics of Smad activation and complex formation by FRET
4. Analyze the rate-limiting step of BMP signaling
5. Complete the kinetic model of BMP signaling with Smad biosensors
6. Use Smad biosensors to analyze signaling under different physiological conditions

2. Materials and Methods

2.1 Materials

Bacteria strains	
E.coli BL-21 DE3	Stratagene
E.coli Top 10	Stratagene
Plasmid vectors	
pcDNA3	Invitrogen
pcDNA3-BRII	Petra Knaus, Berlin
pcDNA3-BRIa/b	Petra Knaus, Berlin
pcDNA3-Smad1	Petra Knaus, Berlin
pcDNA3-Smad4	Petra Knaus, Berlin
pEYFP	Clontech
pECFP	Clontech
pcDNA3-GFPSmad2	Caroline Hill, London
pcDNA3-SBELuc	Caroline Hill, London
Template cDNA	
Smad1	Petra Knaus, Berlin
Smad4	Petra Knaus, Berlin
BRII	Petra Knaus, Berlin
BRI	Petra Knaus, Berlin
YFP	Clontech
CFP	Clontech
Oligonucleotides	MWG Biotech AG, Martinsried and Invitrogen
Chemicals	
Agar	Roth
Agarose	Roth

Ampicillin	Roth
Acetic acid	Roth
APS	Roth
BMP-4	Sigma
BSA	Sigma
Disoxyribonucleotides (dNTPs)	Promega
DNA ladders	Promega
DTT	Roth
EDTA	Roth
Ethanol	Roth
Etidium Bromid	Roth
Glycerin	Roth
Glycin	Roth
HEPES	Roth
HCL	Roth
KCL	Roth
KOH	Roth
NaCl	Roth
NaOH	Roth
TGF-β	Roth
TEMED	Sigma
Tween 100	Roth
PAAG	Roth
Parathormone	Sigma
Ponceau-S	Upstate
SDS	Roth
Tris	Roth
Trypton	Roth
Yeast extract	Roth

Enzymes and kits	
Pfu DNA-polymerase	Promega
Restriction enzymes	Promega
T4 DNA-ligase	Promega
Blocking reagent	Upstate
Luciferase detection kit	Promega
DNA-Maxiprep	Macherey and Nagel
Plasmid Mini Kit	Macherey and Nagel
Gel Extraction Kit	Macherey and Nagel
PCR purification Kit	Macherey and Nagel
Western blot ECL detection kit	Upstate
Cell culture	
DMEM, 4.5 % glucose	Gibco BRL
DMEM/F12, 1% glucose	Gibco BRL
FCS	Invitrogen
Glutamine	Invitrogen
PBS buffer	Invitrogen
Penicillin/Streptomycin	Invitrogen
Tripsin	Sigma
Other materials	
Antibody	Cell Signaling, Abcam
Cell culture dishes and multiwells	NUNC
96-well reader plates	Costar
Glass coverslips 24 mm	Hartenstein
DNA/Protaen Markers	Fermentas
Pipettes	Gilson
Filter for sterile filtration FP30/0.2	Roth
Film	Piercenet
Hybond-C Extra	Amersham biosciences

2. 2 Methods

For generation of Smad1/Smad4 biosensors, common and well established techniques were applied. They are described in sufficient detail elsewhere to reproduce the experiments presented in the study. The details specific to carry out this study that is not considered general and that cannot be found elsewhere is what is presented here.

2.1.1 Molecular biology techniques

To produce a functional biosensor of Smad1 and Smad4, DNA sequences encoding Smad1, Smad4 were fused with CFP and YFP to produce a chimeric fusion protein. The DNA constructs encoding for Smad1 and Smad4 sensing proteins were generated by polymerase chain reaction (PCR) with the human Smad1 (GenBank Acc.No. Q15797) and the Smad4 (Acc.No. Q13485). The CFP and YFP sequences were amplified with standard primers from pEYFP- and pECFP plasmids and attached to different sequences of Smad1 and Smad4 at the N- or C-terminus via different restriction sites to produce genetic constructs encoding for fusion proteins. First, a PCR was performed to amplify the respective DNA fragments. The standard PCR mix contained: Water (in all experiments ultrapure water was used from NANOpure system, Barnstead) in 100 µl, 10x Pfu polymerase buffer 10 µl with 10 mM Mg^{2+}, deoxyribonucleotide triphosphates mix 2 µl, 20 µM forward primer, 20 µM reverse primer, Pfu polymerase 1 µl (0,1U/µl). The PCR program was run on a Biometra thermal cycler (Whatman): 94°C – 5 min, 20x (94°C – 30 s, 50-55°C – 30-240 s, 72°C – t), 72°C – 7 min, 4°C - ∞. Time and temperature was calculated depending on the length of the fragment amplified and % of GC pairs in primers, 1000 base pairs per 120 s. The primers were designed to contain a restriction site and a DNA sequence of Smads or GFP-variant with a length corresponding to the amplification temperature.

PCR fragments were run on a 1% agarose gel prepared with TAE puffer (40 mM Tris, 0.1 mM EDTA, 1 mM (CH_3COO) Na, pH=8.5) using the same as the running buffer. DNA was purified directly from the gel using a Qiaquick Gel Extraction Kit according to the manufacturer's protocol. The DNA fragments were then cut using the appropriate restriction enzymes and subcloned into pcDNA3 expression vector for mammalian cell expression.

Cloning of PCR fragments or oligonucleotides was performed by ligation of the cut fragments into the restriction sites of the vector for 2h at room temperature using T4 DNA ligase.

The ligation mix was then introduced into competent *E. coli* Top-10 bacteria using electroporation: 1 µl ligation mix, 60 µl 10% glycerin, 40 µl Top10, then 100 µl mix was imported into cuvette for electroporation, incubated 20 min with 200 µl added LB medium and plated on a selective LB-medium plate, containing 1.5 % agar and 100 µg/ml ampicillin. LB medium was sterilized by autoclaving ex tempore (Varioklav) and contained (m/v): 1% NaCl, 1% trypton and 0.5% yeast extract. Bacterial colonies were grown overnight and checked for the presence of the cloned construct by plasmid DNA isolation (Qiagen Plasmid Mini Kit) with subsequent restriction analysis. Positive colonies were then grown overnight in 200 ml LB medium plus 100 µg/ml ampicillin and used for plasmid DNA purification (Qiagen Plasmid Maxi Kit).

Concentration of plasmid DNA was calculated from the light absorption at 260 nm measured in a spectrophotometer (Eppendorf). Absorption of 1 corresponds to a plasmid DNA concentration of 50 µg/µl.

2.2.2 Cell culture and transfections

HeLa, HEK 293, C2C12, COS-1 and MDA-MB468 cell lines were grown in DMEM medium with 10% FCS, 4.5 g/l glucose, 2 mM L-glutamine, 100 U/ml penicillin, and 100 µg/ml streptomycin at 37°C and 5% CO_2.The confluence of cells after transfections was not more that 60 %. Cells were plated onto 6 well plates for Western blot analysis, 24 well plates for luciferase assays, or 24 mm glass coverslips in 60 mm dishes for microscopy live cell experiments. The cells were transiently transfected with FuGENE 6 (Roche Molecular Biochemicals), Effectene, or Superfect (Qiagen) transfection reagents. Cells C2C12ΔNp73 were provided by Dr. Thorsten Stiewe from the same institut.

2.2.3 Biochemical techniques

Western Blots - COS-1 cells were transiently transfected with Smad fusion protein and BMP receptor expression plasmids in a 6-well plate. Twenty-four hours after transfection, cells were starved in DMEM supplemented with 0.5% fetal calf serum for

6 hours. After incubation with 20nM of BMP-4 for 1, 5, 15, 30, or 60 minutes cells were harvested and lysed in lysis buffer (Cell Signaling Technology). The lysates were subjected to sodium dodecyl sulfate-polyacrylamide gel electrophoresis using 8 or 12% gels. After electrophoresis, electrotransfer (PEQLAB Biotechnologie) and blocking (10 mM Tris, pH 7.9, 150 mM NaCl, 0.1% Tween 20, and 5% dry milk; 20°C, 1 h), the blot was incubated with monoclonal rabbit antibodies against Phospho-Smad1 (Ser463/465), with anti-Smad1 (Cell Signaling Technology) or anti-GFP polyclonal antibodies (Abcam) for 20 h at 4°C. Amounts of protein were also determined with a monoclonal rabbit antibody against β-actin (Cell Signaling Technology). Detection of adsorbed antibodies was performed by enhanced chemiluminescence (LumiGLO, SuperSignal WestPico, Upstate), using an HRP-conjugated secondary anti-rabbit polyclonal IgG antibody (Upstate) in blocking buffer.

Luciferase Assays - Twenty-four hours before transfection, MDA-MB468 cells were seeded in triplicate at 2 $x10^5$ cells per well in a 6-well plate. 0.2 µg each of pSBE-Luciferase construct (from C. H. Heldin, Ludwig Institute for Cancer Research, Uppsala, Sweeden), 0.05 µg of BMP receptors constructs, and 0.4 µg of indicated fusion Smad1/Smad4 vectors were co-transfected per well. Thirty-six hours after transfection, cells were starved in DMEM (0.5% FCS) for 10 hours and then incubated in DMEM (0.5% FCS) with 20 nM BMP-4 for 8h. To control protein expression levels and normalize luciferase activity, all samples were transfected with a *Renilla* Luciferase coding vector (0.1 µg each). The cells were subsequently lysed with reporter lysis buffer, and luciferase activity was determinated with a Dual-Luciferase assay kit (Promega) on a FLUOstar (BMG Labtech) luminometer. Each experiment was repeated at least three times.

2.2.4 Fluorescent microscopy techniques

Confocal microscopy - HeLa or COS-1 cells were grown to 50% confluence on 26-mm glass cover slips, transiently transfected, and incubated in complete DMEM medium for 24 hours. After this, cells were incubated for 2 to 5 hours with DMEM containing 0.5% FBS. Cells were analyzed before or after treatment with 20 nM BMP-4 or 20 nM leptomycin B (LMB). All live cell imaging was performed at 37°C. The fluorescence

images were recorded on either a modified confocal microscope (LSM-410, Carl Zeiss and LSM Tech) with a 100x NA 1.3 objective (Carl Zeiss) or a Leica SP5 confocal microscope with a 63x NA 1.2 objective. The fluorescence emission resulted from excitation with 458 (for CFP) and 514 (for YFP) nm laser lines from an argon ion laser (Coherent Innova, I-308) from the modified Zeiss LSM-410 or Lasos (DMI 600B, Germany) with the Leica SP5 LSM confocal with internal spectral parameter settings of 488 for CFP and 514 nm for YFP. The fluorescence was detected with either optical filter sets from the microscope manufacturer using a 475-495 band pass filter for CFP and a 530-585 band pass filter for YFP or with the spectral detectors SP5 set at 490-500 nm for CFP and 520-590 nm for YFP.

FRET Microscopy Measurements.

In this study, a fluorescence microscope was used to perform FRET measurements in living cells (148, 151, 173). For all cells, used for FRET experiments, were calculated (buy intensity levels) approximatet concentrations of fusion proteins, they were about 0.7-1.4 μM in single cell. The ratios between CFP:YFP (for intermolecular FRET experiments) in single cell were from 1.5:1 to 1:1. We quantified the FRET signal by calculating excess acceptor emission using FRET ratios from defined regions of interest in, for example, the cytoplasm. The setup for fluorescence resonance energy transfer between the cyan and yellow fluorescent proteins comprises an inverted microscope (Axiovert 200, Carl Zeiss) equipped with a high numerical aperture objective (Plan Apochromat 100x, 1.4 NA, Carl Zeiss). Samples were excited with wide-field light from a competer-driven monochromator Xenon lamp source (Polychrome IV, Till Photonics) at 436 ±5 nm (CFP) and 480 ±5nm (YFP) that was connected to the microscope with an optical light guide and optical focusing system (Till Photonics) with the excitation light reflected by a dichroic beamsplitter (for CFP and FRET measurements, DCLP 460 or for YFP measurements, DCLP 490, Chroma) into the microscope objective. The fluorescence CFP and YFP signals were detected in the emission light train of the microscope by avalanche photodiodes (Till Photonics) separated by a dichroic beam splitter at 505 nm (DCLP 505, Chroma) and with bandpass filters in front of each of the detectors, one at 480 ± 20 nm (HQ480/40, Chroma) for CFP emission and the other at 535 ± 15 nm (HQ535/30, Chroma,) for YFP

emission, and were digitalized using an AD converter (Digidata1322A, Axon Instruments) and stored on a personal computer using Clampex 8.1 software (Axon Instruments) that also synchronized the excitation wavelength with the data acquisition. In a few cases fluorescence images and recordings were made by detection from a CCD camera (Coolsnap HQ, Photometrics) with the image on the CCD camera split spectrally in half and re-imaged on the CCD with a relay system with a dichroic beam splitter at 505 nm and two filtered split images bandpass filtered again with the a 480 ± 20 nm for CFP emission and the other at 535 ± 15 nm for YFP emission (Dual View, Optical Insights). FRET (including the individual CFP and YFP) signals and images were acquired every 0.1 or 1 sec.

FRET is calculated as the ratio of the corrected YFP and CFP emission intensities at 535 ± 15 nm(I_{YFP}) and 480 ± 20 nm ($I_{CFP}(436)$): $I_{YFP}/I_{CFP}(436)$ upon excitation of CFP at 436 ± 5 nm (beam splitter DCLP 460 nm). The YFP (acceptor) direct excitation factor was determined with YFP transfected cells only. The YFP fluorescence was recorded first with 436±5 nm excitation ($F_{Y,436}$). Next the YFP emission was recorded with 480 nm excitation ($F_{Y,480}$). The direct excitation crosstalk was calculated by $F_{Y,436}$ / $F_{Y,480}$ and was equal to 0.06±0.01. The YFP only cells did not show any emission intensity in the CFP emission channel with 436±5 nm excitation. The bleed-through or spillover crosstalk of CFP (donor) into the 535-nm channel was determined first from cells expressing CFP with 436±5 nm excitation (and also of pure recombinant CFP) only showed that the 535 nm channel had 80% of the intensity of the 480 nm channel. The FRET ratio calculation was performed in the following steps to ensure correct subtractions of signals for FRET (108): 1) we identify and subtract the spillover of the CFP in the YFP channel to determine the pure YFP component due to FRET and direct excitation: $YFP_{sum} = I_{yfp}(436nm) - I_{cfp}(436nm) * 0.8$, 2) we identify and subtract the direct excitation component to determine the YFP signal due to FRET: YFP_{FRET} (or I_{YFP}) = YFP_{sum} - 0.06 * YFP(480nm), and 3) the FRET ratio was then calculated by the formula: FRETratio = $I_{YFP}/I_{CFP}(436nm)$. FRET data was acquired for a long time periods before ligand addition to make sure that both the cyan and yellow fluorescent protein signals were stable and were not photobleaching. Otherwise, the measurements were discontinued and not included in these results. To study agonist-induced changes

in FRET, cells were placed in FRET-buffer or in DMEM (0.5% FCS) and BMP-4 (20mM) was applied. As a negative control on the cell was applied the FRET-buffer or DMEM (0.5% FCS) to show that the FRET change induced by BMP-4 addition but not by buffer or media. The imaging data were analyzed with Origin (Microcal) software. ImageJ and MetaMorph 5.0 (Universal Imaging) were also used in some cases. All live cell imaging was performed at 37°C. We proved FRET by photobleaching the acceptor and then observe the donor dequenching (donor signal increase) and also by FLIM FRET imaging (see below). The calculation of relative CFP:YFP concentrations for the intermolecular FRET were corrected by dividing by the brightness of the individual, initial CFP ($I_{CFP}(436)$) and YFP ($I_{YFP,corr}$) intensities: $I_{CFP}(436)/(t_{CFP}\ \varepsilon_{CFP,436}\ \varphi_{CFP})$ and $I_{YFP,\ corr}/(t_{YFP}\ \varepsilon_{YFP,436}\ \varphi_{YFP})$ where t_{CFP} and t_{YFP} are the optical transmissions for CFP and YFP in the respective CFP (0.35) and YFP (0.60) detection channels, $\varepsilon_{CFP,436}$ and $\varepsilon_{YFP,436}$ are the molar extinction coefficients of CFP (28,000 $M^{-1}cm^{-1}$) and YFP (7,000 $M^{-1}cm^{-1}$) at 436±5 nm excitation, respectively, and φ_{CFP} and φ_{YFP} are the fluorescence quantum yields of CFP (0.36) and YFP (0.76) [45, 46].

Fluorescence Liftime Imaging (FLIM) and FLIM FRET determinations

HeLa or COS-1 cells were grown to 50% confluence on 26-mm glass cover slips, transiently transfected with the CFP-Smad1 and YFP-Smad-4 plasmids (as individuals for control and co-transfected for the FRET experiments), and incubated in full DMEM medium for 24 hours. After this, cells were incubated for 2 to 5 hours with DMEM without serum. Cells were analyzed before and after treatment with 20 nM BMP-4 (Sigma) every 15 minutes after addition of BMP-4 upto 45 minutes.

All imaging experiments were performed on a Leica SP5 confocal laser scanning microscope (Leica) using a DMI 6000 inverted microscope stand with a HCX PL APO lamda blue 63x/1.4 OIL UV objective, equipped with a "multi-function port" and a mechanically controlled beamsplitter that could be automatically placed in the excitation and imaging beam pathway for reflection of the laser excitation light and transmission of the fluorescence emission light and also with two built-in spectrally selective photon counting detectors (set at 460 – 500 nm for CFP and 530 – 590 nm for YFP, respectively for each channel) with a detector response time of less than 200 ps (Leica "Spectral FLIM" internal detectors). The FLIM excitation source was a Ti:

Sapphire femtosecond pulsed laser (MaiTai HP, Spectra-Physics). The laser was tuned to provide a wavelength of 860 nm. A second harmonic generation (SHG) crystal (LBO-Crystal for SHG wavelength: 800-1100nm, LINOS Photonics) was used to frequency double the wavelength from 860 nm to 430 nm which efficiently excites CFP and causes minimal excitation of YFP. All remaining 860 nm light was filtered out by a 510 dcxrt dichroic (Chroma) which reflected the 430 nm pulsed excitation beam into the "multifunction port" and, thus, the Leica SP5 scanning and imaging system. The 430 nm laser power for all experiments was measured at the objective to be 5µW. Live cells on glass coverslips (26 mm) were imaged using a homebuilt incubation chamber kept at 37°C via an objective heater (PeCon).The FLIM measurements were carried out by time-correlated single photon counting (TCSPC) recording and used the 'reversed start-stop' approach, with accurate laser synchronization from a Becker & Hickl SPC-830 card (Becker & Hickl) together with a PHD-400-N reference photodiode recording the 80 MHz pulse frequency of the excitation light. The Leica SP5 software recorded images and split the amplified signal between the Leica imaging software (LASAF, Leica) and the SPC-830 TPSPC card controlled by the SPC-830 software on a separarte computer with the imaging synchronized via the external output of the frame, line, and pixel clock from the Leica SP5 into the SPC-830.FLIM (TCSPC) recordings were acquired routinely for between 120 sec and 150 sec. The mean photon counts were between 10^4 and 10^5 counts per second to avoid pulse pileup. Images were recorded with 256×256 Pixels at 400 Hz line scanning speed. During all FRET-FLIM experiments was no significant CFP photobleaching occurred.

FLIM data analysis and FRET calculations

Off-line FLIM data analysis was used pixel-based fitting software (SPCImage 2.8, Becker & Hickl), able to import the binary data generated with the FLIM module. The fluorescence usually fit best and, thus, was always assumed to follow a two-exponential decay which was used to calculate a weighted mean liftime per pixel for complete images. The fitting procedure also included an adaptive offset correction and also convolution procedures to remove timing jitter occurring from both the detectors and the electronics for accuracy (see User's Manual for SPC-830 Software). ImageJ 1.37 (NIH) was used for the determination of mean lifetime in cell areas. Although the

both the CFP and YFP intensity signals were checked for appropriate levels (data not shown), we focussed our attention to the CFP lifetime in the purely expressed case of the CFP-fusion protein (τ_{CFP} = 2.40 ±0.04 ns for CFP-Smad1) or in the case of FRET (with co-transfection of the YFP fusion protein, $\tau_{CFP,\ FRET}$). The FRET efficiency from this data can be calculated from the equation

$$FRET = \left(1 - \frac{\tau_{CFP,FRET}}{\tau_{CFP}}\right)$$

The difference in calculated FRET before and after BMP-4 ligand addition was multiplied by 100 and reported for pixel (and thus entire FRET images) and also whole cell regions in % FRET change.

The calculation of relative CFP/YFP concentrations for the intermolecular FRET-FLIM were performed by the same procedure listed above FRET Microscopy section but with CFP ($I_{CFP}(430)$) and YFP ($I_{YFP,\ 430}$) photon counting intensities from cellular regions with 430 nm excitation. The YFP spillover or bleed-through correction into the CFP emission channel at 430 nm excitation was 0.02. The YFP direct excitation crosstalk was determined to be 0.02. The CFP bleed-through or spillover crosstalk was determined to be 0.31. The calculation of relative CFP/YFP ratios were also corrected by dividing by the brightness of the individual, initial CFP ($I_{CFP}(430)$) and YFP ($I_{YFP,\ corr}$) intensities: $I_{CFP}(430)/(t_{CFP}\ \varepsilon_{CFP,430}\ \varphi_{CFP})$ and $I_{YFP,\ corr}/(t_{YFP}\ \varepsilon_{YFP,430}\ \varphi_{YFP})$ where t_{CFP} and t_{YFP} are the optical transmissions for CFP and YFP in the respective CFP (0.53) and YFP (0.80) detection channels, $\varepsilon_{CFP,430}$ and $\varepsilon_{YFP,430}$ are the molar extinction coefficients of CFP (28,000 $M^{-1}cm^{-1}$) and YFP (2,000 $M^{-1}cm^{-1}$) at 430 nm excitation and φ_{CFP} and φ_{YFP} are the fluorescence quantum yields of CFP (0.36) and YFP (0.76) [45, 46]

The level of CFP photobleaching was initially tested to be insignificant according to the levels reported by Tramier et al (2006) [54]. First the CFP lifetimes were measured multiple times in CFP only transfected control cells and showed no photobleaching under the experimental conditions and no significant difference in lifetime. Second CSmad1and YLSmad4 transfected cells, 5 min before and immediately after BMP addition showed less than 10% photobleaching and less than 2% change in fluorescence lifetime between the two successive images. Furthermore, we calculated the “apparent photobleaching ratio" (as defined by Tramier *et al* (2006) [54]) for the CFP ($I_{CFP}(430)$)

in the CSmad1 and YLSmad4 transfected cells from the intensity with images recorded at 15, 30, and 45 min after BMP addition and used the t=0 min (i.e. immediately after BMP addition) as the initial reference in every case.

TIRF

The total internal reflection fluorescence microscopy or evanescent wave microscopy has opened the possibilities to look on important cellular processes taking place near the basolateral surface at plasma membrane (Fig. 3.11). The TIRF microscopy was done on Leica TIRF module. With this modul was performing "Objective Type TIRF". This TIRF system consists of a HCX PLAPO 100X1.46 OIL objective (Leica) and a high-performance 3D scanner. The 3D scanner automatically adjusts the laser critical angle (488 for YFP exitation, 405 for CFP exitation from EL6000 external light source) to a specified TIRF and penetration depth (for our experiments it was 70nm) while also performing corrections for wavelength and for the best azimuthal angle. Image recordings were made with detection with a CCD camera (Cascade, Photometrics, Arizona, USA), 512X512 Pixl, 90% peak QE, cooling at -80ºC with the image on the CCD camera split spectrally in half and reimaged on the CCD with a relay system with a dichroic beam splitter at 505nm and two filtered split images badpass filtered again with the a 480/30nm for CFP emission and the other at 535/40nm for YFP emission (Dual View, Optical Insights, USA). Images were acquired every 3 sec with exposure time 109 msec. To study agonist-induced changes in FRET, cells were transfected with Smad1YC and in 24h placed in FRET-buffer or in DMEM (0.5% FCS) and BMP-4 (20mM) was applied. As a negative control on the cell was applied the FRET-buffer or DMEM (0.5% FCS) to show that the FRET change induced by BMP-4 addition but not by buffer or media. FRET is calculated as the ratio of the backdround corrected YFP and CFP emission intensities at 535±20nm (Fyfp) and 480±15nm (Fcfp): Fyfp/Fcfp. Spillover of CFP into the 535-nm channel was determined first from cells expressing CFP only showed that the 535 nm channel had 80% of the intensity of the 480 channel, (80%; spillover of YFP into the 480-nmchannel was negligible) was substracted to give a corrected FRET ratio.

3. Results

3. 1 The full length Smad1 biosensor

3. 1. 1 Development of a full-length Smad1 FRET biosensor

To better understand the kinetics of Smad1 activation, a FRET biosensor for Smad1 phosphorylation was created by a fusing Smad1 with two fluorescent proteins, CFP and YFP. This fusion contruct was subsequently used for intramolecular FRET experiments. As Smad1 is known to change its conformation upon phosphorylation (180, 232), the hypothesis was that it might lead to a change in the distance between the fluorophores upon activation by the BMP receptors. Thus, the FRET changes were expected to reflect the conformational change of Smad1 upon activation by phosphorylation. A decrease of the FRET signal was expected because Smad1 changes its conformation from a closed to an open state (Fig. 3.1), and apparently this helps Smad1 to dissociate from BRI and others membrane proteins. However, the Smad1 MH2 domain conformation change has also been shown to occur with homo- and heterocomplex formation after stimulation with a ligand. This could mean that there are two conformational changes occurring during Smad1 activation, and a FRET change could be caused by either of these processes (152).

To develop a highly sensitive Smad1 biosensor, a number of different Smad1 fusion constructs were analyzed for their ability to demonstrate a clearly detectable change in FRET upon stimulation with BMP-4 (Fig. 3.2). The aim was to construct a Smad1 biosensor that yields a FRET change of at least 5% or more so that the sensor can be used with various microscope systems, even if they have a lower sensitivity than the one used in our laboratory

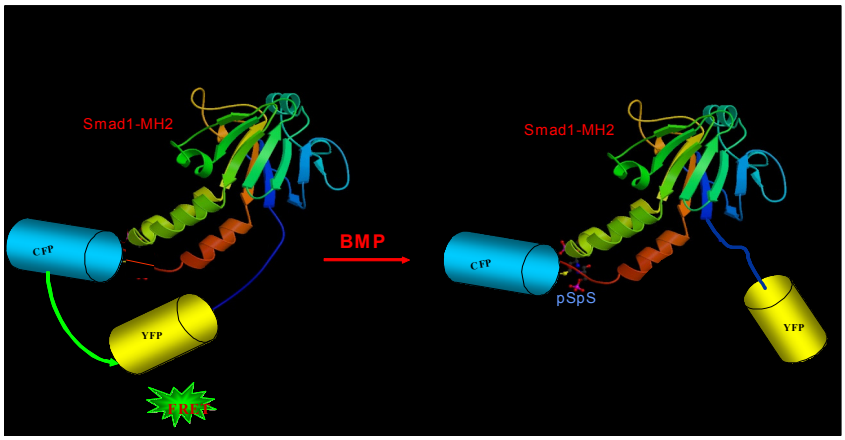

Fig. 3.1. *Schematic representation and principles of Smad1-based biosensors with BMP-4-induced conformational change. Crystal structure of the Smad1 MH2 domain schematically fused to CFP and YFP, respectively, and basal FRET is presented. After BMP-4 activation, the Smad1 MH2 domain is phosphorylated at two distal Ser residues, which induces the conformation change from closed to open and results in the loss of FRET.*

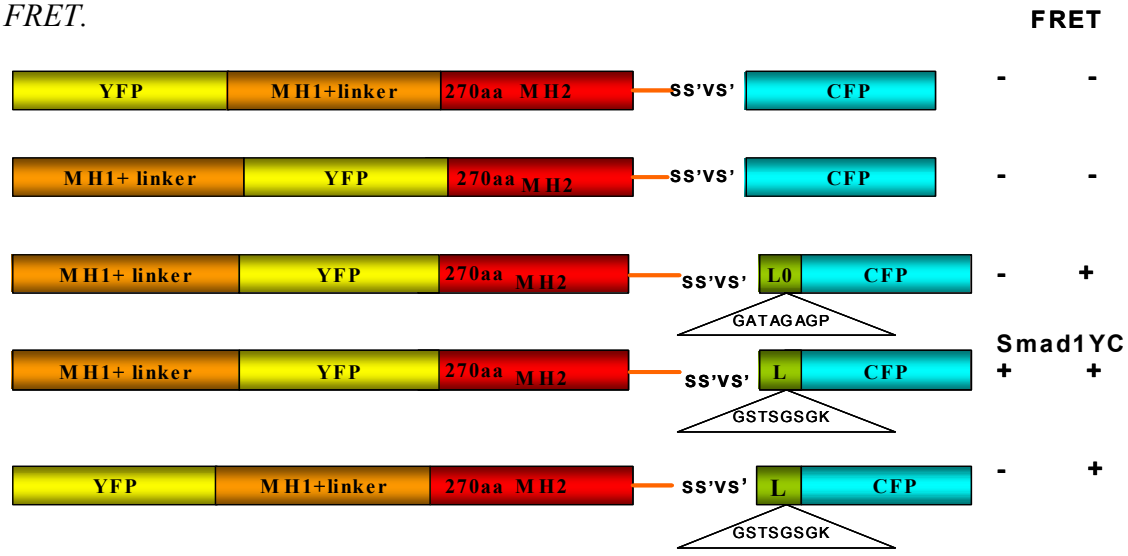

Fig. 3.2. *Development of a full-length Smad1 biosensor. Schematic representation of the constructs designed to observe the activation of the entire Smad1. These are fusion proteins, containing the sequence of the MH1 domain and a linker fused to YFP, the MH2 domain, and CFP attached to the C-terminal end with a specific linker (L or L0). A relative change in FRET measured in COS1BR cells upon full receptor activation (with BMP-4 20nM) is presented by + signs (significance of one, two +, significance meaning - + was positive in minority of trials and + + was positive in majority of trials).*

It was necessary to insert a linker between the C-terminus of Smad1 and CFP in order to avoid impairing phosphorylation of Smad1 at its C-terminal SSXS motif. Without a linker, no FRET change could be detected (Fig. 3.2). This finding is in agreement with results of others authors who have shown that most fusion proteins of RSmads with extensions at the C-terminus lose or at least compromise their activity (235). However, the linker placed between Smad1 and CFP in this study apparently helped to preserve the functionality of Smad1. In fact, different linkers were tested, and a GSTSGSGK peptide linker (L) proved to be most effective in FRET experiment. The functional activity of the Smad1 protein with CFP fused to the C-terminus after the linker (Smad1-L-CFP) (Fig. 3.3A) was tested in detail because the fusion Smad1-CFP without linker (as discussed above) did not show any functional activities. To prove that the chosen linker was appropriate for preserving the functional activity of the Smad1 fusion, a number of experimental assays were performed. First, the nuclear translocation of Smad1-L-CFP upon BMP-4 addition was tested, as this would be an indicator of physiologically normal behavior as has been shown for endogenous Smads. To test this, COS-1 cells were transfected with Smad1-L-CFP, which in about 30% induced cells accumulated in the nucleus after 60 minutes of induction with BMP-4 (Fig. 3.3B).

Second, a luciferase reporter assay that previously was used by Nicholas and co-workers (Nicolas et al., 2004) was also used in this work to determine the transcriptional activity of the Smad1-L-CFP. To do this, the Smad1-L-CFP was transiently transfected together with the Smad1/Smad4-dependent luciferase reporter plasmid, pSBELuciferase, in COS-1 cells. As shown in Fig.3.3C, the Luciferase activity was enhanced by co-transfecting the Smad1-L-CFP expression plasmid, indicating that the fusion protein was able to bind to the Smad1/4 binding element (SBE) present on the luciferase reporter plasmid.

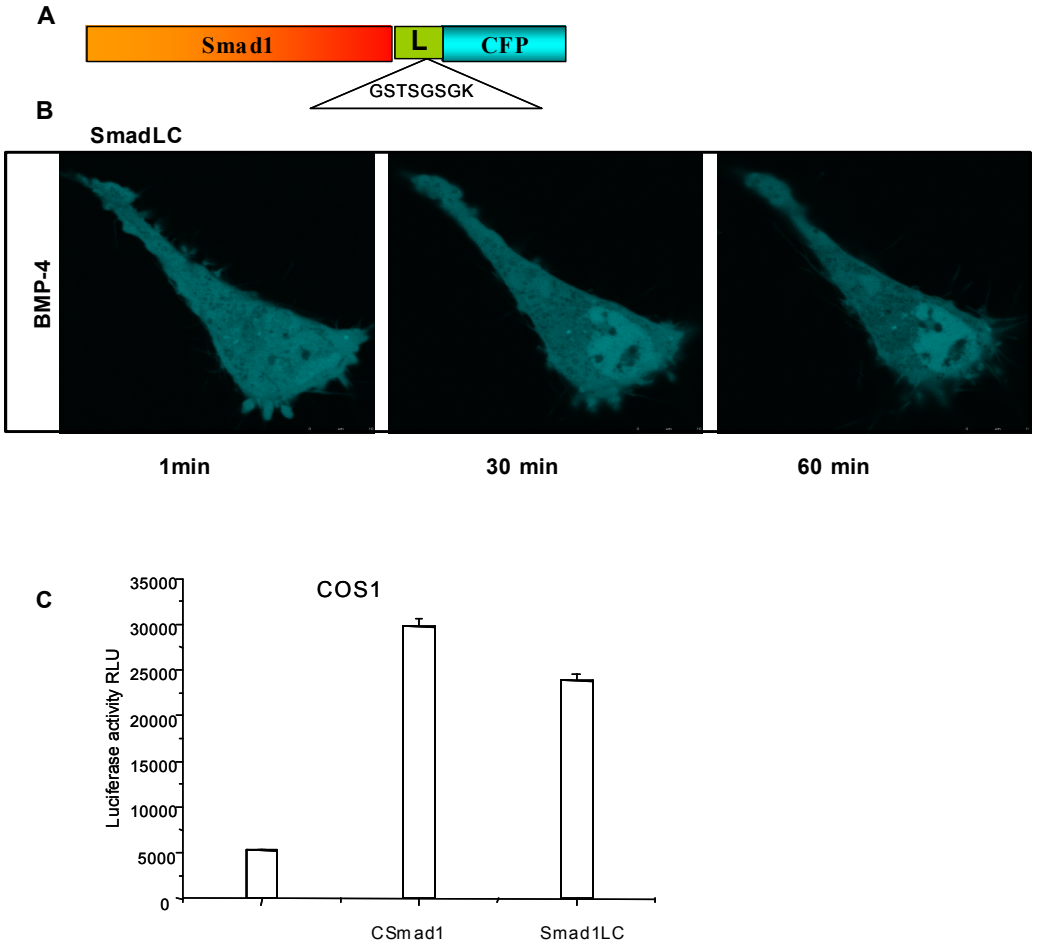

Fig. 3.3 *Linker selection between the C-terminus of Smad1 and CFP. A, The Smad1LC fusion protein was constructed by inserting a short peptide (GSTSGSGK) between the C-terminus of Smad1 and CFP. B, The Smad1LC time series (1, 30 and 60 min) of nuclear translocation after BMP-4 addition. COS-1 cells were transiently transfected with plasmids expressing Smad1LC and BMP receptors. Cells were treated with BMP-4 (20nM). The experiments shown are representative of at least three independent experiments. C, COS1 cells were transfected with the pSBE Luciferase reporter plasmid and plasmids expressing CSmad1 or Smad1LC. Cells were treated with BMP-4 for 8 hours, and luciferase activity was measured. The data are means and standard deviations of the experiment performed in triplicate. All experiments were repeated three times.*

The L linker could, thus, be used in construction of the mono- molecular Smad1 biosensor. The Smad1 biosensor in which CFP was fused to the C-terminus with a selected linker peptide (GSTSGSGK), and YFP was fused between the MH2 domain and the MH1 domain + inker (Fig. 3.4A). This biosensor construct was named Smad1YC.

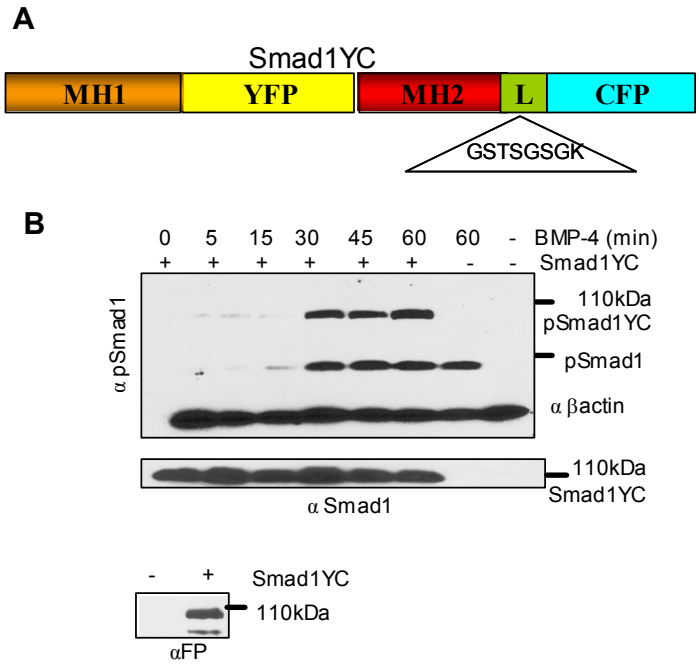

Fig. 3.4. *Full length Smad1 FRET biosensor. A, The Smad1YC fusion protein was constructed by inserting YFP between the MH1 and MH2 domains of human Smad1. CFP was attached with a specific short linker sequence (L) to the C-terminus. B, COS1 cells transfected with the Smad1YC expression plasmid were stimulated with BMP-4. Cells were harvested at the indicated times after BMP-4 stimulation and analyzed by Western blot for the presence of phosphorylated Smad1 (pSmad1). The pSmad1 antibody recognizes both, endogenous pSmad1 and pSmad1YC. Total Smad1YC and β actin are shown as controls. The identity of the 110 kDa protein as Smad1YC was verified using an anti-fluorescent protein (αFP) antibody.*

3. 1. 2 Biological application of a full-length Smad1 FRET biosensor

First, it was determined whether the Smad1YC biosensor retained the phosphorylation properties of wild type Smad1. To do this, COS-1 cells were transfected with the Smad1YC expression plasmid for Western blot analysis. The fusion protein was phosphorylated at a similar time as the endogenous Smad1 in response to BMP-4 (Fig. 3.4B). The phosphorylated bands for both, fusion and wild-type Smad1, appeared only after a delay of 10 min. Apparently, Smad1YC could be a good model to study the kinetic of activation by FRET. The number of kinetic experiments (n=10) by FRET microscopy in living cells was conducted in order to more precisely understand whether the Smad1YC fusion protein functions as a biosensor reflecting Smad1 phosphorylation and more details of this process. COS-1 cells were transiently transfected with plasmids encoding Smad1YC and BMP receptors, and FRET between CFP and YFP was measured. A signal decrease in the YFP channel and an increase in the CFP channel were measured, and the FRET signal was calculated as the ratio between the YFP and CFP signals (Fig. 3.5 A and C). Computerized analysis of the calculated FRET data was used to determine the average kinetics of FRET change (Fig. 3.5B). In cells stimulated with BMP-4, the FRET signal decreased slowly with an average time of 315±70 sec but only after an initial delay of 284±45 sec with no FRET change (Fig. 3.5B).

To determine if different cell lines show a similar delay or whether this phenomenon appears only in COS-1 cells, the same FRET experiments were conducted using C2C12 (n=5) and HEK 293 (n=4) cells (Fig.3.6). A same computerized analysis of the calculated FRET data was used to determine the average FRET change kinetics in these cells. In C2C12 cells stimulated with BMP-4, the FRET signal decreased slowly with a time constant of 300±15 sec after an initial delay of 150±45 sec (Fig. 3.6A), in stimulated HEK 293 cells the FRET signal decreased with the same average time after a delay of 200±45 sec with no FRET change (Fig. 3.6B).

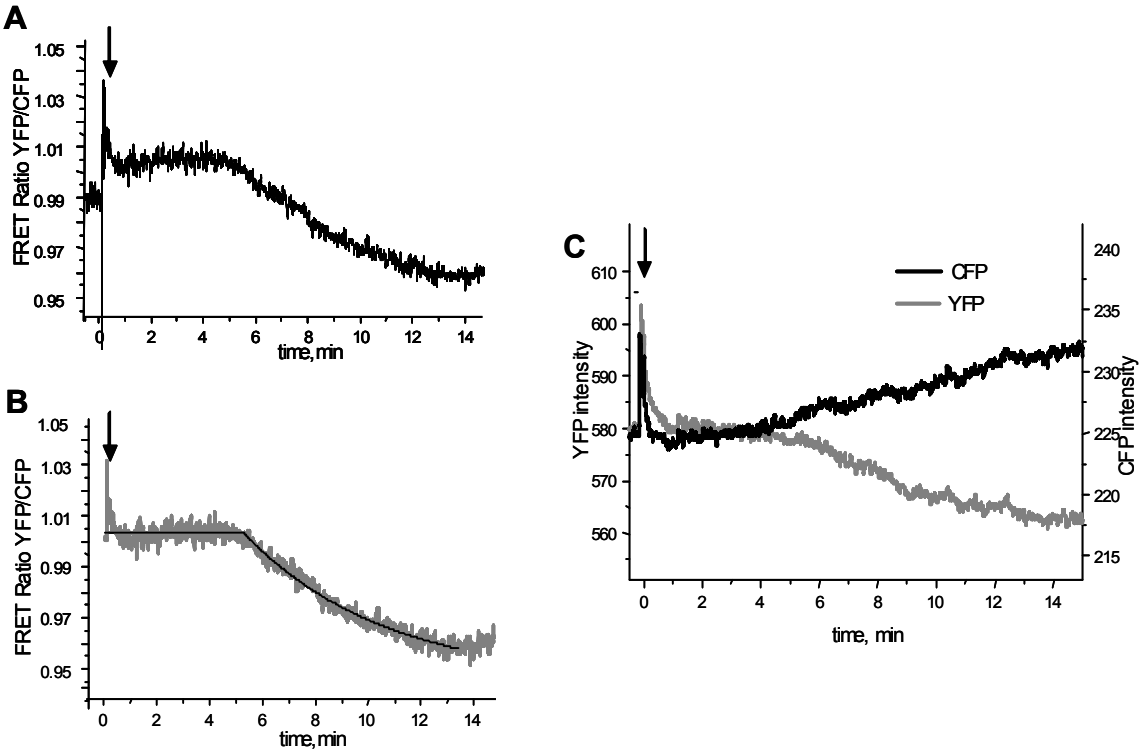

Fig. 3.5 *Intra-molecular FRET kinetics measurement with Smad1YC. A, measurement and B, computerized analysis of FRET (black line of fit in the gray calculated measurement points) represented by the ratio F_{YFP}/F_{CFP} from C, the individual F_{YFP} and F_{CFP} corrected measurements in single COS-1 cell transiently co-transfected with Smad1YC and BMP receptors. Stimulation with BMP-4 began with nearly no response in the FRET ratio until after about 300 sec, when a FRET change with a exponential time constant of about 300 sec was observed with corresponding decrease in the YFP channel and increase in the CFP channel.*

Figure 3.6D shows the time constants and the mean errors of FRET delay and decay for COS-1, C2C12, and HEK 293 cell lines. Thus, a clear delay was detected in all three cell lines tested, but the duration of the delay varied from cell type to cell type.

Control experiments (n=3) was performed, in which FRET was determined in COS-1 cells before BMP-4 addition by acceptor photobleaching (Fig.3.7). The acceptor was selectively photobleached, and, as expected, this maneuver significantly decreased the fluorescence of YFP accompanied by successive increase in the fluorescence of CFP by 20%.

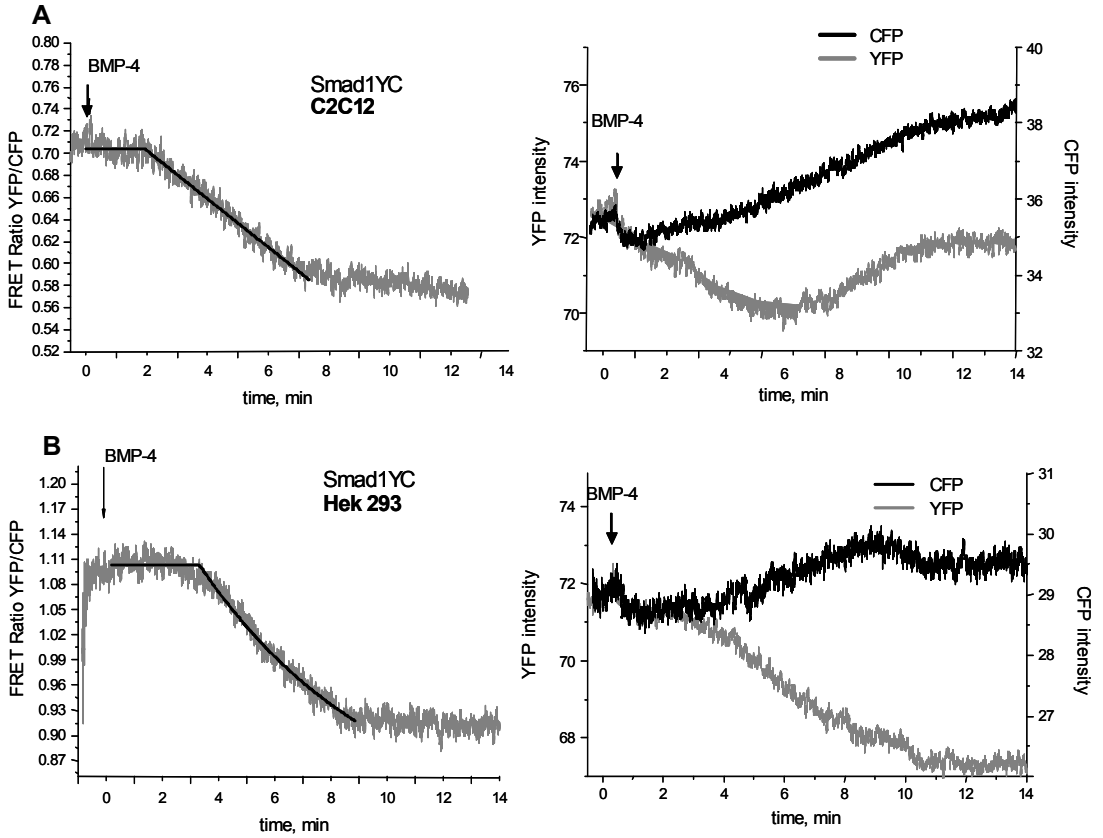

Fig. 3.6 *Measurement and computerized analysis of FRET in C2C12 and HEK 293 cell lines. FRET (represented by the ratio FYFP/FCFP) in single C2C12cell (A) and HEK 293 (B). Cells were transiently transfected with Smad1YC and BMP receptors. Stimulation with BMP-4 began with nearly no response in the FRET ratio until in 102 seconds (A) or in 120 seconds (B). Then FRET changed with an exponential time constant of about 400 seconds. FRET change was also observed with a corresponding decrease in the YFP channel and an increase in the CFP channel.*

The initial FRET level apparently indicated that the biosensor has a closed conformation before stimulation with BMP-4 (Fig. 3.7). To demonstrate that the FRET signal change reflects Smad1 phosphorylation, a mixture of 6 different serine/threonine kinase inhibitors (inhibitor cocktail) was used, which should be able to prevent phosphorylation of wild-type Smad1.

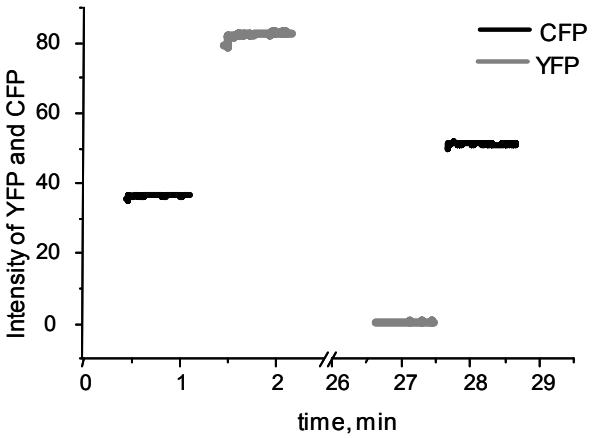

Fig. 3.7 *Donor Dequenching after Acceptor Photobleaching of Smad1YC. FRET was analyzed by Donor Dequenching after Acceptor Photobleaching in COS1 cell transiently expressing BMP receptors and Smad1YC. Emission Intensities of YFP (535nm) and CFP (480nm) were recorded before and after the acceptor fluorophore was completely photobleached with 500 nm excitation light.*

This inhibitor cocktail was used in FRET experiments (n=5) with all conditions as in the previous FRET experiments. COS-1 cells (which were transfected with the Smad1 biosensor) were pre-incubated with the inhibitor cocktail, and then the FRET signal was recorded after BMP-4 addition. As shown in Fig. 3.8, a FRET change did not appear after BMP-4 stimulation, indicating the absence of a conformational change of the biosensor. However, this inhibitor cocktail is not specific for BRI receptor kinases, and this is why a second control experiment was done.

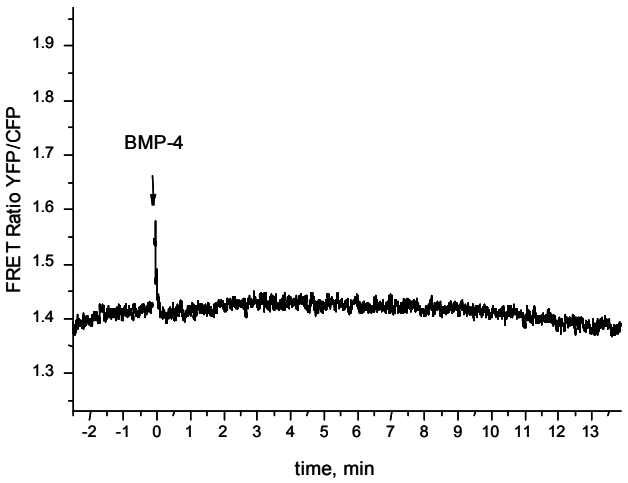

Fig. 3.8 *FRET measurements after incubation with a serine/threonine inhibitor cocktail which is able to prevent phosphorylation of Smad1YC. COS1 cells transfected with biosensor SmadYC were pre-incubated with an inhibitor cocktail, and then the FRET signal was recorded after BMP-4 addition. FRET change did not appear after BMP-4 stimulation, indicating the absence of a conformational change of the biosensor.*

The Smad1 phosphorylation motif (SSXS) was removed by exchanging the three serines for alanines. The fusion protein was named Smad1(SA)YC. COS-1 cells were transiently transfected with plasmids encoding Smad1(SA)YC and BMP receptors and analyzed by FRET. The Smad1(SA)YC did not produce the same FRET change after BMP-4 addition as the Smad1YC biosensor did (Fig. 3.9). The signals in some cases rather showed an immediate slow decay with a time constant of 800±180 sec (n=3) (Fig. 3.9B) or in other cases showed no significant decay at all (n=5) (Fig. 3.9A). The smaller and slower FRET decrease occurring in the minority of cases of the non-phosphorylating mutant might be due to interactions with other proteins (as indicated previously) that could form a complex and thus slightly alter the conformational changes in the of non-phosphorylated mutated Smad1YC constructions. In summary, the approximate 300 sec delay and 300 sec decay is shown to be linked to the active, phosphorylating Smad1YC biosensor.

Apparently, the 300 sec FRET decay and 120-300 sec delay observed with the full-length Smad1 biosensor was shown to be dependent on phosphorylation of the SSXS motif within the Smad1YC biosensor.

The p53 protein family plays a very important role as a tumor suppressor. Smads interact with p53 family proteins in the cytoplasm and in the nucleus (5, 37, 219, 224). The ΔNp73 protein is antagonist of the complete p53 family (68, 103). Members of this family of proteins induce apoptosis, with ΔNp73 being the antagonist of this process. ΔNp73 also inhibits multiple differentiation processes. The ΔNp73 inhibits BMP2-induced conversion of myoblasts to the osteoblast lineage. The question whether ΔNp73 inhibits the Smad signaling pathway at the level of Smad1 phosphorylation was addressed in this study. To do this, FRET experiments in C2C12 cells (n=10), which were cotransfected with Smad1YC and ΔNp73 or just Smad1YC were conducted (Fig. 3.10). The change in FRET after BMP-4 addition for both cases was analyzed. Computer-assisted analyses of the results it showed the same kinetics of FRET change for cells with ΔNp73 (Fig. 3.10B) as for cells with wt p73 (Fig. 3.10A) stimulated with BMP-4: the FRET signal decreased slowly of 300±15 sec after an initial delay of 150±45 sec. These results indicated that ΔNp73 does not inhibit the BMP-4-induced conformational change of Smad1.

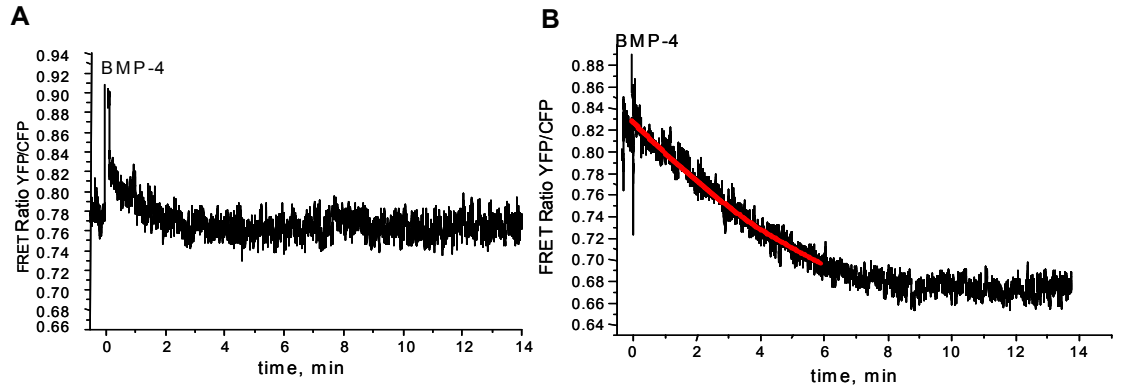

Fig. 3.9 *FRET of Smad1(SA)YC. Measurement and computerized analysis of FRET (represented by the ratio FYFP/FCFP) in single COS-1 cells transiently transfected with Smad1(SA)YC and BMP receptors. A. Stimulation with BMP-4 showed no response in FRET ratio. B. Stimulation with BMP-4 began with a slow decrease in the FRET channel of about 880 seconds.*

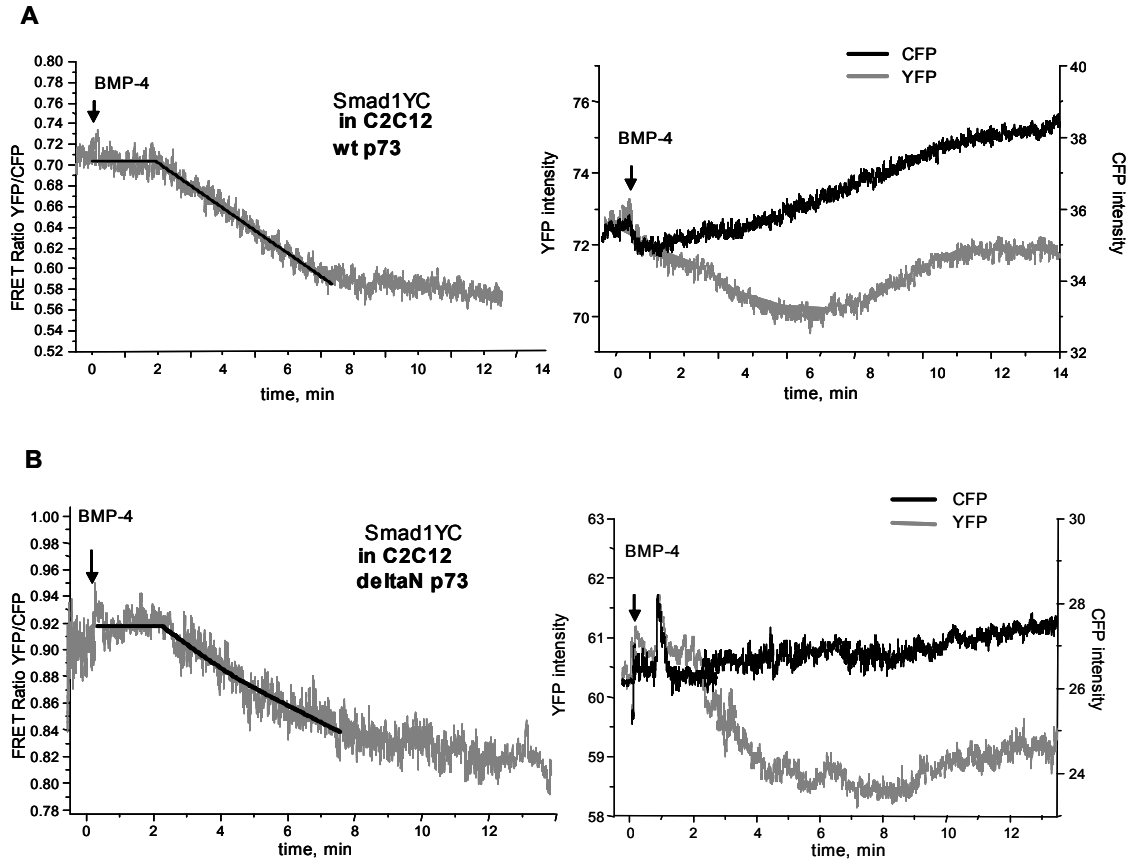

Fig. 3.10 *Measurement and computerized analysis of FRET in C2C12 cells with co-expression of wt p73 or ΔNp73. FRET (represented by the ratio FYFP/FCFP) in single C2C12 cell with co-expression of wt p73 (A) or ΔNp73 (B). Cells were transiently transfected with Smad1YC, BMP receptors and wt p73 or ΔNp73. Stimulation with*

BMP-4 began with nearly no response in the FRET ratio for 102 seconds (A, B). Then FRET changed with an exponential time constant of about 431 seconds. FRET change was also observed with a corresponding decrease in the YFP channel and an increase in the CFP channel.

3. 1. 3 Full-length Smad1 FRET biosensor with TIRF microscopy

The next experiment was designed to determine if the FRET signal starts only after BMP receptor internalization. If this is the case, one should not record any FRET change provided that FRET is measured only at the cell membrane of the cell expressing Smad1YC. There are more assumptions to this, namely that the internalized vesicles will not be within the penetration depth of excitation. The total internal TIRF microscopy technique allowed us to do FRET measurements specifically at the cell surface and measure fluorescence events on it with avoiding auto-fluorescence and fluorescence from deeply internal cell structures (Fig. 3.11).

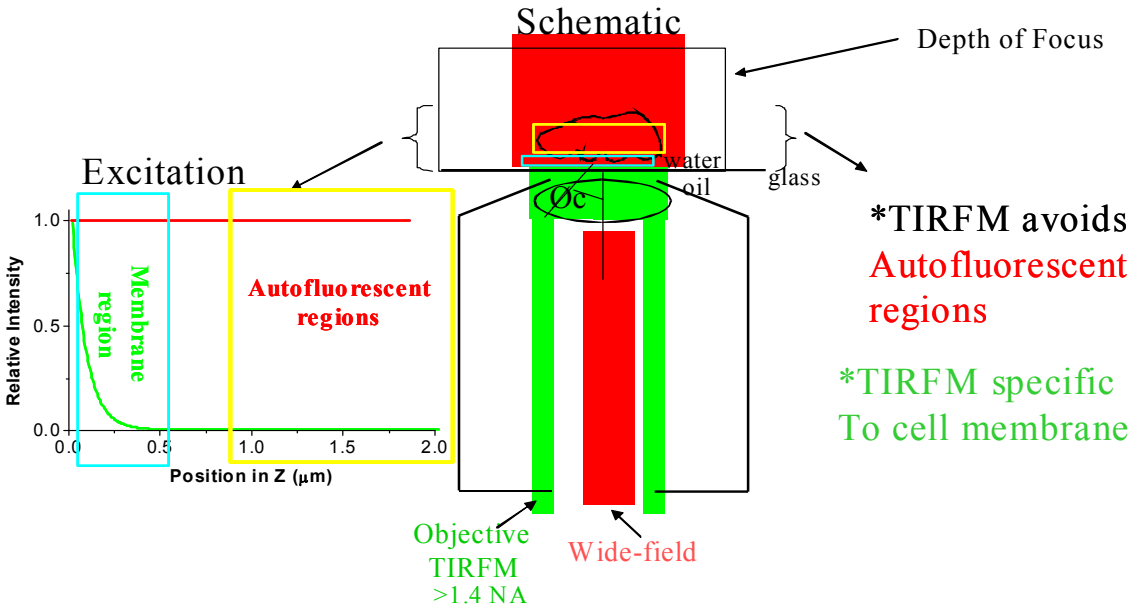

Fig. 3.11 *TIRF. Comparison of Excitation Methods: Wide-field vs. Total Internal Reflection (TIRF) microscopy. With TIRF microscopy it is possible to avoid autofluorescent regions of the cell and excite only membrane regions. With TIRF microscopy one can measure FRET only on the membrane.*

With a TIRF microscope it is possible to excite the fluorophore at a cell membrane with 70 nm penetration depth. To do TIRF experiments, COS-1 cells were transiently transfected with plasmids encoding Smad1YC and BMP receptors, and FRET between CFP and YFP was measured using a TIRF microscope (Fig. 3.12). The signal decrease in the YFP channel and an increase in the CFP channel were clearly observed (Fig. 3.12A), and FRET was presented as a ration between YFP and CFP (Fig. 3.12B). A number of FRET experiments on the cell membrane by TIRF microscopy in living cells were conducted (n=3). Computerized analysis of the calculated FRET data was used to determine the average kinetics of FRET change (Fig. 3.12B). In cells stimulated with BMP-4, the FRET signal decreased slowly with an average time of 300 sec but only after an initial delay of 200 sec with no FRET change (Fig. 3.12B). From these results one can conclude that FRET change and Smad1 activation start already at the cell membrane or very close to it, but not only after receptor internalization. The time delay between stimulation with BMP-4 and activation of Smad1 appeared already at the membrane as well.

3. 2 Smad1 biosensor based solely on the MH2 domain

3. 2. 1 Development of a Smad1-MH2 domain FRET biosensor.

To analyze the role of the MH1 domain in more detail and improve the understanding of the kinetics of Smad1 activation by phosphorylation, a Smad1-MH2 biosensor without the MH1 domain and linker was created. The aim was to create a biosensor, with a faster response upon BMP-4 activation as compared to the full Smad1 biosensor. The Smad1 MH2 domain was fused with both fluorescent proteins, CFP and YFP, and used for intramolecular FRET experiments. As it is the MH2 domain that changes its conformation upon phosphorylation (180, 232), it was hypothesized that this MH2-only biosensor might lead to a similar change in the distance between the fluorophores upon activation by the BMP receptors as for full Smad1 biosensor. In other words, the FRET changes were supposed to reflect the MH2 domain conformation change after phosphorylation. A decrease in the FRET signal was expected, similar to the one observed for the full-length Smad1 biosensor (Fig. 3.1). However, it is

important to note that the Smad1 MH2 domain conformation change has also been shown to occur upon homo- and heterocomplex formation after stimulation with a ligand (152).

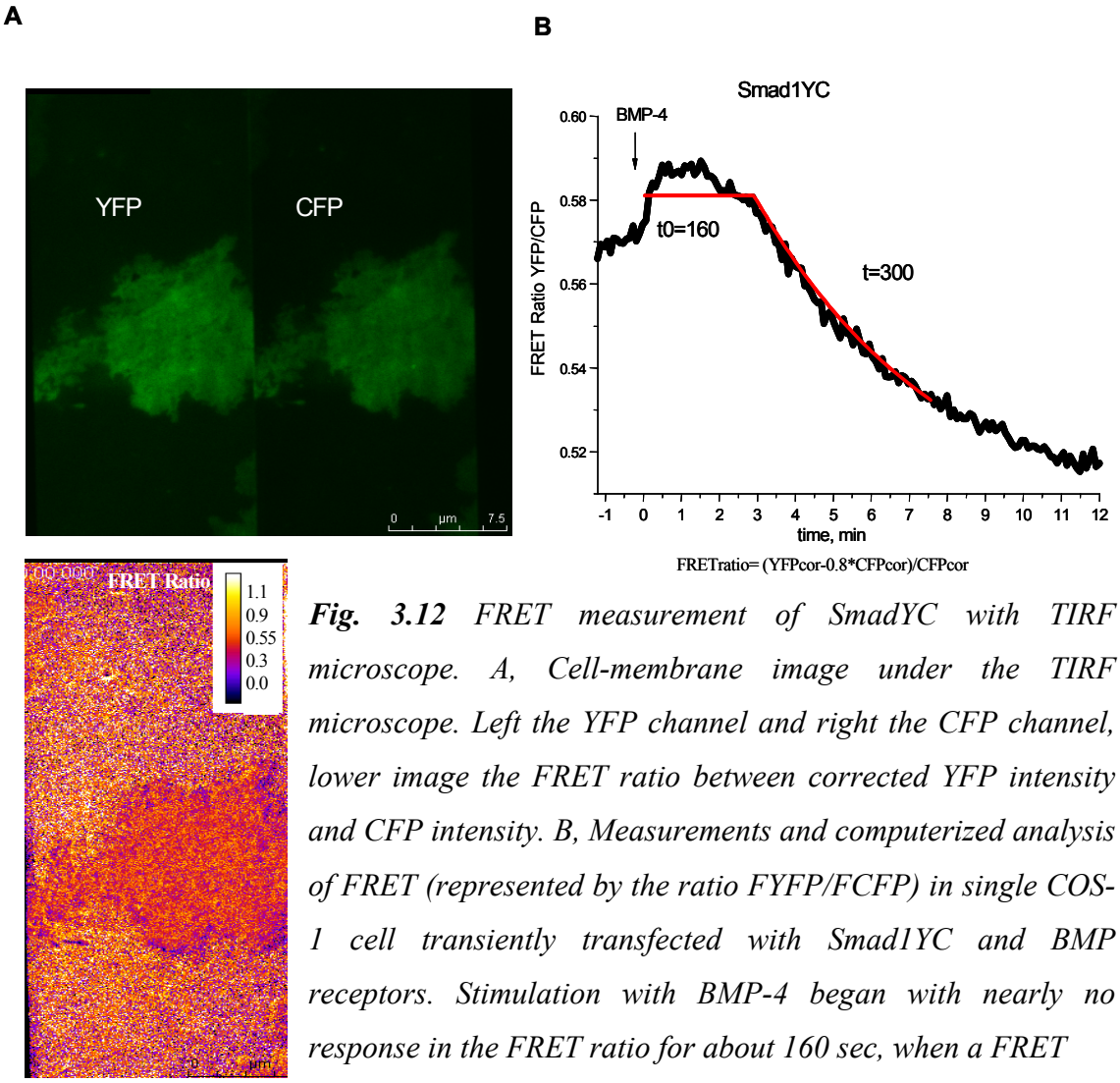

Fig. 3.12 *FRET measurement of SmadYC with TIRF microscope. A, Cell-membrane image under the TIRF microscope. Left the YFP channel and right the CFP channel, lower image the FRET ratio between corrected YFP intensity and CFP intensity. B, Measurements and computerized analysis of FRET (represented by the ratio FYFP/FCFP) in single COS-1 cell transiently transfected with Smad1YC and BMP receptors. Stimulation with BMP-4 began with nearly no response in the FRET ratio for about 160 sec, when a FRET change with an exponential time constant of about 300 seconds was observed with corresponding decrease.*

To develop a highly sensitivity Smad1-MH2 domain biosensor, a number of different fusion Smad constructs were analyzed for their ability to demonstrate a detectable change in FRET upon stimulation with BMP-4 (Fig. 3.13). In all attempted

constructs, the MH1 domain and the linker were deleted, and only parts of the MH2 domain or the full MH2 domain were fused between YFP and CFP (Fig. 3.13).

The same linker L as for Smad1YC was inserted between the C terminus of Smad1 and CFP. The Smad1-MH2-only biosensor that worked best in FRET experiments was named YSmad1C and used in all subsequent experiments (Fig. 3.14A).

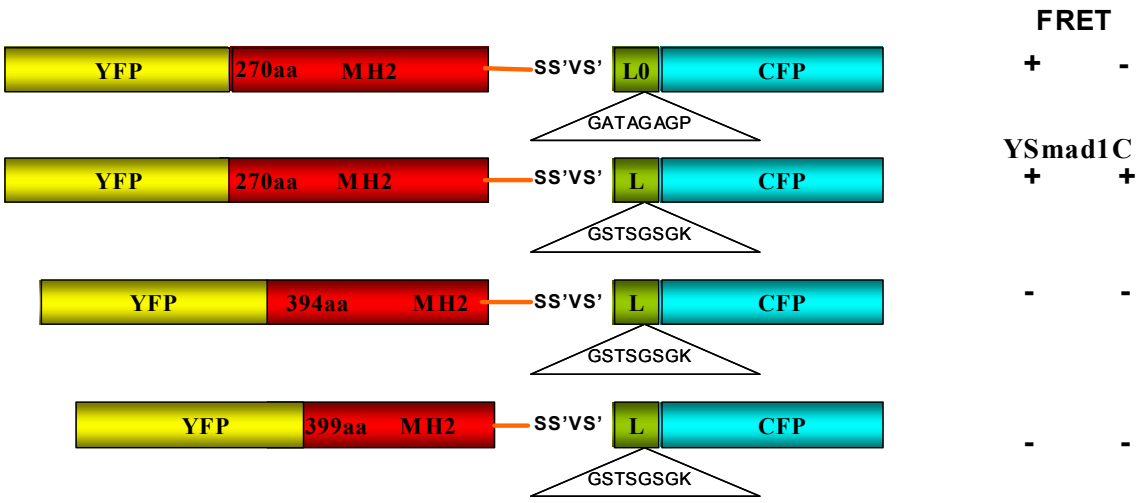

Fig. 3.13. *Development of MH2 domain-based Smad1 biosensors. Schematic representation of the constructs designed to observe the activation of the MH2 domain of Smad1. These are fusion proteins containing a sequence of the MH2 domain fused to YFP and CFP with a specific linker (L or L0) at the C-terminus. Two lowest fusion proteins are containing a truncated sequence of the MH2 domain. A relative change in FRET measured in COS1BR cells upon full receptor activation (with BMP-4 20nM) is presented by + signs (significance of one, two +, significance meaning - + was positive in minority of trials and + + was positive in majority of trials).*

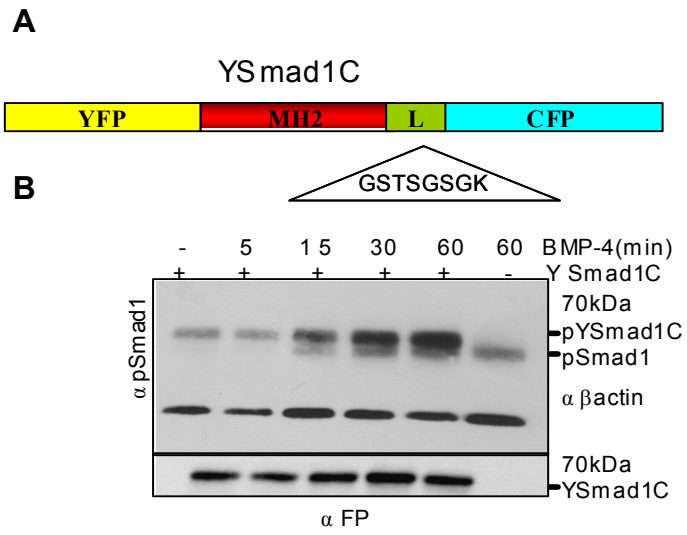

Fig. 3.14 *Smad1 MH2 domain-based FRET biosensor. A, The YSmad1C fusion protein was constructed by flanking the human Smad1 MH2 domain with YFP and CFP. CFP was attached with the specific short linker sequence (L) to the C-terminus. The construct does not contain the MH1 domain and the MH1 linker. B, COS1 cells transfected with the YSmad1C expression plasmid were stimulated with BMP-4. Cells were harvested at the indicated times after BMP-4 stimulation and analyzed by Western blot for the presence of phosphorylated Smad1 (pSmad1). Total YSmad1C was detected using an anti-fluorescent protein (αFP) antibody.*

3. 2. 2 Biological application of the Smad1-MH2 FRET biosensor.

COS-1 cells were transfected with plasmids encoding YSmad1C and BMP receptors for Western blot analysis of the phosphorylation properties (Fig. 3.14B). The Western blots indicated that the YSmad1C showed a notably constant phosphorylation than wild-type Smad1. The band reflecting the phosphorylated fusion protein could be detected already without BMP-4 stimulation, and the signal increased within the first minute after BMP-4 addition indicating that Smad1 without MH1 domain was phosphorylated without delay (Fig. 3.14B). By contrast, phosphorylation of the endogenous Smad1 protein (as a control in the same cells) showed no significant phosphorylation within the first 5 minutes after BMP-4 addition (Fig. 3.14B). Next, COS-1 cells were transiently transfected with YSmad1C for FRET observations

between CFP and YFP (Fig. 3.15). All FRET data (n=9) was subjected to computerized analysis to determine the average kinetics of FRET change (Fig. 3.15B).

After stimulation of the cells with BMP-4, a fast decrease (that demonstrated that the YSmad1C sensor lacking an MH1 domain was phosphorylated almost immediately after addition of BMP-4) with subsequent slow recovery of FRET ratios was recorded with time constants of the decrease of 300±40 sec and with the slow increase of 600±140 sec (about 50% of the cells) (Fig. 3.15A and C) or without increase (also about 50% of the cells) (Fig. 3.16).

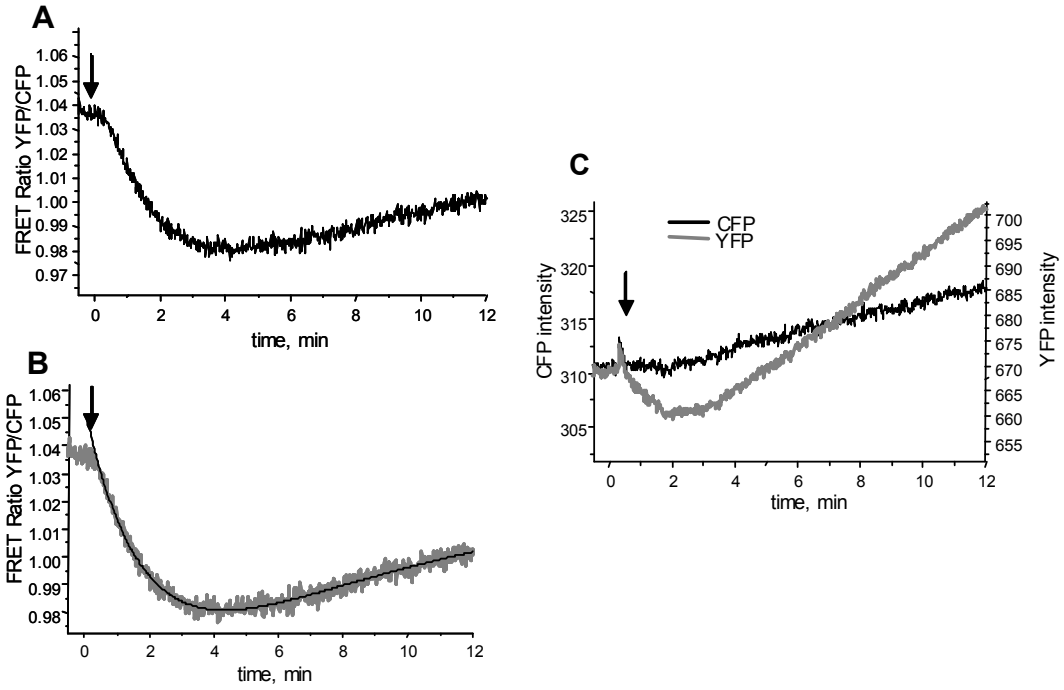

Fig. 3.15*. Intra-molecular FRET kinetics measurement with YSmad1C. A, measurement and B, computerized analysis of FRET (black line of fit in the gray calculated measurement points) represented by the ratio FYFP/FCFP from C, the individual FYFP and FCFP corrected measurements in single COS-1 cell transiently transfected with YSmad1C and BMP receptors. Stimulation of the YSmad1C transfected cells with BMP-4 leads to a rapid decrease of FRET in about 300 sec and a slow recovery phase of about 600 sec with corresponding and decreases in YFP channel and increases in CFP.*

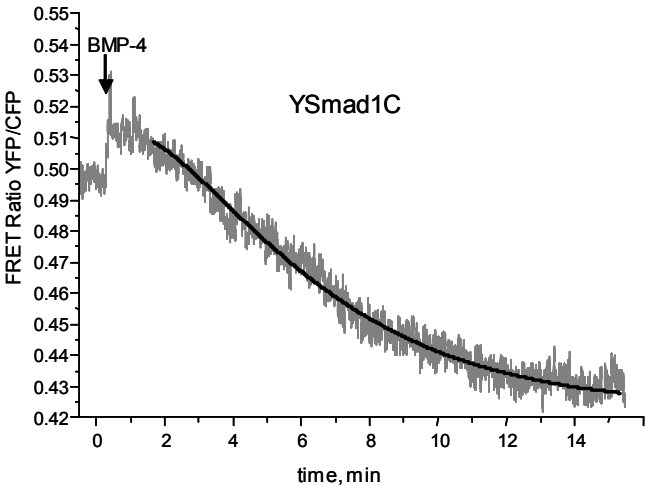

Fig. 3.16 *FRET experiments with* YSmad1C. *Measurement and computerized analysis of FRET ratio in single COS-1 cell transiently transfected with YSmad1C and BMP receptors. Stimulation of YSmad1C-transfected cells with BMP-4 leads to a rapid decrease of FRET in 290 seconds and without recovery phase with corresponding decreases in the YFP channel and increases in the CFP channel.*

The same control experiments (n=4) as for Smad1YC sensor were performed in order to reliably determine FRET in the COS-1 cell before BMP-4 addition by acceptor photobleaching (Fig. 3.17A). The acceptor was photobleached, and this maneuver significantly decreased the fluorescence of YFP accompanied by a successive increase in the fluorescence of CFP by about 30%. This indicated that a baseline FRET exists in the absence of stimulation, because this biosensor has a closed conformation before BMP stimulation (Fig. 3.17A). BMP signaling is a slow process. After cell stimulation with BMP-4, the signal can continue for 1-2 hours, and Smad proteins are able to recycle after dephosphorylation, which appears in the nucleus. Part of the dephosphorylated Smad1 will bind again to the receptors, while the other part of the Smad1 proteins will be degraded. Therefore, it would be interesting to detect a reversal of the FRET signal in cells which were co-transfect with a more robust biosensor like YSmad1C. The reversibility was tested by first observing (Fig. 3.17B) a second FRET change of the YSmad1C biosensor in the COS-1 cells (n=3 out of 20) by waiting for 30 min after the first BMP addition to allow for recovery, followed by another BMP addition. 15 min after the first BMP-4 addition the BMP-containing medium was washed away with 3 ml of FRET buffer, and 30 min later BMP-4 was added again. As shown in figure 3.17B, a second FRET decrease was clearly observed. Thus, the BMP-induced conformational change of YSmad1C was indeed reversible.

To demonstrate that the FRET signal changes reflected Smad1 phosphorylation, the same serine/threonine inhibitor cocktail was used as for the full-length Smad1 biosensor. COS-1 cells were transfected with Smad1-MH2 biosensor and pre-incubated with the inhibitor cocktail, and then the FRET signal after BMP-4 addition was measured (n=4) as shown of Fig. 3.18. A FRET change did not appear after BMP-4 stimulation, indicating the absence of a conformation change of the biosensor.

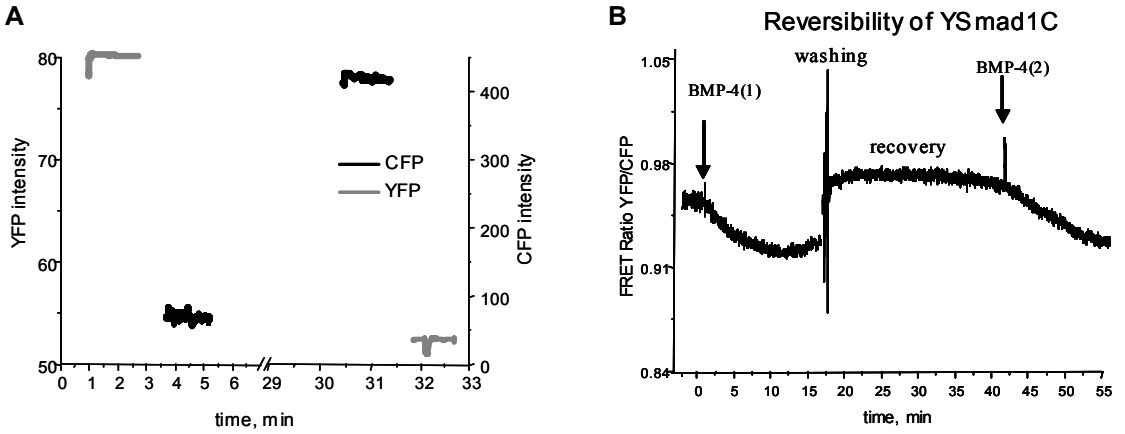

Fig. 3.17 *A, Donor Dequenching after Acceptor Photobleaching of YSmad1C. COS1 cell transiently transfected with BMP receptors and YSmad1C FRET was analyzed by a technique called Donor Dequenching after Acceptor Photobleaching. Emission Intensities of YFP (535 nm, yellow) and CFP (480 nm, cyan) were recorded before and after the acceptor fluorophore (YFP) was completely photobleached with 500 nm excitation light. B, Reversibility of YSmad1C biosensor. Measurement of FRET (represented by the ratio FYFP/FCFP) in single COS-1 cell transiently transfected with YSmad1C and BMP receptors. Stimulation of YSmad1C-transfected cells with BMP-4 (1) leads to a rapid decrease of FRET in 300 seconds. Then the cell were washed with FRET buffer (3 ml), and after a recovery phase the cell were stimulated with BMP-4 again (2) that leads also to a slow decrease.*

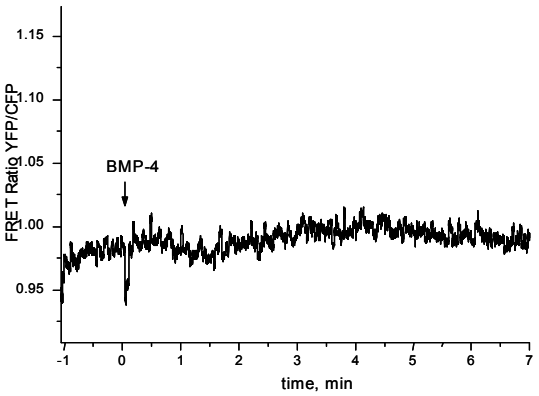

Fig. 3.18 *FRET measurements after incubation with a serine/threonine kinase inhibitor cocktail which is able to prevent phosphorylation of YSmad1C. COS1 cells transfected with biosensor YSmadC were pre-incubated with a kinase inhibitor cocktail, and then the FRET signal was recorded after BMP-4 addition. FRET change did not appear after BMP-4 stimulation after BMP-4 stimulation indicating the absence of conformation change of the biosensor.*

Nonetheless, a second control experiment was performed: the YSmad1C fusion protein was modified by exchange of the three distal serines to alanines. This fusion protein was named YSmad1(SA)C (Fig.3.19). COS-1 cells were transiently transfected with plasmids encoding YSmad1(SA)C and BMP receptors and analyzed by FRET microscopy (n=6). As shown in figure 3.19, the serine-to-alanine mutations abolished the FRET change, indicating that phosphorylation of the SSXS motif is required for the FRET change.

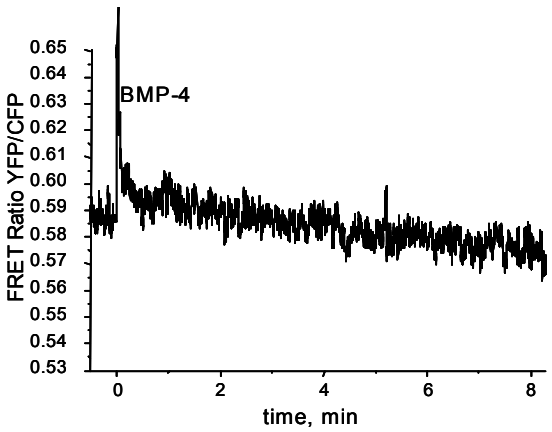

Fig. 3.19 *FRET of YSmad1(SA). Measurement of FRET (represented by the ratio FYFP/FCFP) in single COS-1 cells transiently transfected with YSmad1(SA)C and BMP receptors. Stimulation with BMP-4 caused no response in the FRET signal.*

3. 3 Smad1 and Smad4 biosensors

3. 3 .1 Development of Smad1 and Smad4 biosensors for intermolecular FRET

The next goal was to develop Smad1 and Smad4 biosensors to study the kinetics of heterocomplex formation with intermolecular FRET. To develop highly sensitive

Smad1 and Smad4 intermolecular biosensors, a number of different fusion Smad constructs (YFP for Smad4 and CFP for Smad1) were analyzed for their ability to demonstrate functional activity and a detectable change in FRET upon stimulation with BMP-4. In these FRET experiments we expected an increase in FRET signal because it was based on an interaction between two proteins (Smad1 and Smad4) upon receptor stimulation with its ligand.

To start, a number of different fusion Smad proteins were constructed (Fig. 3.20), which were subsequently tested for their ability to translocate to the nucleus upon BMP-4 addition. This was considered to be an indicator of physiologically normal behavior, as has been shown for endogenous Smads. To test this, COS-1 were transfected with Smad1 or Smad4 fusion constructs, and their intracellular-localization after 60 minutes of induction with BMP-4 was observed. As will be discussed in next chapter, after 60 min of BMP-4 stimulation, each of the fusions Smad proteins was separately translocated into the nucleus. Secondly, fusion Smad proteins were tested in an established assay to ensure that they retained the activity of wild-type Smads. A luciferase reporter assay was done to test the transcriptional activity of the fusions. To do this, plasmids encoding (also will be shown in next chapter) the Smad1 and Smad4 fusion proteins were transiently transfected together with the Smad1/Smad4-dependent luciferase reporter plasmid, pSBELuciferase, into COS-1 or MDA-MB cells, and the luciferase activity was measured 48 hours after transfection and after 8 hours of BMP-4 stimulation. For those fusion proteins, which were positive in both fuctional assays (i.e. nuclear localization 1 h after BMP-4 addition and increased luciferase activity derived from the pSBELuciferase reporter plasmid) (Fig. 3.20A), intermolecular FRET experiments were conducted (Fig. 3.20B). To do this, COS-1 cells were transiently transfected with Smad1 and Smad4 fusion constructs (Fig. 3.20A), and the FRET signal upon stimulation with BMP-4 was recorded (Fig. 3.20B). The best combinations of two fusion proteins (one Smad1 and one Smad4), which demonstrated the highest FRET increase, were used as a model for more precise measurements of the interaction kinetic of Smad1–Smad4 and heterocomplex formation by FRET. The Smad1 fusion proteins CSmad1 and Smad1-L-C, and the Smad4 fusion protein YL1Smad4 (Fig. 3.20B) were

chosen as the best combination for studying the kinetics of complex formation with FRET in living cells (see chapter 3.3.3).

The linker L1 (SGLRSRV) between YFP and Smad4 apparently preserved the functional activity of Smad4. This linker is part of the multiple cloning site (MCS) of the plasmid vector pGFP-C1 (Clontech), and it was shown that with this linker Smad4 preserves its functional activity. Apparently the Smad4 C-terminal fusion protein that was fused directly to YFP without any linker did not show functional activity. A linker was not necessary for the CSmad1 fusion protein but necessary for Smad1LC as was previously shown (Fig. 3.21A).

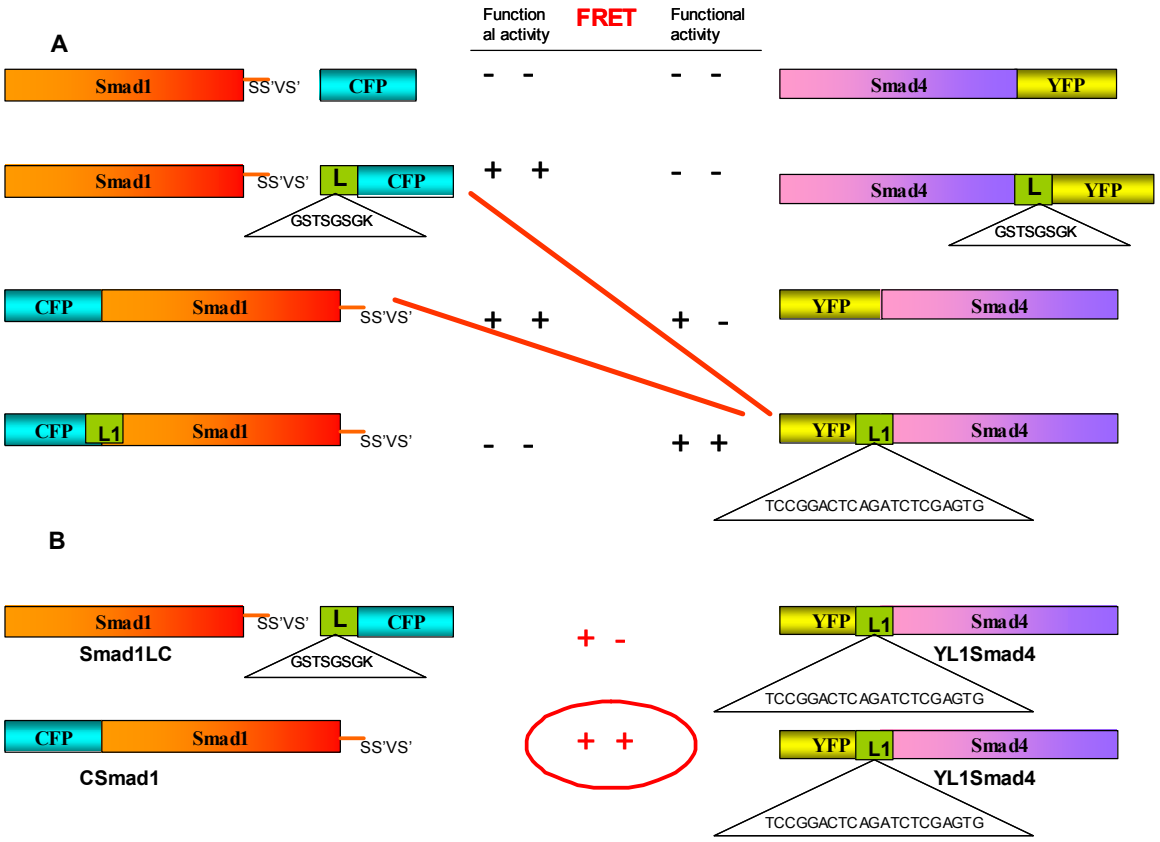

Fig. 3.20 *Development of the Smad1 and Smad4 biosensors. A. Schematic representation of the constructs designed to observe complex formation between Smad1 and Smad4. These are fusion proteins, containing a sequence of Smad1 fused to CFP at the C- or N-terminus with or without specific linker, L or L1, and Smad4 fused to YFP at the C- or N-terminus with or without a specific linker, L or L1. First the nuclear translocation and luciferase activity of the fluorescent Smad proteins after BMP-4 stimulation was tested. The results are presented by + signs, and the constructs with*

two + were selected for intermolecular FRET experiment. B. A relative increase in FRET measured in COS1BR cells upon full receptor activation (with BMP-4 20nM) is presented by + signs (significance of one, two +, +, significance meaning - + was positive in minority of trials and + + was positive in majority of trials).

3.3. 2 BMP4-induced nuclear translocation and transcriptional activity of fluorescent Smad fusion proteins

In this chapter the experiments of nuclear translocation and luciferase activity upon BMP-4 stimulation and also Western blot analysis with the chosen Smad1-L-C, CSmad1 and YLSmad4 are demonstrated.

COS-1 cells or HEK 293 cells were transfected with the fluorescent Smad fusion expression plasmids, and the behavior of the fusion proteins after BMP-4 addition was analyzed (Fig. 3.21). First, to ensure that the CFP/YFP Smads perform nucleocytoplasmic shuttling in the absence of BMP-4 stimulation, cells were pretreated with leptomycin B (LMB), which inhibits the nuclear export by CRM1/exportin-1. CRM1 has previously been identified as the nuclear transporter for NES-dependent export of Smads (44). CSmad1, Smad1-L-C (data not show), and YL1Smad4 were predominantly cytoplasmic in untreated cells and predominantly nuclear in cells treated with LMB (Fig. 3.21B and C). Similarly, the fusion proteins accumulated in the nucleus (but only in about 30% of observed cells) after 60 minutes of induction with BMP-4 (Fig. 3.21B and C). To test whether co-expression of the two Smad fusion proteins, CSmad1 and YL1Smad4, impairs nuclear translocation, COS-1 cells were co-transfected with both CSmad1 and YLSmad4 expression plasmids to observe in parallel nuclear translocation of each fusion protein over time upon BMP-4 or LMB addition. With confocal microscopy, it was clearly observed that co-expression does not prevent nuclear translocation of both fusion proteins upon LMB addition (Fig. 3.21D).

The parallel observation of nuclear translocation of each fusion protein over time upon BMP-4 addition was more difficult. Previously published results of others indicated that nuclear translocation in complexes is less favored in comparison to the translocation of endogenous Smads (134) because fluorescent proteins fused to Smads have a lower

mobility and apparently lower nuclear translocation probabilities spatially in heterocomplex.

Nonetheless, nuclear translocation of the fusion proteins upon BMP addition was observed by means of confocal fluorescence lifetime imaging (FLIM), a technique which can determine FRET efficiency. The technique is able to determine FRET by changes in the fluorescence lifetime of the donor in the presence of the acceptor on a pixel-by-pixel basis for time-lapsed images on the minute time-scale (see materials and methods). The nuclear translocation of CSmad1/YLSmad4 upon BMP-4 addition with FLIM was observed and will be described it in the next section.

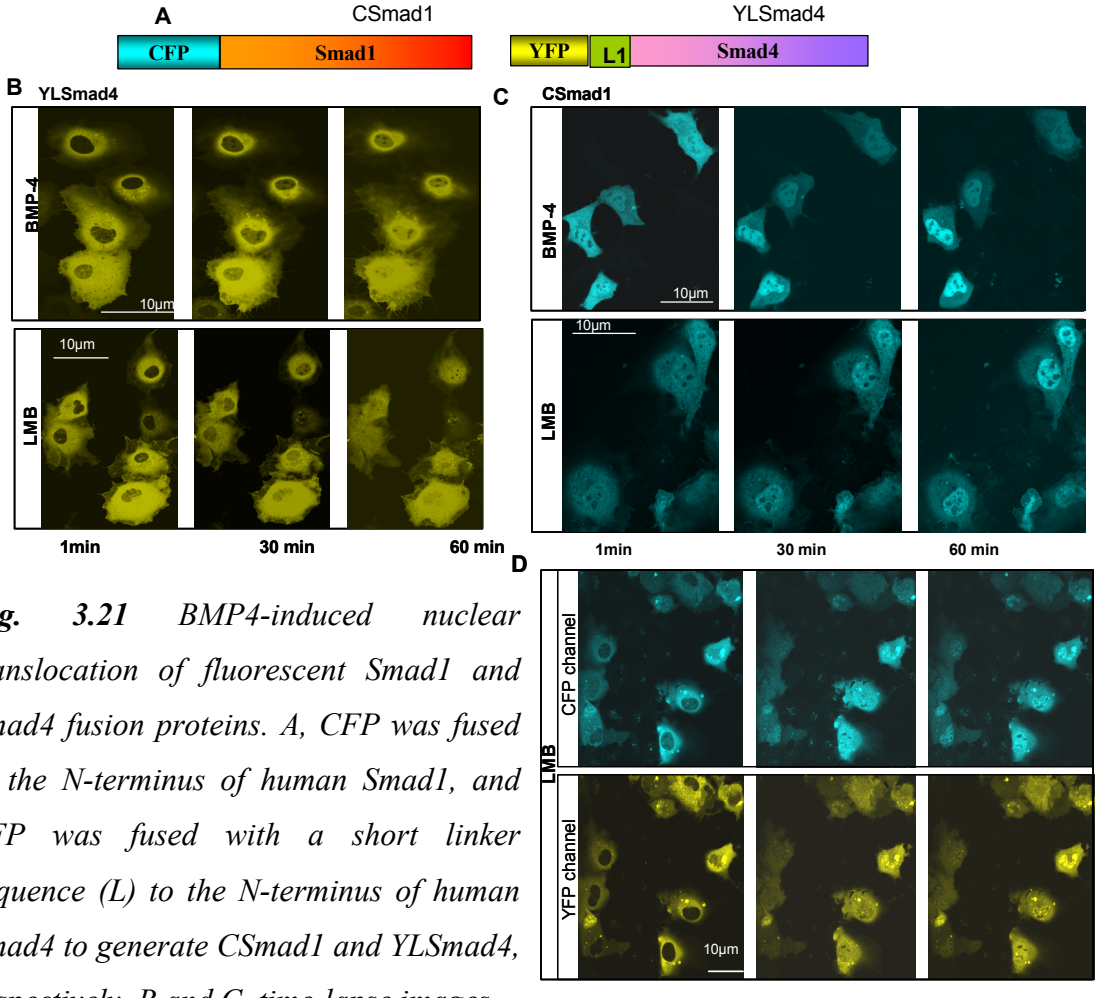

Fig. 3.21 *BMP4-induced nuclear translocation of fluorescent Smad1 and Smad4 fusion proteins. A, CFP was fused to the N-terminus of human Smad1, and YFP was fused with a short linker sequence (L) to the N-terminus of human Smad4 to generate CSmad1 and YLSmad4, respectively. B and C, time-lapse images of nuclear localization of CSmad1 and YLSmad4 after BMP-4 and LMB addition (1, 30 and 60 min). COS-1 cells were transiently transfected with plasmids expressing CSmad1 or YLSmad4 and the BMP receptors. Cells were treated with BMP-4 (20nM)*

or LMB (2nM). The experiments shown are representative of at least three independent experiments. D, The CSmad1/YLSmad4 time-lapse images of nuclear localization after LMB addition (1, 30 and 60 min). COS-1 cells were transiently co-transfected with plasmids expressing CSmad1 and YLSmad4 and the BMP receptor. Cells were treated with LMB (2nM). The experiments shown are representative of at least three independent experiments.

The transcriptional activity of CSmad1 and YL1Smad4 were tested using the pSBELuciferase reporter assay (n=3) (Fig. 3.22B and C). For this assay, the Smad fusion proteins were expressed in MDA-MB468 cells, which lack endogenous Smad4, but contain R-Smads. The results of the luciferase assays were difficult to obtain without long periods of starvation (see materials and methods) due to over-expression of endogenous R-Smads mixed with normal cell signaling activities creating unfavorable basal activities. The starvation apparently reduces the endogenous Smad1 levels so that co-transfection of both Smad1 and Smad4 were necessary to observe the difference between the active and non-active cells. The Smad1/Smad4-dependent luciferase reporter plasmid, pSBELuciferase, was transiently transfected together with the CSmad1 (Fig. 3.22B) or YL1Smad4 (Fig. 3.22C) expression plasmid. As shown in figure 3.22B and C, luciferase expression was enhanced by co-transfecting wtSmad4 with CSmad1. YLSmad4 co-transfected with wt Smad1 also increased the luciferase activity. From the data presented in this part we concluded that CSmad1 and YLSmad4 retain the normal function as a transcription factor.

Next, CSmad1 phosphorylation was observed upon BMP-4 addition (Fig. 3.22A). COS-1 cells were transfected with these expression plasmids for Western blot analysis. YL1Smad4 was detected with a Smad4-specific antibody in Western blot experiments. The Western blots indicated that CSmad1 was phosphorylated efficiently in response to BMP-4, as was endogenous Smad1, with same rate of the phosphorylation (Fig. 3.22A).

The next parameter is an increase in FRET signal after BMP-4 addition. The FRET signal between CSmad1 and YL1Smad4 was most pronounced and reproducible. The FRET signal between Smad1LC and YL1Smad4 was less reproducible but similar to the FRET signal between CSmad1 and YL1Smad4 (Fig. 3.23). Nevertheless, the

kinetics is appearing to be different. This indicated that the intensity, but not the kinetics, of the FRET signal does not depend on the position of the fluorescent proteins in Smad fusion proteins. Thus, one can conclude that CSmad1 and YL1Smad4 can be used in fluorescence microscopy investigations to study the kinetics of Smad1-Smad4 complexation in detail by FRET.

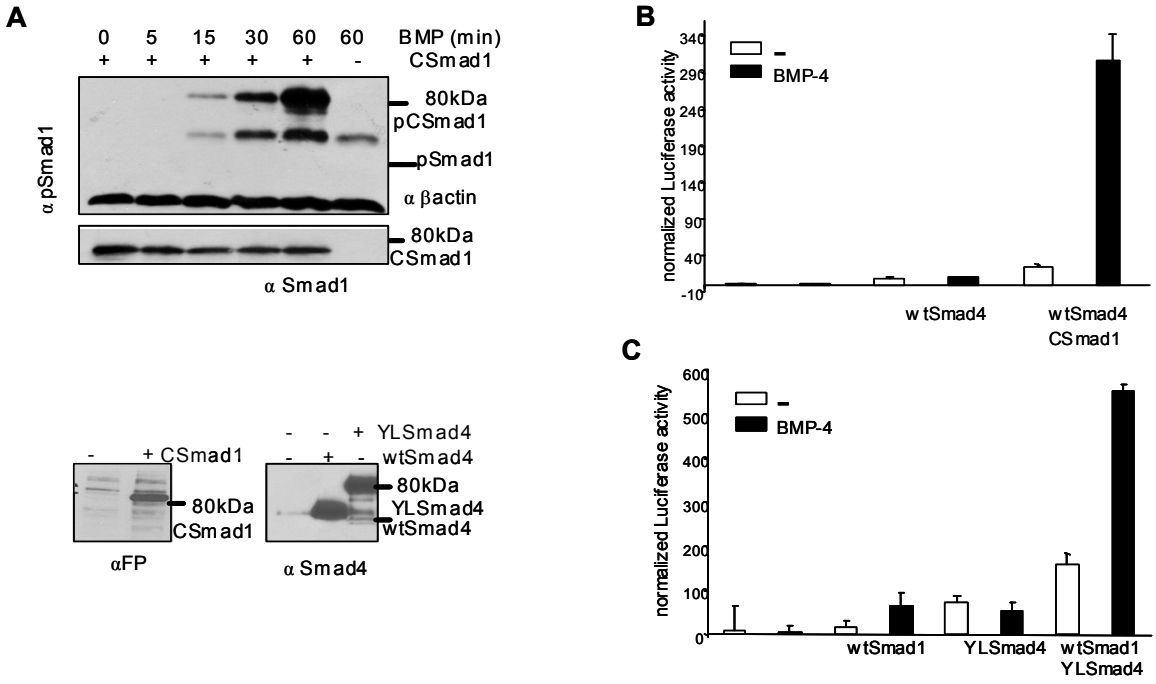

Fig. 3.22*. BMP4-induced functional activity of fluorescent Smad1 and Smad4 fusion proteins. A, CSmad1 and YLSmad4 were expressed in COS-1 by transient transfection. Cell extracts were harvested at different times after BMP-4 stimulation and analyzed by Western blot with antibodies recognizing phosphorylated Smad1 (αpSmad1), total Smad1, Smad4, or fluorescent proteins (αFP). B and C, MDA-MB468 cells lacking endogenous Smad4 were transfected with the pSBE Luciferase reporter plasmid and plasmids expressing wild-type Smad4, YLSmad4 (for B,), or wtSmad4 and CSmad1 (for C,). Cells were treated with BMP-4 for 8 hours, and luciferase activity was measured. The data are means and standard deviations of experiment performed in triplicate. All experiments were repeated three times.*

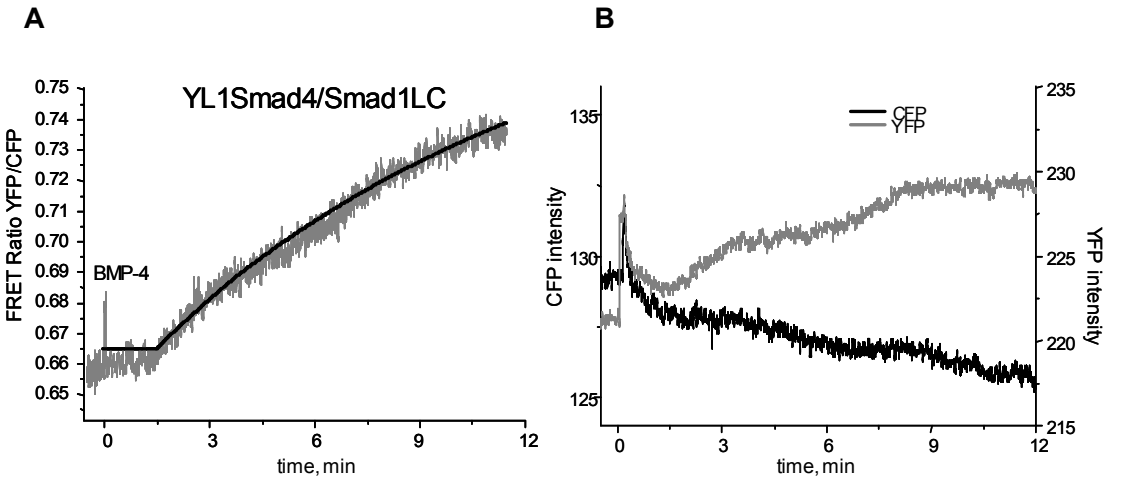

Fig. 3.23 *Measurement of FRET with Smad1LC. A and B, Measurement of FRET (represented by the ratio FYFP/FCFP) in single COS-1 cell transiently transfected with Smad1LC, YLSmad4, and BMP receptors. Stimulation with BMP-4 caused almost no response in the FRET channel for a dormant period of about 100 seconds, after which a FRET increase occurred with a time constant of about 700 seconds with a corresponding increase in the YFP and a decrease in the CFP channel.*

3. 3. 3 Kinetic studies of Smad1/Smad4 fusion proteins complex formation.

The CSmad1 and YL1Smad4 fusion constructs were used to measure the complex formation rate between Smad1-Smad4 by FRET (Fig. 3.24). COS-1, HeLa, and MDA-MB468 cells (n=3 for each cell line) were transiently transfected with plasmid constructs expressing CSmad1, YL1Smad4, and BMP receptors. Then, the kinetics of heteromeric complex formation of these fusion proteins was observed before and after stimulation with BMP-4. The experiments in figure 3.24 A and B demonstrated that FRET occurred between these constructs in COS-1 and HeLa cell after addition of BMP-4 with corresponding increases in the YFP channel and decreases in the CFP channel. Computer-assisted analysis of the FRET data revealed an increase of the FRET signal in the cells with an average time constant of 517±160 sec, but only after a 260±48 sec delay with no FRET change (Fig. 3.24 A and B). A two times higher amplitude of FRET increase was observed in MDA-MB468 breast cancer cells. This could be explained by the absence of the endogenous Smad4 that likely serves as a competitor of the Smad4 fusion protein (Fig. 3.24C). In this situation the measured intermolecular FRET, the intracellular molar ratio between donor and acceptor was

difficult to control, and different concentrations of the two fluorophores may be misinterpreted as FRET. In this case, the recorded change in donor and acceptor fluorescence can be identified as a true change in FRET by monitoring donor and acceptor fluorescence intensity over time. A true FRET change corresponds to a symmetric change of donor and acceptor fluorescence intensity as one can see on figure 3.24 (e.g. in case of an increase in FRET – simultaneous increase in the acceptor and decrease in donor fluorescence). Another approach to prove FRET consists in collecting the donor emission before and after photobleaching of the acceptor (Fig. 3.24D). FRET was determined in the MDA-MB468 cell line (30 min after BMP-4 addition) by acceptor photobleaching (n=3). The acceptor was photobleached selectively, and, as expected, this maneuver significantly decreased the fluorescence of YFP accompanied by successive increase in the fluorescence of CFP by 15% (Fig. 3.24D).

The donor to acceptor ratios ranges measured for all of the CSmad1/YLSmad4 intermolecular FRET cells from figure 7 (and further measured cells for statistics with data not shown) were between 0.7 and 2.1. Between these values, no major trends of FRET change and CFP/YFP ration were observed. Although a few trials were attempted well above and well below these CFP/YFP ratio ranges, a stable FRET was never observed. These observations are in accordance with the predicted donor to acceptor concentration range of 0.1 to 10 by Berney *et a*l (2003) [51] for a stable, detectable FRET to occur.

As an additional method for proving intermolecular FRET, fluorescence lifetime imaging (FLIM) was used. HeLa cells were transiently co-transfected with plasmid constructs expressing CSmad1, YLSmad4, and BMP receptors. The kinetics of FRET of these fusion proteins were observed before and after stimulation with BMP-4 for 45 min (Fig. 3.25A (left panels)) and measured every 15 min.

An analysis of the CFP fluorescence lifetime of the 17 HeLa cells in Fig. 3. 25A (left panels) revealed a significant decrease in fitted and averaged decay time constants from 2.27 ± 0.06 nsec before addition to 1.87 ± 0.03 nsec 45 min after addition of BMP-4.

Shorter fluorescence lifetimes in comparison to the pure CFP fluorescence lifetime (in this case of singly expressed CSmad1 in HeLa cells) are due to the interaction with the acceptor molecule (YLSmad4) causing the FRET (34, 35, 51). Furthermore, the ratio of

the CFP (FRET) lifetime to the pure CFP lifetime can be used to calculate the FRET efficiency (see materials and methods).

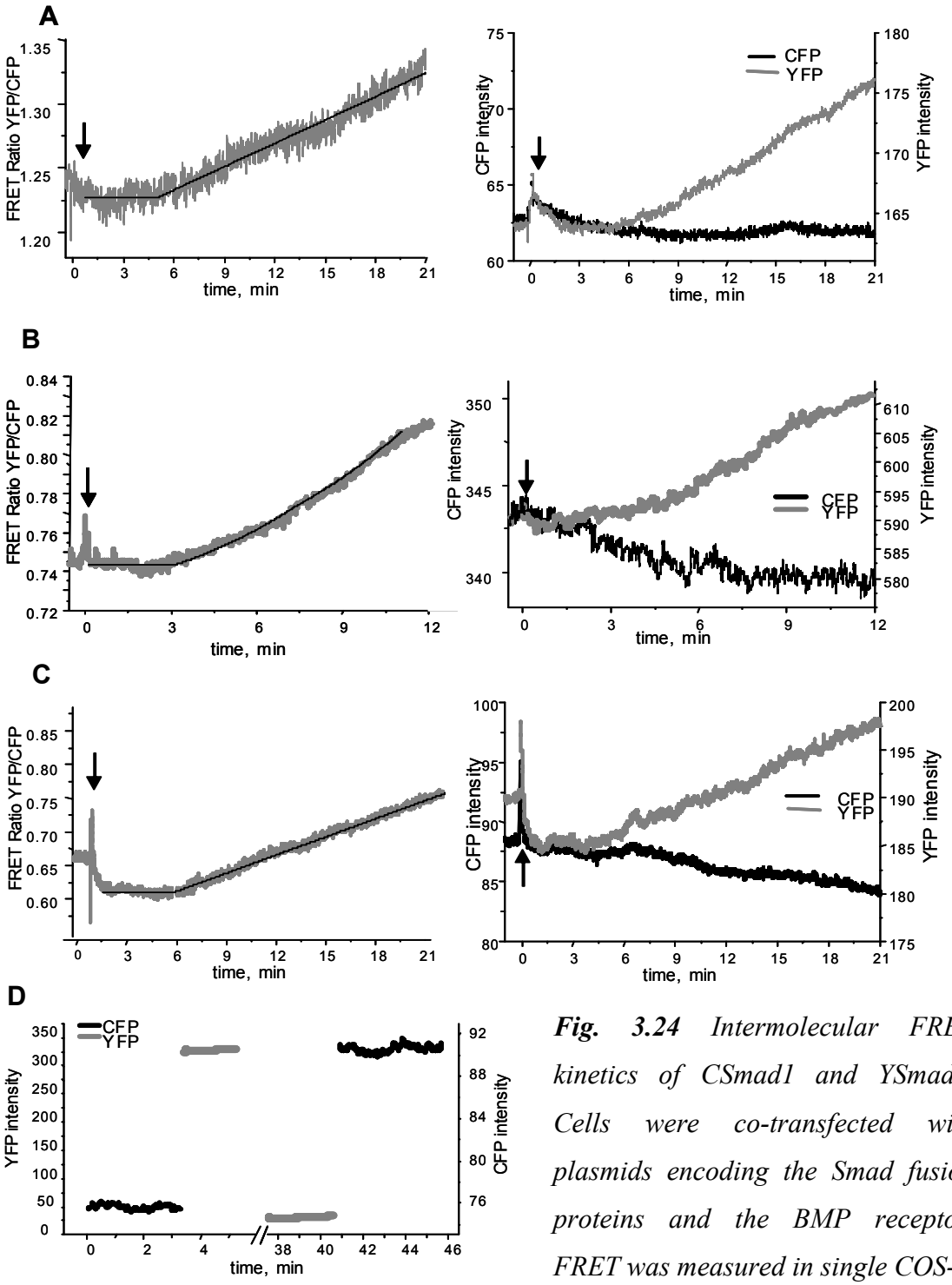

Fig. 3.24 *Intermolecular FRET kinetics of CSmad1 and YSmad4. Cells were co-transfected with plasmids encoding the Smad fusion proteins and the BMP receptor. FRET was measured in single COS-1 (A), HeLa (B), or MDAMB468 (C) cells. Stimulation with BMP-4 caused very little response in the FRET channel for a dormant period of about 300 sec, after which a*

FRET increase occurred with a time constant of about 600 sec with a corresponding increase in the YFP and a decrease in the CFP channel. D, MDA-MB468 cell transiently expressing BMP receptors and YLSmad4 and CSmad1 fusion proteins were analyzed by a technique called Donor Dequenching after Acceptor Photobleaching. Emission Intensities of YFP (535 nm, yellow) and CFP (480 nm, cyan) were recorded before and after the acceptor fluorophore (YFP) was completely photobleached with 500 nm excitation light.

Before BMP addition of the co-transfected CSmad1/YLSmad4 HeLa cells (n=17), the CFP fluorescence lifetime indicated a baseline FRET efficiency of 5 ± 2% in contrast to 45 minutes after addition revealing a FRET efficiency of 22 ± 2% giving rise to a total FRET change (ΔFRET) of 17 ± 4%.

The ΔFRET was calculated on a pixel-by-pixel basis for all of the 17 cells showing a normal distribution (see Fig. 3.25B for 15 min and 45 min after BMP addition) to verify mean and standard error distribution of the FRET change (6±1% for 15 min and 11±1% for 45 min after BMP addition). The slight differences in FRET change calculation here (in comparison to the 17% calculated above) are almost entirely due to pixel shifts in time during image acquisition mostly due to the slow migration of the cells.

The FRET change (ΔFRET) was also determined for the 17 individual cells at 15, 30, and 45 min after BMP addition to show the dynamics and statistics contributing to this FRET (Fig. 3.25C). A majority of cells (11 of 17 and 12 of 17) show a significant ΔFRET increase of >6% at 30 and 45 min after BMP addition, respectively, with nearly half (7 of 17) showing a >6% ΔFRET already at 15 min after addition. The range of CFP/ YFP ratios where ΔFRET occurred was found to be between 0.3 to 3.1 agreeing to the acceptable range as reported by Berney et al. (2003). However, due to the possibility of photobleaching (discussed below), and removal of data from photobleaching, the dynamic range would be reduced to 0.7 to 3.1, overlapping the values reported above.

Photobleaching of CFP has also been shown to affect fluorescence lifetime measurements and, thus, could cause a falsely reported FRET or ΔFRET [54] . Care was taken to use experimental conditions that did not allow photobleaching (see

Materials and Methods). However, upon application of the “apparent photobleaching ratio" (as defined by Tramier *et al* (2006) [54]) for the CFP (see Materials and Methods for calculation and figure 8C for individual cell values), 7 cells showed a significant “apparent photobleaching” (> 0.3) and two cells showed a slight “apparent photobleaching” (< 0.3 but > 0.1) causing greater than 20% shorter CFP fluorescence lifetimes in the significant case and less than 10% shorter lifetimes in the slight case. Because the possibility exists that further CFP fluorescence intensity decreases, indicated by a lower “apparent photobleaching” value, could occur to either reorganization (by nuclear localization or cell shifting) or to photobleaching, we have further categorized all of the form from CFP for measurements into four possible cases: no photobleaching and no reorganization, no photobleaching and reorganization, photobleaching and reorganization, and photobleaching and no reorganization. The ΔFRET remains to be highly significant after rejection for any possibility of photobleaching with 5 of the 8 cells > 0.04. The ΔFRET improves even further in dynamics and statistics if the reorganization of CFP rules out the photobleaching rejection with 12 of 15 cells > 0.04 and 9 of 15 cells > 0.06.

As mentioned above, figure 3.25A (left panels) shows FLIM images of CSmad1 before and after BMP-4 addition that have significantly decreasing donor (CFP) lifetimes in the majority of cases in the cytosol (12 of 17 cells) and that also show in some cases the FRET change slowly traveling in to the nucleus of HeLa cells (4 of 17 cells). Only one cell showed an absolutely clear pure CSmad1 and YLSmad4 nuclear translocation to complement the nuclear translocating FRET (Fig. 3.25A, encircled cell in left panels and right panels).

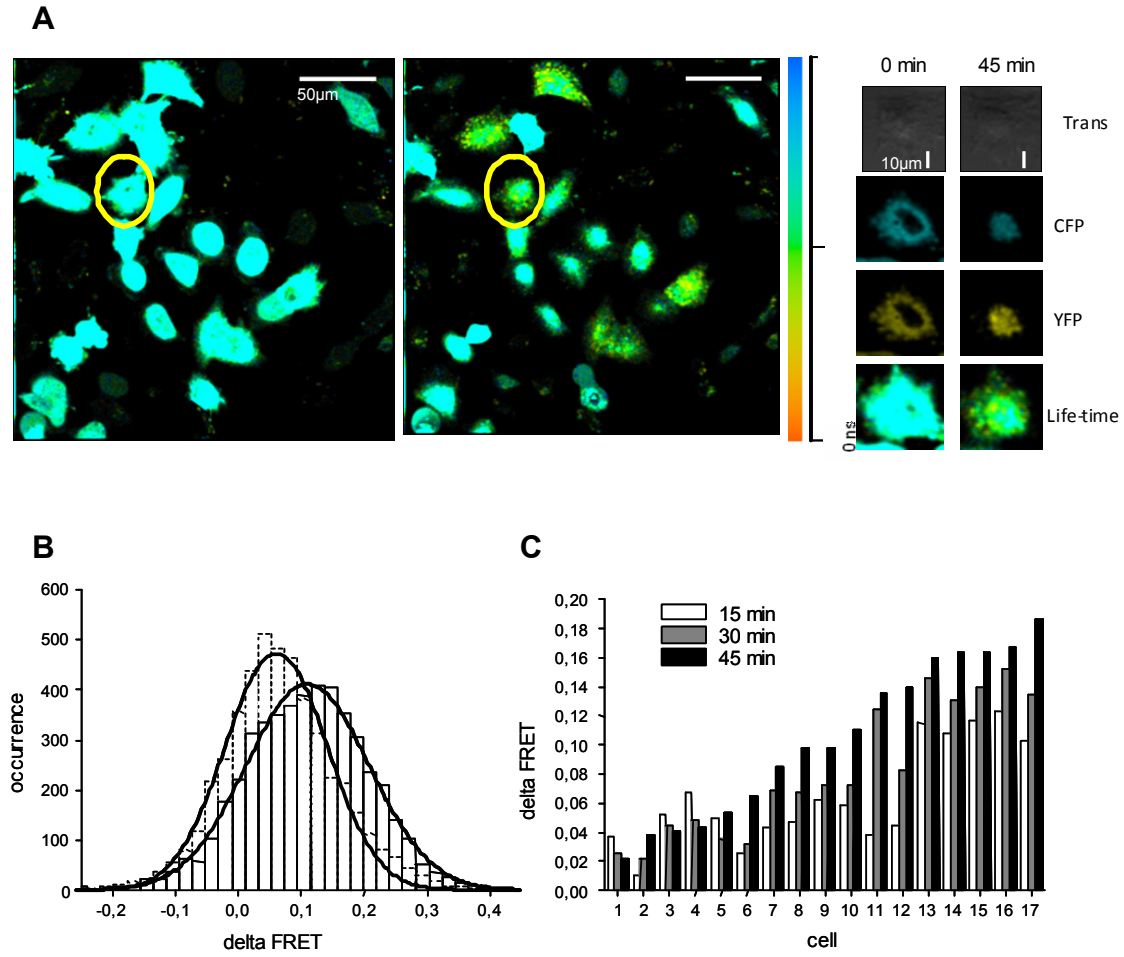

Fig. 3.25 *Observation of intermolecular FRET kinetics of CSmad1 and YSmad4 in HeLa cells with FLIM. A (left panels), Fluorescence lifetime image (FLIM) analysis of CSmad1 in 17 Hela cells co-transfected with CSmad1 and YLSmad4 (left) before (t=0 min) and (right) t=45min after addition of BMP-4. The donor mean lifetime decreases from 2.27 ± 0.03 nsec to 1.87 ± 0.03 nsec for the 17 HeLa cells 45 min after BMP-4 addition (scale bar, 50 µm). A cell is encircled as it shows nuclear translocation of FRET shown in detail in the right panels. A (right panels), shows a zoomed transmission, pure CFP, pure YFP, and FLIM of the nuclear translocation FRET as an example from the left panels before (t = 0 min) and 45 min after BMP-4 addition (scale bar, 10µm). B, histogram and distribution of FRET dynamics from the pixels of the 17 Hela cells co-transfected with CSmad1 and YLSmad4 from A. ΔFRET efficiencies were calculated at 15 min (dashed lines) and at 45 min (solid lines) after BMP addition subtracted from the FRET at t=0 min before BMP addition. Both column graphs were*

fitted with single Gaussian curves and reveal a change in FRET efficiency of 6 ± 1 % at t=15min and 11 ± 1 % at t=45min. C, FRET efficiency change of 17 Hela cells transfected with CSmad1 and YLSmad4. TCSPC data from sample and control experiment were taken for calculation of FRET efficiency. The FRET efficiency before BMP addition serves as reference to show the dynamics of FRET. The white column indicates the change in FRET efficiency after 15 min, the gray columns after 30 min and the black columns after 45 min of BMP-4 addition.

4. Discussion

In this study, fluorescent biosensors for direct visualization of Smad signaling were developed. With these Smad biosensors, the kinetics of Smad1 activation, which is defined by phosphorylation-induced, concerted structural changes of Smad1, were investigated. In addition, the kinetics of Smad1/Smad4 complex formation was analyzed by FRET using YFP and CFP fusions of Smad1 and Smad4, respectively. These Smad fusion proteins closely mimic the behavior of endogenous Smad1 and Smad4 in terms of their activation and their formation of active Smad transcription factor complexes on Smad-responsive elements.

4. 1 Advantages and disadvantages of FRET biosensors

The most difficult part of this work was the creation of functionally active fluorescent Smad fusion proteins that can be used as FRET biosensors. It is of utmost importance that these fusion proteins have the same or at least very similar functional properties as the wild-type proteins, and, in addition, they have to be usable for detection of FRET.

To create the Smad fusions, different strategies of placing the fluorescent proteins in sequence with Smads were tested. YFP or CFP were fused to the C- or N-terminus of different Smad domains, and at least 2-3 different tests for their functional activity were performed. Phosphorylation as a marker of activation was analyzed by Western blot, nuclear translocation was visualized with time-lapse microscopy, and the transcriptional activating activity of the fusion proteins was measured with a luciferase assay. All functional assays performed with the full-length Smad biosensors with YFP or CFP on the C- or N-terminus indicated that the fluorescent fusion Smads mimic the behavior wild-type Smads in cultured cells. However, it is still possible that some functional aspects or specific interactions with other signaling pathways could still be impaired. Therefore, the FRET biosensors should be used only as a model to probe Smad signaling pathways. It is important to keep in mind that the validity of any model needs to be confirmed with independent functional assays.

With the Smad1YC and YSmad1C biosensors, it was possible to detect phosphorylation upon BMP-4 addition with same rate as phosphorylation of the wt Smad1 (in case of Smad1YC), but transcriptional activation was not detected with these biosensors using a luciferase assay with vector containing a Smad-binding element (SBELuciferase). The reason for this has not been determined, but it could be that fusing the entire Smad1 protein or only the Smad1 MH2 domain with two fluorescent proteins created a problem for the relatively large fusion protein to translocate into the nucleus or to interact with different transcription factors or DNA. If this was the case, it might indicate that monomolecular Smad1 biosensors can only be used to study the kinetics of Smad phosphorylation.

Another issue to consider when using FRET microscopy to study processes in living cell is that overexpression of fusion proteins could be harmful for cells. Fluorescent proteins could be toxic for cells if they are overexpressed and induce aberrant signaling or apoptosis (176). Thus, it is important to find a suitable expression level of fusion proteins that allows FRET measurements without toxicity to the cell and keep it for all FRET measurements. To provide stable and reproducible FRET measurements it is important to have similar amounts of the CFP and YFP fusion proteins inside of the cell. For all cells, used for FRET experiments, concentrations of fusion proteins were about 0.7-1.4 μM in single cell.This is of particular importance for intermolecular FRET experiments. Here, control experiments using acceptor acceptor photobleaching or FLIM are needed.

In spite of the limitations mentioned above, the FRET technique in general has a lot of important advantages. First of all, with FRET microscopy one can visualize processes in living cells in real time, very fast, and without severely damaging or killing the cell due to lysis, necessary for biochemical techniques. FRET microscopy is more sensitive than standard biochemical techniques as it allows observing the signaling processes from the very beginning and visualizing and recording even very small changes in the kinetics of these signaling processes under different physiological conditions. It would be great if the Smad biosensor could be used not only in living cells, but even in tissues and organs of a whole organism, provided that the fusion proteins can be expressed stably in cells of this organism. For example FRET changes could be recorded in real time in different

parts of an embryo during embryogenesis or in different tissues during wound healing. On the cellular level, the FRET biosensors can be used drug screening in order to find new inhibitors or activators of the BMP singling pathway.

4. 2 Creation of fusion Smad proteins

The most important and at the same time most difficult step in creating Smad fusion proteins is to place the Smad domains and the fluorescent protein domains in a way that this fusion Smad still retains its functional activity. A useful assembly of protein domains can sometimes be reached only after trying many different cloning strategies. Some fusion construct can have functional activity but do not show FRET change after activation. The reason for this could be an unfavorable distance and/or orientation between donor and acceptor. The distance should be not more then 10-20 nm, and the orientation should not be perpendicular, but these parameters are very difficult if not impossible to predict. During constructions of fusion proteins it is in some cases necessary to insert linkers between the Smad- and the fluorescent protein domains. In the present study, the first attempt was to place the fluorescent protein at the C- or N-terminus of Smad1 without linkers and test these fusion proteins for functional activity. Some of them retained functional activity, while others needed modifications, particularly the incorporation of suitable linker sequences. For the construction of the Smad1YC and YSmad1C biosensors it was necessary to place CFP at the C-terminus of Smad1. This became a potential problem for the specific phosphorylation properties of Smad1, because Smad1 is phosphorylated by the BMP receptor at two C-terminal serine residues. To avoid compromising Smad1 phosphorylation, a linker (L) was inserted between CFP and the distal serines. To find a suitable linker, a search of the published literature was performed to find examples of linkers, which had been used previously for the creation of fusion proteins for FRET experiments. Some of these linkers were modified, and finally a functionally active Smad1 biosensor was obtained that could be phosphorylated by the BRI receptor. For the analysis of signaling using the YSmad1C biosensor it was also important how the YFP domain was placed at the N-terminus. It was attempted to separate YFP by a few

amino acids from the MH2 domain. However, only one construct was useful for FRET experiments.

Smad4 had previously been fused to GFP using a short linker (235), and from these data it was unclear whether a linker was needed for the function of the fusion protein. With more intense investigations, it was found out that in all previous fusions of Smad4 with fluorescent proteins at the N- terminus, the authors "used" a fortuitous linker derived from the multiple cloning site (MCS) of the eYFP plasmid (Clontech), but unfortunately this was not mentioned in the publications. We used this linker (L1) with some modifications and develop a functionally active YL1Smad4 fusion protein.

4. 3 The rate--limiting step of the BMP signaling

The kinetics of activation of RSmads is a paradox in that the mobile fraction of these proteins (an immobile fraction of the fusion Smad2 protein was also observed with FRAP (134)) diffuse quickly (in about msec rate) though the cell but phosphorylate slowly. The first question addressed with FRET was: What is the rate-limiting step of the BMP signaling cascade?

BMP-4 signals via two types of receptors (BRI and BRII) that are expressed at the cell surface as homomeric or heteromeric complexes. The ligand, in this case BMP-4, has two options for binding to the receptors. It can bind to the high-affinity receptor BRI and then recruit BRII into a hetero-oligomeric complex. This process leads to activation of the Smad-independent p38 MAPK pathway. The other alternative is to bind simultaneously to the preformed hetero-oligomeric complexes which are then endocytosed via CCP into the cytoplasm, and this may have an influence on the duration of Smad signaling. The complexes then activate the Smad signaling pathway (140). In previous publications (49, 139, 140) and own unpublished data), a high concentration of preformed complexes of BMP receptors which signal towards the Smad pathway was observed on the cell surface. Thus, the presumption was made that activated receptor should be instantaneously available upon BMP-4 binding to phosphorylate Smad1, provided that Smad signaling starts at the cell membrane and receptor internalization is not required. Therefore, BMP receptor activation should not be a limiting step of the Smad signaling pathway.

Recently, the cytosolic diffusion constants were reported for Smad2 before activation. The diffusion was so fast that there should nearly always be Smad2 available for phosphorylation (170). A similarly fast diffusion can be assumed also for the related molecule Smad1. However, the kinetics of Smad2 phosphorylation as deduced from Western blot analyses showed that the phosphorylated Smads were observed after 10-15 min incubation with ligand (170). Thus, the question was addressed: is Smad1 phosphorylation the rate-limiting step of BMP-4 signaling? To answer this question, fluorescent biosensors of Smad1 that reflect the kinetics of Smad1 phosphorylation were used. First, a full-length Smad1 fusion with YFP and CFP (Smad1YC) was created and analyzed. Western blot experiments demonstrated that this biosensor had phosphorylation kinetics similar to wild-type Smad1. Upon activation by phosphorylation, Smad1 undergoes a conformational switch (152, 180, 232) that should be reflected by a FRET change when using the engineered Smad biosensor. However, several processes could occur that could slow the signaling process such as diffusion-driven events, protein binding, or dissociation from different anchor membrane protein upon phosphorylation by the type one BMP receptor. In any case, the changes in the FRET level serve as an indicator of the progression for cytosolic Smads to become phosphorylated and free for complexation.

In the FRET experiments with Smad1YC, high initial FRET ratio levels were observed. After BMP-4 stimulation of COS-1 cells, FRET signals from Smad1YC displayed an initial “non-response” period about 300 sec with a subsequent slow decrease with an average time constant of about 300sec indicating that there are dynamic events occurring up to the phosphorylation process. In C2C12 and HEK 293 cells, a slightly shorter “non-response” period of 100-300 sec followed by a slow signal decrease with an average time of 300 sec was observed. Thus, the following explanations for the non-instantaneous FRET response could be suggested: (1) endocytosis of the BMP receptors (73), (2) binding to other proteins before phosphorylation, (3) Smad1 stays bound to the receptor after phosphorylation and not allowing more to be bound, or (4) that the event is complex formation. The bottom line is that all these processes can cause retardation in Smad signaling. After phosphorylation the Smad1 MH2 domain undergoes a conformation change and

interacts with the C-terminal tails of other Smad1 MH2 domains forming a homotrimer (152). Thus, it is possible that both, phosphorylation and homotrimerization contribute to the FRET changes.

As was mentioned before, Smad1 is activated by preformed complexes of the BMP receptors that are endocytosed. This suggests that the kinetics of Smad1 activation may to some extent be cell type-specific, leading to the hypothesis that the delay originates from the endocytosis rate of the BMP receptors on the plasma membrane as the corresponding delays reflect cell-type specific internalization rates (56). Hence the question was addressed: is endocytosis of preformed BMP receptor complexes the rate-limiting step of BMP-4 signaling? To answer this question, FRET experiments with biosensor Smad1YC on the cell plasma membrane was conducted. We presumed that if Smad1 activation starts only after endocytosis of the receptor, we should not observe FRET changes at the plasma membrane. To do this experiment the TIRF microscope was used. It turned out that FRET started to change (decrease) already at the membrane with about 150 sec delay after BMP-4 addition. Apparently, Smad1 activation starts at the membrane area and does not depend on BMP receptor internalization. Activation again starts only after 100-300 sec delay, indicating that some second process needs to occur.

In summary, for the period of 100-300 sec after BMP-4 addition when no changes in the FRET signal could be observed, we suggest that a slow, gated type of diffusion-controlled reaction is naturally occurring in the cells. The interpretation of the "dead" response time after stimulation with BMP-4 is that it is an important kinetic factor of the Smad signaling process and perhaps even a major bottleneck to the kinetics of Smad signaling.

4. 4 MH1 domain and Smad1 activation

The experiments showed that the 100-300 sec delay in Smad1 activation was not caused by endocytosis of the BMP receptors or at least was not caused by endocytosis of these receptors occurring within the 70 nm penetration depth of the TIRF microscopy. Apparently, the key reason for the delay could be in a complex process of interactions of Smads with others proteins at the membrane. It has been shown that R-

Smads are anchored at the cell membrane by interacting with various cytoplasmic proteins, including SARA, which recruits and stabilizes the monomeric form of Smad2/3 (208). This protein could also be responsible for the delay in Smad1 activation (208). Smad1 was also observed to interact with the cytoplasmic domain of CD44 and Endofin, which anchors Smad1 at the plasma membrane (150). Furthermore, the complete number of Smad interacting proteins at the membrane still remains to be determined (22, 113). All these factors could cause the delayed FRET response after BMP-4 stimulation. In fact, the complex regulatory process of R-Smad activation could be one of the rate limiting steps of the BMP receptor-signaling pathway in general.

Previous studies have shown that the MH1 domain of Smad1 is responsible for binding not only to specific DNA sequences and transcription factors, but also to cytoskeletal proteins near the membrane (113). Moreover, the MH1 domain has a regulatory role in inhibition of the Smad molecule in the cytoplasm prior to activation. This inhibition is mediated through the binding of the MH1 domain to an opposing MH2 domain of Smad1, and Smad phosphorylation upon activation is thought to relieve it (57, 66, 106, 113, 118). However, there is no direct evidence that the MH1 domain could be responsible for regulation of Smad1 phosphorylation, and that it can delay the process of Smad1 activation. Therefore, the question was addressed whether the MH1 domain could be responsible for the delay in Smad1 phosphorylation by developing a sensor based solely on the MH2 domain. To answer this question, the MH2-only Smad1 biosensor lacking the MH1 domain (YSmad1C) was used. With this biosensor it was demonstrated how the MH1 domain influences the kinetics of Smad1 activation. Both, FRET measurements and Western blot analysis clearly showed that the YSmad1C was activated without the delay that wild-type Smad1 and the Smad1YC displayed. After stimulation with BMP-4 we observed that the FRET ratio quickly dropped (without the delay observed with the full sensor) with a time constant of about 300 sec, suggesting that this reflects the dynamics without the delay observed in the full Smad biosensor. These FRET experiments and those with the mutated sensor, YSmad1(SA)C, indicated that the FRET decrease reflected phosphorylation of the MH1-deficient Smad1, which start immediately without delay after BMP-4 addition. Thus, YSmad1C FRET signals

can be robustly and more quickly detected than with the full sensor and potentially many times faster than with Western blot or luciferase assays.

The data demonstrate the important role of the MH1 domain in regulating Smad1 phosphorylation (Fig. 4.1) However, homotrimerization of the MH2 domain of Smad1 upon BMP stimulation could also contribute to the FRET changes as for the Smad1YC biosensor. Also, the usefulness of the YSmad1C biosensor was further shown in that it is reversible in a low number of cases (~10%) tested by first observing the FRET decrease upon BMP-4 addition, removal of the BMP-4, waiting for a long period (>30 min) for recovery, and observation of the FRET decrease again in the same cell upon a second addition of BMP-4.

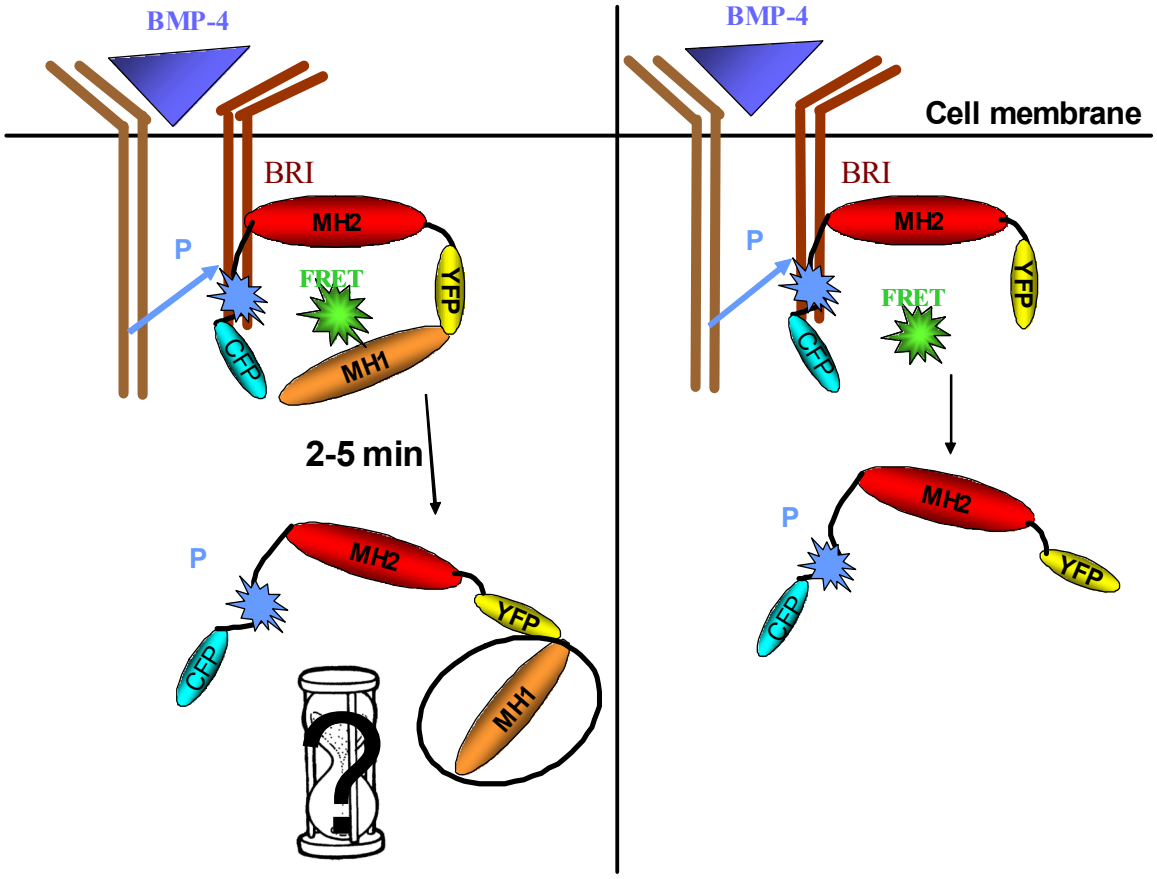

Fig. 4.1 *Conformational change of the Smad1 biosensors observed by FRET. This FRET change reflects the specific phosphorylation of two distal serines upon BMP-4 stimulation. A rate-limiting delay of 2 - 5 minutes occurred between BMP stimulation and Smad1 activation. The delay is dependent on the MH1 domain of Smad1.*

4. 5 Kinetics and rate-limiting step of Smad1/Smad4 complexation

The next step of this work was to link the processes of Smad1 activation with Smad1/Smad4 complex formation. After Smad1 dissociates from the type I BMP receptor, it forms a complex with the Co-Smad, Smad4 (116, 253, 254). However, after phosphorylation by BRI, Smad1 performs a phosphorylation-induced trimerization with other Smad1 molecules. After this trimerization, Smad4 is exchanged with one of the Smad1 molecules via the conserved trimer interface. It has been suggested that such a process should occur slowly (152).

In the present work, FRET experiments were done to study the kinetics of the Smad1/Smad4 complex formation in more detail. The results demonstrated that CSmad1 and YLSmad4 form a heteromeric complex in BMP-4-stimulated cells after a delay of about 300seconds. The time constant calculated from the FRET ratio increase after stimulation with BMP-4 is on the order of about 600 sec and indicates how slow the complex formation process between CSmad1 and YLSmad4 is. This expectable result and that allow us to us this tool as a model for studying Smad complexation.

With the addition of FLIM, the statistics of positive recordings of the CSmad1/YLSmad4 complexation upon BMP addition in individual cells is quite high (70%). It was also shown by confocal microscopy and FLIM that the activated CSmad1 and YLSmad4 complexes can enter the nucleus to further add to the usefulness of the biosensors.

4. 6 The role of FRET-based Smad biosensors as tools

Recent studies have shown an important role of TGF-β signaling in the regulation of cancer (10, 74). For example, specific mutations and deletions of the genes for R-Smad proteins occur in different human carcinomas (55). Therefore, fluorescent Smad biosensors could be used as new fast tool for the screening of drugs against certain cancers. Smad biosensors could be used in different cancer cell lines to identify differences in kinetics of activation and complexation in comparison with normal cells. One example, which demonstrates that biosensors can be used for drugs screening is the experiment where a serine-threonine kinase inhibitor cocktail was used. This inhibitor

cocktail was used in the FRET experiments for Smad1YC and YSmad1C biosensors, and the lack of FRET change after BMP-4 stimulation indicated inhibition of phosphorylation of both biosensors. Also, FRET biosensors could be used to analyze the influence of different cytoplasmic proteins on Smad signaling. For this, different cells could be transfected with Smad biosensors together with some proteins that play role in activation or deactivation of Smad signaling.

In a side collaborative project with the group of Thorsten Stiewe at the Rudolf Virchow Center, the influence of p73, a p53 family protein, on Smad1 signaling was studied. The p53 family plays a very important role as family of tumor suppressors. These proteins induce apoptosis, and an N-terminally truncated version of the p53 family protein p73, ΔNp73, can serve as an antagonist of this processes (5, 37, 219, 224). In other words, the ΔNp73 protein is an antagonist of the complete p53 family. The ΔNp73 inhibits multiple differentiation processes, for instance the BMP2-induced conversion of myoblasts to the osteoblast lineage (68, 103). The question was asked if ΔNp73 inhibits Smad signaling pathways at the level of Smad1 phosphorylation. To answer this question, FRET experiment in the C2C12 cell line were conducted. The cells were cotransfected with Smad1YC and ΔNp73 or with Smad1YC and wild-type p73. The results showed that the ΔNp73 did not interfere with the Smad1 phosphorylation process. Apparently, the inhibition of BMP signaling by ΔNp73 can occur at a different level of BMP signaling, not on the level of Smad1 activation.

Further applications to use of these biosensors are currently being developed in our group. One aim is to observe the expression of Smad biosensors in living organisms, organs, or part of organs by using the Selective Plane Illumination Microscopy (SPIM) technique. With this microscopy technique it is possible to observe the kinetics of Smad signaling with the Smad biosensors in living embryos of drosophila and zebrafish. Such experiments could allow specifically observing the role of Smad expression during initial phases of embryogenesis and giving important new insights into the role of the BMP signaling pathway during development.

Conclusions

1. The cellular fluorescence Smad based biosensors for direct visualization with FRET of Smad-dependent signaling in live mammalian cells was developed.

2. A rate-limiting delay of 2 - 5 minutes between BMP stimulation and Smad1 activation was identified.

3. A similar delay in the Smad1/Smad4 complexation was observed.

4. This delay is dependent on the MH1 domain of Smad1.

5. These results give new insights into the dynamics of the BMP receptor – Smad1/4 signaling process and provide a new tool for studying Smads.

5. References

1. Abdollah, S., M. Macias-Silva, T. Tsukazaki, H. Hayashi, L. Attisano, and J. L. Wrana. 1997. TbetaRI phosphorylation of Smad2 on Ser465 and Ser467 is required for Smad2-Smad4 complex formation and signaling. J Biol Chem 272:27678-85.
2. Adams, S., B. Bacskai, A. T. Harootunian, M. Mahaut-Smith, P. J. Sammak, S. S. Taylor, and R. Y. Tsien. 1993. Imaging of cAMP signals and A-kinase translocation in single living cells. Adv Second Messenger Phosphoprotein Res 28:167-70.
3. Adams, S. R., A. T. Harootunian, Y. J. Buechler, S. S. Taylor, and R. Y. Tsien. 1991. Fluorescence ratio imaging of cyclic AMP in single cells. Nature 349:694-7.
4. Akhurst, R. J., and R. Derynck. 2001. TGF-beta signaling in cancer--a double-edged sword. Trends Cell Biol 11:S44-51.
5. Ariazi, E. A., Y. Satomi, M. J. Ellis, J. D. Haag, W. Shi, C. A. Sattler, and M. N. Gould. 1999. Activation of the transforming growth factor beta signaling pathway and induction of cytostasis and apoptosis in mammary carcinomas treated with the anticancer agent perillyl alcohol. Cancer Res 59:1917-28.
6. Attisano, L., J. L. Wrana, E. Montalvo, and J. Massague. 1996. Activation of signalling by the activin receptor complex. Mol Cell Biol 16:1066-73.
7. Baker, J. C., and R. M. Harland. 1996. A novel mesoderm inducer, Madr2, functions in the activin signal transduction pathway. Genes Dev 10:1880-9.
8. Beck, S. E., B. H. Jung, E. Del Rosario, J. Gomez, and J. M. Carethers. 2007. BMP-induced growth suppression in colon cancer cells is mediated by p21(WAF1) stabilization and modulated by RAS/ERK. Cell Signal.
9. Beck, S. E., B. H. Jung, A. Fiorino, J. Gomez, E. D. Rosario, B. L. Cabrera, S. C. Huang, J. Y. Chow, and J. M. Carethers. 2006. Bone morphogenetic protein signaling and growth suppression in colon cancer. Am J Physiol Gastrointest Liver Physiol 291:G135-45.
10. Bierie, B., and H. L. Moses. 2006. Tumour microenvironment: TGFbeta: the molecular Jekyll and Hyde of cancer. Nat Rev Cancer 6:506-20.
11. Brejc, K., T. K. Sixma, P. A. Kitts, S. R. Kain, R. Y. Tsien, M. Ormo, and S. J. Remington. 1997. Structural basis for dual excitation and photoisomerization of the Aequorea victoria green fluorescent protein. Proc Natl Acad Sci U S A 94:2306-11.
12. Brown, D. A., and J. K. Rose. 1992. Sorting of GPI-anchored proteins to glycolipid-enriched membrane subdomains during transport to the apical cell surface. Cell 68:533-44.
13. Bunemann, M., M. Frank, and M. J. Lohse. 2003. Gi protein activation in intact cells involves subunit rearrangement rather than dissociation. Proc Natl Acad Sci U S A 100:16077-82.
14. Carcamo, J., F. M. Weis, F. Ventura, R. Wieser, J. L. Wrana, L. Attisano, and J. Massague. 1994. Type I receptors specify growth-inhibitory and transcriptional responses to transforming growth factor beta and activin. Mol Cell Biol 14:3810-21.

15. Celeste, A. J., J. A. Iannazzi, R. C. Taylor, R. M. Hewick, V. Rosen, E. A. Wang, and J. M. Wozney. 1990. Identification of transforming growth factor beta family members present in bone-inductive protein purified from bovine bone. Proc Natl Acad Sci U S A 87:9843-7.
16. Celeste, A. J., V. Rosen, J. L. Buecker, R. Kriz, E. A. Wang, and J. M. Wozney. 1986. Isolation of the human gene for bone gla protein utilizing mouse and rat cDNA clones. Embo J 5:1885-90.
17. Centrella, M., S. Casinghino, C. Gundberg, T. L. McCarthy, J. Wozney, and V. Rosen. 1996. Changes in bone morphogenetic protein sensitivity relative to differentiation in fetal rat bone cell cultures. Ann N Y Acad Sci 785:224-6.
18. Centrella, M., S. Casinghino, J. Kim, T. Pham, V. Rosen, J. Wozney, and T. L. McCarthy. 1995. Independent changes in type I and type II receptors for transforming growth factor beta induced by bone morphogenetic protein 2 parallel expression of the osteoblast phenotype. Mol Cell Biol 15:3273-81.
19. Centrella, M., V. Rosen, J. M. Wozney, S. R. Casinghino, and T. L. McCarthy. 1997. Opposing effects by glucocorticoid and bone morphogenetic protein-2 in fetal rat bone cell cultures. J Cell Biochem 67:528-40.
20. Ceresa, B. P., and S. L. Schmid. 2000. Regulation of signal transduction by endocytosis. Curr Opin Cell Biol 12:204-10.
21. Chen, D., M. A. Harris, G. Rossini, C. R. Dunstan, S. L. Dallas, J. Q. Feng, G. R. Mundy, and S. E. Harris. 1997. Bone morphogenetic protein 2 (BMP-2) enhances BMP-3, BMP-4, and bone cell differentiation marker gene expression during the induction of mineralized bone matrix formation in cultures of fetal rat calvarial osteoblasts. Calcif Tissue Int 60:283-90.
22. Chen, H. B., J. Shen, Y. T. Ip, and L. Xu. 2006. Identification of phosphatases for Smad in the BMP/DPP pathway. Genes Dev 20:648-53.
23. Chen, R. H., and R. Derynck. 1994. Homomeric interactions between type II transforming growth factor-beta receptors. J Biol Chem 269:22868-74.
24. Cicchetti, G., M. Biernacki, J. Farquharson, and P. G. Allen. 2004. A ratiometric expressible FRET sensor for phosphoinositides displays a signal change in highly dynamic membrane structures in fibroblasts. Biochemistry 43:1939-49.
25. Cody, C. W., D. C. Prasher, W. M. Westler, F. G. Prendergast, and W. W. Ward. 1993. Chemical structure of the hexapeptide chromophore of the Aequorea green-fluorescent protein. Biochemistry 32:1212-8.
26. Cohen, M. M., Jr. 2002. Bone morphogenetic proteins with some comments on fibrodysplasia ossificans progressiva and NOGGIN. Am J Med Genet 109:87-92.
27. de Caestecker, M. P., E. Piek, and A. B. Roberts. 2000. Role of transforming growth factor-beta signaling in cancer. J Natl Cancer Inst 92:1388-402.
28. Dennler, S., M. J. Goumans, and P. ten Dijke. 2002. Transforming growth factor beta signal transduction. J Leukoc Biol 71:731-40.
29. Derynck, R., R. J. Akhurst, and A. Balmain. 2001. TGF-beta signaling in tumor suppression and cancer progression. Nat Genet 29:117-29.
30. Derynck, R., and X. H. Feng. 1997. TGF-beta receptor signaling. Biochim Biophys Acta 1333:F105-50.

31. Derynck, R., and Y. E. Zhang. 2003. Smad-dependent and Smad-independent pathways in TGF-beta family signalling. Nature 425:577-84.
32. Di Guglielmo, G. M., C. Le Roy, A. F. Goodfellow, and J. L. Wrana. 2003. Distinct endocytic pathways regulate TGF-beta receptor signalling and turnover. Nat Cell Biol 5:410-21.
33. Dong, C., Z. Li, R. Alvarez, Jr., X. H. Feng, and P. J. Goldschmidt-Clermont. 2000. Microtubule binding to Smads may regulate TGF beta activity. Mol Cell 5:27-34.
34. Duncan, R. R. 2006. Fluorescence lifetime imaging microscopy (FLIM) to quantify protein-protein interactions inside cells. Biochem Soc Trans 34:679-82.
35. Duncan, R. R., A. Bergmann, M. A. Cousin, D. K. Apps, and M. J. Shipston. 2004. Multi-dimensional time-correlated single photon counting (TCSPC) fluorescence lifetime imaging microscopy (FLIM) to detect FRET in cells. J Microsc 215:1-12.
36. Dupont, S., L. Zacchigna, M. Adorno, S. Soligo, D. Volpin, S. Piccolo, and M. Cordenonsi. 2004. Convergence of p53 and TGF-beta signaling networks. Cancer Lett 213:129-38.
37. Dupont, S., L. Zacchigna, M. Cordenonsi, S. Soligo, M. Adorno, M. Rugge, and S. Piccolo. 2005. Germ-layer specification and control of cell growth by Ectodermin, a Smad4 ubiquitin ligase. Cell 121:87-99.
38. Ebisawa, T., M. Fukuchi, G. Murakami, T. Chiba, K. Tanaka, T. Imamura, and K. Miyazono. 2001. Smurf1 interacts with transforming growth factor-beta type I receptor through Smad7 and induces receptor degradation. J Biol Chem 276:12477-80.
39. Ebisawa, T., K. Tada, I. Kitajima, K. Tojo, T. K. Sampath, M. Kawabata, K. Miyazono, and T. Imamura. 1999. Characterization of bone morphogenetic protein-6 signaling pathways in osteoblast differentiation. J Cell Sci 112 (Pt 20):3519-27.
40. Elangovan, M., H. Wallrabe, Y. Chen, R. N. Day, M. Barroso, and A. Periasamy. 2003. Characterization of one- and two-photon excitation fluorescence resonance energy transfer microscopy. Methods 29:58-73.
41. Eppert, K., S. W. Scherer, H. Ozcelik, R. Pirone, P. Hoodless, H. Kim, L. C. Tsui, B. Bapat, S. Gallinger, I. L. Andrulis, G. H. Thomsen, J. L. Wrana, and L. Attisano. 1996. MADR2 maps to 18q21 and encodes a TGFbeta-regulated MAD-related protein that is functionally mutated in colorectal carcinoma. Cell 86:543-52.
42. Feng, X. H., and R. Derynck. 1997. A kinase subdomain of transforming growth factor-beta (TGF-beta) type I receptor determines the TGF-beta intracellular signaling specificity. Embo J 16:3912-23.
43. Feng, X. H., and R. Derynck. 1996. Ligand-independent activation of transforming growth factor (TGF) beta signaling pathways by heteromeric cytoplasmic domains of TGF-beta receptors. J Biol Chem 271:13123-9.
44. Fornerod, M., M. Ohno, M. Yoshida, and I. W. Mattaj. 1997. CRM1 is an export receptor for leucine-rich nuclear export signals. Cell 90:1051-60.
45. Freedman, V. H., and S. I. Shin. 1974. Cellular tumorigenicity in nude mice: correlation with cell growth in semi-solid medium. Cell 3:355-9.

46. Fujii, M., K. Takeda, T. Imamura, H. Aoki, T. K. Sampath, S. Enomoto, M. Kawabata, M. Kato, H. Ichijo, and K. Miyazono. 1999. Roles of bone morphogenetic protein type I receptors and Smad proteins in osteoblast and chondroblast differentiation. Mol Biol Cell 10:3801-13.
47. Fukuchi, M., T. Imamura, T. Chiba, T. Ebisawa, M. Kawabata, K. Tanaka, and K. Miyazono. 2001. Ligand-dependent degradation of Smad3 by a ubiquitin ligase complex of ROC1 and associated proteins. Mol Biol Cell 12:1431-43.
48. Funaba, M., C. M. Zimmerman, and L. S. Mathews. 2002. Modulation of Smad2-mediated signaling by extracellular signal-regulated kinase. J Biol Chem 277:41361-8.
49. Gilboa, L., A. Nohe, T. Geissendorfer, W. Sebald, Y. I. Henis, and P. Knaus. 2000. Bone morphogenetic protein receptor complexes on the surface of live cells: a new oligomerization mode for serine/threonine kinase receptors. Mol Biol Cell 11:1023-35.
50. Goggins, M., M. Schutte, J. Lu, C. A. Moskaluk, C. L. Weinstein, G. M. Petersen, C. J. Yeo, C. E. Jackson, H. T. Lynch, R. H. Hruban, and S. E. Kern. 1996. Germline BRCA2 gene mutations in patients with apparently sporadic pancreatic carcinomas. Cancer Res 56:5360-4.
51. Gordon, G. W., G. Berry, X. H. Liang, B. Levine, and B. Herman. 1998. Quantitative fluorescence resonance energy transfer measurements using fluorescence microscopy. Biophys J 74:2702-13.
52. Gorlich, D., and U. Kutay. 1999. Transport between the cell nucleus and the cytoplasm. Annu Rev Cell Dev Biol 15:607-60.
53. Hahn, S. A., M. Schutte, A. T. Hoque, C. A. Moskaluk, L. T. da Costa, E. Rozenblum, C. L. Weinstein, A. Fischer, C. J. Yeo, R. H. Hruban, and S. E. Kern. 1996. DPC4, a candidate tumor suppressor gene at human chromosome 18q21.1. Science 271:350-3.
54. Hanai, J., L. F. Chen, T. Kanno, N. Ohtani-Fujita, W. Y. Kim, W. H. Guo, T. Imamura, Y. Ishidou, M. Fukuchi, M. J. Shi, J. Stavnezer, M. Kawabata, K. Miyazono, and Y. Ito. 1999. Interaction and functional cooperation of PEBP2/CBF with Smads. Synergistic induction of the immunoglobulin germline Calpha promoter. J Biol Chem 274:31577-82.
55. Harradine, K. A., and R. J. Akhurst. 2006. Mutations of TGFbeta signaling molecules in human disease. Ann Med 38:403-14.
56. Hartung, A., K. Bitton-Worms, M. M. Rechtman, V. Wenzel, J. H. Boergermann, S. Hassel, Y. I. Henis, and P. Knaus. 2006. Different routes of bone morphogenic protein (BMP) receptor endocytosis influence BMP signaling. Mol Cell Biol 26:7791-805.
57. Hata, A., R. S. Lo, D. Wotton, G. Lagna, and J. Massague. 1997. Mutations increasing autoinhibition inactivate tumour suppressors Smad2 and Smad4. Nature 388:82-7.
58. Hata, A., J. Seoane, G. Lagna, E. Montalvo, A. Hemmati-Brivanlou, and J. Massague. 2000. OAZ uses distinct DNA- and protein-binding zinc fingers in separate BMP-Smad and Olf signaling pathways. Cell 100:229-40.

59. Hata, A., Y. Shi, and J. Massague. 1998. TGF-beta signaling and cancer: structural and functional consequences of mutations in Smads. Mol Med Today 4:257-62.
60. Hata, H., M. Hamano, J. Watanabe, and H. Kuramoto. 1998. Role of estrogen and estrogen-related growth factor in the mechanism of hormone dependency of endometrial carcinoma cells. Oncology 55 Suppl 1:35-44.
61. Hayes, S., A. Chawla, and S. Corvera. 2002. TGF beta receptor internalization into EEA1-enriched early endosomes: role in signaling to Smad2. J Cell Biol 158:1239-49.
62. Heldin, C. H., K. Miyazono, and P. ten Dijke. 1997. TGF-beta signalling from cell membrane to nucleus through SMAD proteins. Nature 390:465-71.
63. Hemmati-Brivanlou, A., and G. H. Thomsen. 1995. Ventral mesodermal patterning in Xenopus embryos: expression patterns and activities of BMP-2 and BMP-4. Dev Genet 17:78-89.
64. Henis, Y. I., A. Moustakas, H. Y. Lin, and H. F. Lodish. 1994. The types II and III transforming growth factor-beta receptors form homo-oligomers. J Cell Biol 126:139-54.
65. Henningfeld, K. A., H. Friedle, S. Rastegar, and W. Knochel. 2002. Autoregulation of Xvent-2B; direct interaction and functional cooperation of Xvent-2 and Smad1. J Biol Chem 277:2097-103.
66. Hill, C. S. 1999. The Smads. Int J Biochem Cell Biol 31:1249-54.
67. Hoodless, P. A., T. Haerry, S. Abdollah, M. Stapleton, M. B. O'Connor, L. Attisano, and J. L. Wrana. 1996. MADR1, a MAD-related protein that functions in BMP2 signaling pathways. Cell 85:489-500.
68. Huttinger-Kirchhof, N., H. Cam, H. Griesmann, L. Hofmann, M. Beitzinger, and T. Stiewe. 2006. The p53 family inhibitor DeltaNp73 interferes with multiple developmental programs. Cell Death Differ 13:174-7.
69. Imamura, T., M. Takase, A. Nishihara, E. Oeda, J. Hanai, M. Kawabata, and K. Miyazono. 1997. Smad6 inhibits signalling by the TGF-beta superfamily. Nature 389:622-6.
70. Inoue, H., T. Imamura, Y. Ishidou, M. Takase, Y. Udagawa, Y. Oka, K. Tsuneizumi, T. Tabata, K. Miyazono, and M. Kawabata. 1998. Interplay of signal mediators of decapentaplegic (Dpp): molecular characterization of mothers against dpp, Medea, and daughters against dpp. Mol Biol Cell 9:2145-56.
71. Israel, D. I., J. Nove, K. M. Kerns, R. J. Kaufman, V. Rosen, K. A. Cox, and J. M. Wozney. 1996. Heterodimeric bone morphogenetic proteins show enhanced activity in vitro and in vivo. Growth Factors 13:291-300.
72. Ito, Y., and K. Miyazono. 2003. RUNX transcription factors as key targets of TGF-beta superfamily signaling. Curr Opin Genet Dev 13:43-7.
73. Itoh, S., and P. Ten Dijke. 2007. Negative regulation of TGF-beta receptor/Smad signal transduction. Curr Opin Cell Biol 19:176-84.
74. Jakowlew, S. B. 2006. Transforming growth factor-beta in cancer and metastasis. Cancer Metastasis Rev.
75. Janetopoulos, C., T. Jin, and P. Devreotes. 2001. Receptor-mediated activation of heterotrimeric G-proteins in living cells. Science 291:2408-11.

76. Jans, D. A., C. Y. Xiao, and M. H. Lam. 2000. Nuclear targeting signal recognition: a key control point in nuclear transport? Bioessays 22:532-44.
77. Karaulanov, E., W. Knochel, and C. Niehrs. 2004. Transcriptional regulation of BMP4 synexpression in transgenic Xenopus. Embo J 23:844-56.
78. Katagiri, T., S. Akiyama, M. Namiki, M. Komaki, A. Yamaguchi, V. Rosen, J. M. Wozney, A. Fujisawa-Sehara, and T. Suda. 1997. Bone morphogenetic protein-2 inhibits terminal differentiation of myogenic cells by suppressing the transcriptional activity of MyoD and myogenin. Exp Cell Res 230:342-51.
79. Katagiri, T., A. Yamaguchi, T. Ikeda, S. Yoshiki, J. M. Wozney, V. Rosen, E. A. Wang, H. Tanaka, S. Omura, and T. Suda. 1990. The non-osteogenic mouse pluripotent cell line, C3H10T1/2, is induced to differentiate into osteoblastic cells by recombinant human bone morphogenetic protein-2. Biochem Biophys Res Commun 172:295-9.
80. Katagiri, T., A. Yamaguchi, M. Komaki, E. Abe, N. Takahashi, T. Ikeda, V. Rosen, J. M. Wozney, A. Fujisawa-Sehara, and T. Suda. 1994. Bone morphogenetic protein-2 converts the differentiation pathway of C2C12 myoblasts into the osteoblast lineage. J Cell Biol 127:1755-66.
81. Katzmann, D. J., M. Babst, and S. D. Emr. 2001. Ubiquitin-dependent sorting into the multivesicular body pathway requires the function of a conserved endosomal protein sorting complex, ESCRT-I. Cell 106:145-55.
82. Kavsak, P., R. K. Rasmussen, C. G. Causing, S. Bonni, H. Zhu, G. H. Thomsen, and J. L. Wrana. 2000. Smad7 binds to Smurf2 to form an E3 ubiquitin ligase that targets the TGF beta receptor for degradation. Mol Cell 6:1365-75.
83. Kawabata, M., A. Chytil, and H. L. Moses. 1995. Cloning of a novel type II serine/threonine kinase receptor through interaction with the type I transforming growth factor-beta receptor. J Biol Chem 270:5625-30.
84. Kawabata, M., T. Imamura, H. Inoue, J. Hanai, A. Nishihara, A. Hanyu, M. Takase, Y. Ishidou, Y. Udagawa, E. Oeda, D. Goto, K. Yagi, M. Kato, and K. Miyazono. 1999. Intracellular signaling of the TGF-beta superfamily by Smad proteins. Ann N Y Acad Sci 886:73-82.
85. Kawabata, M., T. Imamura, and K. Miyazono. 1998. Signal transduction by bone morphogenetic proteins. Cytokine Growth Factor Rev 9:49-61.
86. Kawabata, M., T. Imamura, K. Miyazono, M. E. Engel, and H. L. Moses. 1995. Interaction of the transforming growth factor-beta type I receptor with farnesyl-protein transferase-alpha. J Biol Chem 270:29628-31.
87. Kawabata, M., H. Inoue, A. Hanyu, T. Imamura, and K. Miyazono. 1998. Smad proteins exist as monomers in vivo and undergo homo- and hetero-oligomerization upon activation by serine/threonine kinase receptors. Embo J 17:4056-65.
88. Kim, J., K. Johnson, H. J. Chen, S. Carroll, and A. Laughon. 1997. Drosophila Mad binds to DNA and directly mediates activation of vestigial by Decapentaplegic. Nature 388:304-8.
89. Kingsley, D. M. 1994. The TGF-beta superfamily: new members, new receptors, and new genetic tests of function in different organisms. Genes Dev 8:133-46.

90. Kirsch, T., J. Nickel, and W. Sebald. 2000. BMP-2 antagonists emerge from alterations in the low-affinity binding epitope for receptor BMPR-II. Embo J 19:3314-24.
91. Kirsch, T., J. Nickel, and W. Sebald. 2000. Isolation of recombinant BMP receptor IA ectodomain and its 2:1 complex with BMP-2. FEBS Lett 468:215-9.
92. Kirsch, T., W. Sebald, and M. K. Dreyer. 2000. Crystal structure of the BMP-2-BRIA ectodomain complex. Nat Struct Biol 7:492-6.
93. Knockaert, M., G. Sapkota, C. Alarcon, J. Massague, and A. H. Brivanlou. 2006. Unique players in the BMP pathway: small C-terminal domain phosphatases dephosphorylate Smad1 to attenuate BMP signaling. Proc Natl Acad Sci U S A 103:11940-5.
94. Koenig, B. B., J. S. Cook, D. H. Wolsing, J. Ting, J. P. Tiesman, P. E. Correa, C. A. Olson, A. L. Pecquet, F. Ventura, R. A. Grant, and et al. 1994. Characterization and cloning of a receptor for BMP-2 and BMP-4 from NIH 3T3 cells. Mol Cell Biol 14:5961-74.
95. Kretzschmar, M., J. Doody, I. Timokhina, and J. Massague. 1999. A mechanism of repression of TGFbeta/ Smad signaling by oncogenic Ras. Genes Dev 13:804-16.
96. Kurzchalia, T. V., P. Dupree, R. G. Parton, R. Kellner, H. Virta, M. Lehnert, and K. Simons. 1992. VIP21, a 21-kD membrane protein is an integral component of trans-Golgi-network-derived transport vesicles. J Cell Biol 118:1003-14.
97. Kusanagi, K., H. Inoue, Y. Ishidou, H. K. Mishima, M. Kawabata, and K. Miyazono. 2000. Characterization of a bone morphogenetic protein-responsive Smad-binding element. Mol Biol Cell 11:555-65.
98. Lagna, G., A. Hata, A. Hemmati-Brivanlou, and J. Massague. 1996. Partnership between DPC4 and SMAD proteins in TGF-beta signalling pathways. Nature 383:832-6.
99. Lakowicz, J. R., I. I. Gryczynski, and Z. Gryczynski. 1999. High Throughput Screening with Multiphoton Excitation. J Biomol Screen 4:355-362.
100. Lakowicz, J. R., H. Szmacinski, K. Nowaczyk, W. J. Lederer, M. S. Kirby, and M. L. Johnson. 1994. Fluorescence lifetime imaging of intracellular calcium in COS cells using Quin-2. Cell Calcium 15:7-27.
101. Lawler, S., X. H. Feng, R. H. Chen, E. M. Maruoka, C. W. Turck, I. Griswold-Prenner, and R. Derynck. 1997. The type II transforming growth factor-beta receptor autophosphorylates not only on serine and threonine but also on tyrosine residues. J Biol Chem 272:14850-9.
102. Lecanda, F., L. V. Avioli, and S. L. Cheng. 1997. Regulation of bone matrix protein expression and induction of differentiation of human osteoblasts and human bone marrow stromal cells by bone morphogenetic protein-2. J Cell Biochem 67:386-96.
103. Lee, A. F., D. K. Ho, P. Zanassi, G. S. Walsh, D. R. Kaplan, and F. D. Miller. 2004. Evidence that DeltaNp73 promotes neuronal survival by p53-dependent and p53-independent mechanisms. J Neurosci 24:9174-84.
104. Li, J., and W. X. Li. 2006. A novel function of Drosophila eIF4A as a negative regulator of Dpp/BMP signalling that mediates SMAD degradation. Nat Cell Biol 8:1407-14.

105. Liu, D., B. L. Black, and R. Derynck. 2001. TGF-beta inhibits muscle differentiation through functional repression of myogenic transcription factors by Smad3. Genes Dev 15:2950-66.
106. Liu, F., A. Hata, J. C. Baker, J. Doody, J. Carcamo, R. M. Harland, and J. Massague. 1996. A human Mad protein acting as a BMP-regulated transcriptional activator. Nature 381:620-3.
107. Lo, R. S., Y. G. Chen, Y. Shi, N. P. Pavletich, and J. Massague. 1998. The L3 loop: a structural motif determining specific interactions between SMAD proteins and TGF-beta receptors. Embo J 17:996-1005.
108. Lohse, M. J., J. P. Vilardaga, and M. Bunemann. 2003. Molecular mechanisms of receptor activation: real-time analysis by fluorescence resonance energy transfer. Auton Autacoid Pharmacol 23:231-3.
109. Lu, S. L., M. Kawabata, T. Imamura, Y. Akiyama, T. Nomizu, K. Miyazono, and Y. Yuasa. 1998. HNPCC associated with germline mutation in the TGF-beta type II receptor gene. Nat Genet 19:17-8.
110. Lu, S. L., M. Kawabata, T. Imamura, K. Miyazono, and Y. Yuasa. 1999. Two divergent signaling pathways for TGF-beta separated by a mutation of its type II receptor gene. Biochem Biophys Res Commun 259:385-90.
111. Luo, K., and H. F. Lodish. 1997. Positive and negative regulation of type II TGF-beta receptor signal transduction by autophosphorylation on multiple serine residues. Embo J 16:1970-81.
112. Luo, K., and H. F. Lodish. 1996. Signaling by chimeric erythropoietin-TGF-beta receptors: homodimerization of the cytoplasmic domain of the type I TGF-beta receptor and heterodimerization with the type II receptor are both required for intracellular signal transduction. Embo J 15:4485-96.
113. Luo, Q., E. Nieves, J. Kzhyshkowska, and R. H. Angeletti. 2006. Endogenous transforming growth factor-beta receptor-mediated Smad signaling complexes analyzed by mass spectrometry. Mol Cell Proteomics 5:1245-60.
114. Luyten, F. P., N. S. Cunningham, S. Ma, N. Muthukumaran, R. G. Hammonds, W. B. Nevins, W. I. Woods, and A. H. Reddi. 1989. Purification and partial amino acid sequence of osteogenin, a protein initiating bone differentiation. J Biol Chem 264:13377-80.
115. MacGrogan, D., and R. Bookstein. 1997. Tumour suppressor genes in prostate cancer. Semin Cancer Biol 8:11-9.
116. Macias-Silva, M., S. Abdollah, P. A. Hoodless, R. Pirone, L. Attisano, and J. L. Wrana. 1996. MADR2 is a substrate of the TGFbeta receptor and its phosphorylation is required for nuclear accumulation and signaling. Cell 87:1215-24.
117. Macias-Silva, M., P. A. Hoodless, S. J. Tang, M. Buchwald, and J. L. Wrana. 1998. Specific activation of Smad1 signaling pathways by the BMP7 type I receptor, ALK2. J Biol Chem 273:25628-36.
118. Massague, J. 1998. TGF-beta signal transduction. Annu Rev Biochem 67:753-91.
119. Massague, J., and D. Wotton. 2000. Transcriptional control by the TGF-beta/Smad signaling system. Embo J 19:1745-54.

120. Mattaj, I. W., and L. Englmeier. 1998. Nucleocytoplasmic transport: the soluble phase. Annu Rev Biochem 67:265-306.
121. Mitchell, H., A. Choudhury, R. E. Pagano, and E. B. Leof. 2004. Ligand-dependent and -independent transforming growth factor-beta receptor recycling regulated by clathrin-mediated endocytosis and Rab11. Mol Biol Cell 15:4166-78.
122. Miyawaki, A. 2003. Fluorescence imaging of physiological activity in complex systems using GFP-based probes. Curr Opin Neurobiol 13:591-6.
123. Miyawaki, A. 2003. Visualization of the spatial and temporal dynamics of intracellular signaling. Dev Cell 4:295-305.
124. Miyawaki, A., J. Llopis, R. Heim, J. M. McCaffery, J. A. Adams, M. Ikura, and R. Y. Tsien. 1997. Fluorescent indicators for Ca2+ based on green fluorescent proteins and calmodulin. Nature 388:882-7.
125. Miyazono, K. 2001. [Recent advances in the research on TGF-beta/Smad signaling pathways]. Tanpakushitsu Kakusan Koso 46:105-10.
126. Miyazono, K., K. Kusanagi, and H. Inoue. 2001. Divergence and convergence of TGF-beta/BMP signaling. J Cell Physiol 187:265-76.
127. Miyazono, K., P. ten Dijke, and C. H. Heldin. 2000. TGF-beta signaling by Smad proteins. Adv Immunol 75:115-57.
128. Miyazono, K., P. ten Dijke, H. Yamashita, and C. H. Heldin. 1994. Signal transduction via serine/threonine kinase receptors. Semin Cell Biol 5:389-98.
129. Moustakas, A., and C. H. Heldin. 2002. From mono- to oligo-Smads: the heart of the matter in TGF-beta signal transduction. Genes Dev 16:1867-71.
130. Nakao, A., T. Imamura, S. Souchelnytskyi, M. Kawabata, A. Ishisaki, E. Oeda, K. Tamaki, J. Hanai, C. H. Heldin, K. Miyazono, and P. ten Dijke. 1997. TGF-beta receptor-mediated signalling through Smad2, Smad3 and Smad4. Embo J 16:5353-62.
131. Namiki, M., S. Akiyama, T. Katagiri, A. Suzuki, N. Ueno, N. Yamaji, V. Rosen, J. M. Wozney, and T. Suda. 1997. A kinase domain-truncated type I receptor blocks bone morphogenetic protein-2-induced signal transduction in C2C12 myoblasts. J Biol Chem 272:22046-52.
132. Newfeld, S. J., E. H. Chartoff, J. M. Graff, D. A. Melton, and W. M. Gelbart. 1996. Mothers against dpp encodes a conserved cytoplasmic protein required in DPP/TGF-beta responsive cells. Development 122:2099-108.
133. Nickel, J., M. K. Dreyer, T. Kirsch, and W. Sebald. 2001. The crystal structure of the BMP-2:BMPR-IA complex and the generation of BMP-2 antagonists. J Bone Joint Surg Am 83-A Suppl 1:S7-14.
134. Nicolas, F. J., K. De Bosscher, B. Schmierer, and C. S. Hill. 2004. Analysis of Smad nucleocytoplasmic shuttling in living cells. J Cell Sci 117:4113-25.
135. Nikolaev, V. O., M. Bunemann, L. Hein, A. Hannawacker, and M. J. Lohse. 2004. Novel single chain cAMP sensors for receptor-induced signal propagation. J Biol Chem 279:37215-8.
136. Nikolaev, V. O., S. Gambaryan, and M. J. Lohse. 2006. Fluorescent sensors for rapid monitoring of intracellular cGMP. Nat Methods 3:23-5.

137. Nishihara, A., J. Hanai, T. Imamura, K. Miyazono, and M. Kawabata. 1999. E1A inhibits transforming growth factor-beta signaling through binding to Smad proteins. J Biol Chem 274:28716-23.
138. Nishimura, R., Y. Kato, D. Chen, S. E. Harris, G. R. Mundy, and T. Yoneda. 1998. Smad5 and DPC4 are key molecules in mediating BMP-2-induced osteoblastic differentiation of the pluripotent mesenchymal precursor cell line C2C12. J Biol Chem 273:1872-9.
139. Nohe, A., S. Hassel, M. Ehrlich, F. Neubauer, W. Sebald, Y. I. Henis, and P. Knaus. 2002. The mode of bone morphogenetic protein (BMP) receptor oligomerization determines different BMP-2 signaling pathways. J Biol Chem 277:5330-8.
140. Nohe, A., E. Keating, P. Knaus, and N. O. Petersen. 2004. Signal transduction of bone morphogenetic protein receptors. Cell Signal 16:291-9.
141. Nohe, A., E. Keating, T. M. Underhill, P. Knaus, and N. O. Petersen. 2005. Dynamics and interaction of caveolin-1 isoforms with BMP-receptors. J Cell Sci 118:643-50.
142. Nohe, A., E. Keating, T. M. Underhill, P. Knaus, and N. O. Petersen. 2003. Effect of the distribution and clustering of the type I A BMP receptor (ALK3) with the type II BMP receptor on the activation of signalling pathways. J Cell Sci 116:3277-84.
143. Oie, H. K., A. F. Gazdar, P. A. Lalley, E. K. Russell, J. D. Minna, J. DeLarco, G. J. Todaro, and U. Francke. 1978. Mouse chromosome 5 codes for ecotropic murine leukaemia virus cell-surface receptor. Nature 274:60-2.
144. Okadome, T., H. Yamashita, P. Franzen, A. Moren, C. H. Heldin, and K. Miyazono. 1994. Distinct roles of the intracellular domains of transforming growth factor-beta type I and type II receptors in signal transduction. J Biol Chem 269:30753-6.
145. Ormo, M., A. B. Cubitt, K. Kallio, L. A. Gross, R. Y. Tsien, and S. J. Remington. 1996. Crystal structure of the Aequorea victoria green fluorescent protein. Science 273:1392-5.
146. Ozanne, B., R. J. Fulton, and P. L. Kaplan. 1980. Kirsten murine sarcoma virus transformed cell lines and a spontaneously transformed rat cell-line produce transforming factors. J Cell Physiol 105:163-80.
147. Pardali, K., and A. Moustakas. 2007. Actions of TGF-beta as tumor suppressor and pro-metastatic factor in human cancer. Biochim Biophys Acta 1775:21-62.
148. Parsons, M., B. Vojnovic, and S. Ameer-Beg. 2004. Imaging protein-protein interactions in cell motility using fluorescence resonance energy transfer (FRET). Biochem Soc Trans 32:431-3.
149. Persson, U., H. Izumi, S. Souchelnytskyi, S. Itoh, S. Grimsby, U. Engstrom, C. H. Heldin, K. Funa, and P. ten Dijke. 1998. The L45 loop in type I receptors for TGF-beta family members is a critical determinant in specifying Smad isoform activation. FEBS Lett 434:83-7.
150. Peterson, R. S., R. A. Andhare, K. T. Rousche, W. Knudson, W. Wang, J. B. Grossfield, R. O. Thomas, R. E. Hollingsworth, and C. B. Knudson. 2004. CD44 modulates Smad1 activation in the BMP-7 signaling pathway. J Cell Biol 166:1081-91.

151. Pollok, B. A., and R. Heim. 1999. Using GFP in FRET-based applications. Trends Cell Biol 9:57-60.
152. Qin, B. Y., B. M. Chacko, S. S. Lam, M. P. de Caestecker, J. J. Correia, and K. Lin. 2001. Structural basis of Smad1 activation by receptor kinase phosphorylation. Mol Cell 8:1303-12.
153. Raftery, L. A., V. Twombly, K. Wharton, and W. M. Gelbart. 1995. Genetic screens to identify elements of the decapentaplegic signaling pathway in Drosophila. Genetics 139:241-54.
154. Reguly, T., and J. L. Wrana. 2003. In or out? The dynamics of Smad nucleocytoplasmic shuttling. Trends Cell Biol 13:216-20.
155. Roberts, A. B., L. C. Lamb, D. L. Newton, M. B. Sporn, J. E. De Larco, and G. J. Todaro. 1980. Transforming growth factors: isolation of polypeptides from virally and chemically transformed cells by acid/ethanol extraction. Proc Natl Acad Sci U S A 77:3494-8.
156. Roberts, K. E., J. J. McElroy, W. P. Wong, E. Yen, A. Widlitz, R. J. Barst, J. A. Knowles, and J. H. Morse. 2004. BMPR2 mutations in pulmonary arterial hypertension with congenital heart disease. Eur Respir J 24:371-4.
157. Rogers, M. B., V. Rosen, J. M. Wozney, and L. J. Gudas. 1992. Bone morphogenetic proteins-2 and -4 are involved in the retinoic acid-induced differentiation of embryonal carcinoma cells. Mol Biol Cell 3:189-96.
158. Rosen, V., J. Capparella, D. McQuaid, K. Cox, R. S. Thies, J. Song, and J. Wozney. 1993. Development of immortalized cells derived from 13DPC mouse limb buds as a system to study the effects of recombinant human bone morphogenetic protein-2 (rhBMP-2) on limb bud cell differentiation. Prog Clin Biol Res 383A:305-15.
159. Rosen, V., J. Nove, J. J. Song, R. S. Thies, K. Cox, and J. M. Wozney. 1994. Responsiveness of clonal limb bud cell lines to bone morphogenetic protein 2 reveals a sequential relationship between cartilage and bone cell phenotypes. J Bone Miner Res 9:1759-68.
160. Rosen, V., J. M. Wozney, E. A. Wang, P. Cordes, A. Celeste, D. McQuaid, and L. Kurtzberg. 1989. Purification and molecular cloning of a novel group of BMPs and localization of BMP mRNA in developing bone. Connect Tissue Res 20:313-9.
161. Rosenthal, R. E., and P. Wozney. 1991. Diagnostic value of gadopentetate dimeglumine for 1.5-T MR imaging of musculoskeletal masses: comparison with unenhanced T1- and T2-weighted imaging. J Magn Reson Imaging 1:547-51.
162. Rosenzweig, B. L., T. Imamura, T. Okadome, G. N. Cox, H. Yamashita, P. ten Dijke, C. H. Heldin, and K. Miyazono. 1995. Cloning and characterization of a human type II receptor for bone morphogenetic proteins. Proc Natl Acad Sci U S A 92:7632-6.
163. Ross, S., E. Cheung, T. G. Petrakis, M. Howell, W. L. Kraus, and C. S. Hill. 2006. Smads orchestrate specific histone modifications and chromatin remodeling to activate transcription. Embo J 25:4490-502.

164. Rothberg, K. G., J. E. Heuser, W. C. Donzell, Y. S. Ying, J. R. Glenney, and R. G. Anderson. 1992. Caveolin, a protein component of caveolae membrane coats. Cell 68:673-82.
165. Sammak, P. J., S. R. Adams, A. T. Harootunian, M. Schliwa, and R. Y. Tsien. 1992. Intracellular cyclic AMP not calcium, determines the direction of vesicle movement in melanophores: direct measurement by fluorescence ratio imaging. J Cell Biol 117:57-72.
166. Sapkota, G., M. Knockaert, C. Alarcon, E. Montalvo, A. H. Brivanlou, and J. Massague. 2006. Dephosphorylation of the linker regions of Smad1 and Smad2/3 by small C-terminal domain phosphatases has distinct outcomes for bone morphogenetic protein and transforming growth factor-beta pathways. J Biol Chem 281:40412-9.
167. Sato, M., T. Ozawa, K. Inukai, T. Asano, and Y. Umezawa. 2002. Fluorescent indicators for imaging protein phosphorylation in single living cells. Nat Biotechnol 20:287-94.
168. Satow, R., A. Kurisaki, T. C. Chan, T. S. Hamazaki, and M. Asashima. 2006. Dullard promotes degradation and dephosphorylation of BMP receptors and is required for neural induction. Dev Cell 11:763-74.
169. Savage, C., P. Das, A. L. Finelli, S. R. Townsend, C. Y. Sun, S. E. Baird, and R. W. Padgett. 1996. Caenorhabditis elegans genes sma-2, sma-3, and sma-4 define a conserved family of transforming growth factor beta pathway components. Proc Natl Acad Sci U S A 93:790-4.
170. Schmierer, B., and C. S. Hill. 2005. Kinetic analysis of Smad nucleocytoplasmic shuttling reveals a mechanism for transforming growth factor beta-dependent nuclear accumulation of Smads. Mol Cell Biol 25:9845-58.
171. Schutte, M., R. H. Hruban, L. Hedrick, K. R. Cho, G. M. Nadasdy, C. L. Weinstein, G. S. Bova, W. B. Isaacs, P. Cairns, H. Nawroz, D. Sidransky, R. A. Casero, Jr., P. S. Meltzer, S. A. Hahn, and S. E. Kern. 1996. DPC4 gene in various tumor types. Cancer Res 56:2527-30.
172. Sebald, W., J. Nickel, J. L. Zhang, and T. D. Mueller. 2004. Molecular recognition in bone morphogenetic protein (BMP)/receptor interaction. Biol Chem 385:697-710.
173. Sekar, R. B., and A. Periasamy. 2003. Fluorescence resonance energy transfer (FRET) microscopy imaging of live cell protein localizations. J Cell Biol 160:629-33.
174. Sekelsky, J. J., S. J. Newfeld, L. A. Raftery, E. H. Chartoff, and W. M. Gelbart. 1995. Genetic characterization and cloning of mothers against dpp, a gene required for decapentaplegic function in Drosophila melanogaster. Genetics 139:1347-58.
175. Shaner, N. C., R. E. Campbell, P. A. Steinbach, B. N. Giepmans, A. E. Palmer, and R. Y. Tsien. 2004. Improved monomeric red, orange and yellow fluorescent proteins derived from Discosoma sp. red fluorescent protein. Nat Biotechnol 22:1567-72.
176. Shaner, N. C., P. A. Steinbach, and R. Y. Tsien. 2005. A guide to choosing fluorescent proteins. Nat Methods 2:905-9.

177. Shi, W., C. Chang, S. Nie, S. Xie, M. Wan, and X. Cao. 2007. Endofin acts as a Smad anchor for receptor activation in BMP signaling. J Cell Sci 120:1216-24.
178. Shi, X., X. Yang, D. Chen, Z. Chang, and X. Cao. 1999. Smad1 interacts with homeobox DNA-binding proteins in bone morphogenetic protein signaling. J Biol Chem 274:13711-7.
179. Shi, Y., A. Hata, R. S. Lo, J. Massague, and N. P. Pavletich. 1997. A structural basis for mutational inactivation of the tumour suppressor Smad4. Nature 388:87-93.
180. Shi, Y., and J. Massague. 2003. Mechanisms of TGF-beta signaling from cell membrane to the nucleus. Cell 113:685-700.
181. Shimizu, A., M. Kato, A. Nakao, T. Imamura, P. ten Dijke, C. H. Heldin, M. Kawabata, S. Shimada, and K. Miyazono. 1998. Identification of receptors and Smad proteins involved in activin signalling in a human epidermal keratinocyte cell line. Genes Cells 3:125-34.
182. Shimizu, S., Y. Nishikawa, K. Kuroda, S. Takagi, K. Kozaki, S. Hyuga, S. Saga, and M. Matsuyama. 1996. Involvement of transforming growth factor beta1 in autocrine enhancement of gelatinase B secretion by murine metastatic colon carcinoma cells. Cancer Res 56:3366-70.
183. Shin, S. I., V. H. Freedman, R. Risser, and R. Pollack. 1975. Tumorigenicity of virus-transformed cells in nude mice is correlated specifically with anchorage independent growth in vitro. Proc Natl Acad Sci U S A 72:4435-9.
184. Simons, K., and E. Ikonen. 1997. Functional rafts in cell membranes. Nature 387:569-72.
185. Simons, K., and G. van Meer. 1988. Lipid sorting in epithelial cells. Biochemistry 27:6197-202.
186. Souchelnytskyi, S., A. Moustakas, and C. H. Heldin. 2002. TGF-beta signaling from a three-dimensional perspective: insight into selection of partners. Trends Cell Biol 12:304-7.
187. Souchelnytskyi, S., P. ten Dijke, K. Miyazono, and C. H. Heldin. 1996. Phosphorylation of Ser165 in TGF-beta type I receptor modulates TGF-beta1-induced cellular responses. Embo J 15:6231-40.
188. Sowa, H., H. Kaji, G. N. Hendy, L. Canaff, T. Komori, T. Sugimoto, and K. Chihara. 2004. Menin is required for bone morphogenetic protein 2- and transforming growth factor beta-regulated osteoblastic differentiation through interaction with Smads and Runx2. J Biol Chem 279:40267-75.
189. Steyer, J. A., and W. Almers. 2001. A real-time view of life within 100 nm of the plasma membrane. Nat Rev Mol Cell Biol 2:268-75.
190. Sun, Y., W. Zhang, F. Ma, W. Chen, and S. Hou. 1997. Evaluation of transforming growth factor beta and bone morphogenetic protein composite on healing of bone defects. Chin Med J (Engl) 110:927-31.
191. Tada, K., H. Inoue, T. Ebisawa, M. Makuuchi, M. Kawabata, T. Imamura, and K. Miyazono. 1999. Region between alpha-helices 3 and 4 of the mad homology 2 domain of Smad4: functional roles in oligomer formation and transcriptional activation. Genes Cells 4:731-41.

192. Takase, M., T. Imamura, T. K. Sampath, K. Takeda, H. Ichijo, K. Miyazono, and M. Kawabata. 1998. Induction of Smad6 mRNA by bone morphogenetic proteins. Biochem Biophys Res Commun 244:26-9.
193. Tang, Y., V. Katuri, A. Dillner, B. Mishra, C. X. Deng, and L. Mishra. 2003. Disruption of transforming growth factor-beta signaling in ELF beta-spectrin-deficient mice. Science 299:574-7.
194. ten Dijke, P., P. Franzen, H. Yamashita, H. Ichijo, C. H. Heldin, and K. Miyazono. 1994. Serine/threonine kinase receptors. Prog Growth Factor Res 5:55-72.
195. ten Dijke, P., K. Miyazono, and C. H. Heldin. 2000. Signaling inputs converge on nuclear effectors in TGF-beta signaling. Trends Biochem Sci 25:64-70.
196. ten Dijke, P., H. Yamashita, H. Ichijo, P. Franzen, M. Laiho, K. Miyazono, and C. H. Heldin. 1994. Characterization of type I receptors for transforming growth factor-beta and activin. Science 264:101-4.
197. ten Dijke, P., H. Yamashita, T. K. Sampath, A. H. Reddi, M. Estevez, D. L. Riddle, H. Ichijo, C. H. Heldin, and K. Miyazono. 1994. Identification of type I receptors for osteogenic protein-1 and bone morphogenetic protein-4. J Biol Chem 269:16985-8.
198. Thiagalingam, A., A. De Bustros, M. Borges, R. Jasti, D. Compton, L. Diamond, M. Mabry, D. W. Ball, S. B. Baylin, and B. D. Nelkin. 1996. RREB-1, a novel zinc finger protein, is involved in the differentiation response to Ras in human medullary thyroid carcinomas. Mol Cell Biol 16:5335-45.
199. Thiagalingam, S., C. Lengauer, F. S. Leach, M. Schutte, S. A. Hahn, J. Overhauser, J. K. Willson, S. Markowitz, S. R. Hamilton, S. E. Kern, K. W. Kinzler, and B. Vogelstein. 1996. Evaluation of candidate tumour suppressor genes on chromosome 18 in colorectal cancers. Nat Genet 13:343-6.
200. Thiagalingam, S., N. A. Lisitsyn, M. Hamaguchi, M. H. Wigler, J. K. Willson, S. D. Markowitz, F. S. Leach, K. W. Kinzler, and B. Vogelstein. 1996. Evaluation of the FHIT gene in colorectal cancers. Cancer Res 56:2936-9.
201. Thies, R. S., M. Bauduy, B. A. Ashton, L. Kurtzberg, J. M. Wozney, and V. Rosen. 1992. Recombinant human bone morphogenetic protein-2 induces osteoblastic differentiation in W-20-17 stromal cells. Endocrinology 130:1318-24.
202. Ting, A. Y., K. H. Kain, R. L. Klemke, and R. Y. Tsien. 2001. Genetically encoded fluorescent reporters of protein tyrosine kinase activities in living cells. Proc Natl Acad Sci U S A 98:15003-8.
203. Todaro, G. J., C. Fryling, and J. E. De Larco. 1980. Transforming growth factors produced by certain human tumor cells: polypeptides that interact with epidermal growth factor receptors. Proc Natl Acad Sci U S A 77:5258-62.
204. Toomre, D., and D. J. Manstein. 2001. Lighting up the cell surface with evanescent wave microscopy. Trends Cell Biol 11:298-303.
205. Truong, K., A. Sawano, H. Mizuno, H. Hama, K. I. Tong, T. K. Mal, A. Miyawaki, and M. Ikura. 2001. FRET-based in vivo Ca2+ imaging by a new calmodulin-GFP fusion molecule. Nat Struct Biol 8:1069-73.
206. Tsien, R. Y. 1998. The green fluorescent protein. Annu Rev Biochem 67:509-44.

207. Tsien, R. Y., B. J. Bacskai, and S. R. Adams. 1993. FRET for studying intracellular signalling. Trends Cell Biol 3:242-5.
208. Tsukazaki, T., T. A. Chiang, A. F. Davison, L. Attisano, and J. L. Wrana. 1998. SARA, a FYVE domain protein that recruits Smad2 to the TGFbeta receptor. Cell 95:779-91.
209. Tsuneizumi, K., T. Nakayama, Y. Kamoshida, T. B. Kornberg, J. L. Christian, and T. Tabata. 1997. Daughters against dpp modulates dpp organizing activity in Drosophila wing development. Nature 389:627-31.
210. Uchida, T., K. Nakakawaji, and J. Sakamoto. 1996. [Administration of oral etoposide for one year as adjuvant chemotherapy for non-small cell lung cancer-side effect]. Gan To Kagaku Ryoho 23:1967-70.
211. Urist, M. R. 1965. Bone: formation by autoinduction. Science 150:893-9.
212. Usui, T., M. Takase, Y. Kaji, K. Suzuki, K. Ishida, T. Tsuru, K. Miyata, M. Kawabata, and H. Yamashita. 1998. Extracellular matrix production regulation by TGF-beta in corneal endothelial cells. Invest Ophthalmol Vis Sci 39:1981-9.
213. van der Wal, J., R. Habets, P. Varnai, T. Balla, and K. Jalink. 2001. Monitoring agonist-induced phospholipase C activation in live cells by fluorescence resonance energy transfer. J Biol Chem 276:15337-44.
214. van Meer, G., and K. Simons. 1988. Lipid polarity and sorting in epithelial cells. J Cell Biochem 36:51-8.
215. Verschueren, K., J. E. Remacle, C. Collart, H. Kraft, B. S. Baker, P. Tylzanowski, L. Nelles, G. Wuytens, M. T. Su, R. Bodmer, J. C. Smith, and D. Huylebroeck. 1999. SIP1, a novel zinc finger/homeodomain repressor, interacts with Smad proteins and binds to 5'-CACCT sequences in candidate target genes. J Biol Chem 274:20489-98.
216. Wachter, R. M., B. A. King, R. Heim, K. Kallio, R. Y. Tsien, S. G. Boxer, and S. J. Remington. 1997. Crystal structure and photodynamic behavior of the blue emission variant Y66H/Y145F of green fluorescent protein. Biochemistry 36:9759-65.
217. Wang, E. A., V. Rosen, P. Cordes, R. M. Hewick, M. J. Kriz, D. P. Luxenberg, B. S. Sibley, and J. M. Wozney. 1988. Purification and characterization of other distinct bone-inducing factors. Proc Natl Acad Sci U S A 85:9484-8.
218. Wang, L., W. C. Jackson, P. A. Steinbach, and R. Y. Tsien. 2004. Evolution of new nonantibody proteins via iterative somatic hypermutation. Proc Natl Acad Sci U S A 101:16745-9.
219. Wang, S. E., A. Narasanna, C. W. Whitell, F. Y. Wu, D. B. Friedman, and C. L. Arteaga. 2007. Convergence of p53 and transforming growth factor beta (TGFbeta) signaling on activating expression of the tumor suppressor gene maspin in mammary epithelial cells. J Biol Chem 282:5661-9.
220. Warren, A., and M. Zimmer. 2001. Computational analysis of Thr203 isomerization in green fluorescent protein. J Mol Graph Model 19:297-303.
221. Whitman, M. 1998. Smads and early developmental signaling by the TGFbeta superfamily. Genes Dev 12:2445-62.
222. Wiersdorff, V., T. Lecuit, S. M. Cohen, and M. Mlodzik. 1996. Mad acts downstream of Dpp receptors, revealing a differential requirement for dpp

signaling in initiation and propagation of morphogenesis in the Drosophila eye. Development 122:2153-62.
223. Wieser, R., J. L. Wrana, and J. Massague. 1995. GS domain mutations that constitutively activate T beta R-I, the downstream signaling component in the TGF-beta receptor complex. Embo J 14:2199-208.
224. Wilkinson, D. S., S. K. Ogden, S. A. Stratton, J. L. Piechan, T. T. Nguyen, G. A. Smulian, and M. C. Barton. 2005. A direct intersection between p53 and transforming growth factor beta pathways targets chromatin modification and transcription repression of the alpha-fetoprotein gene. Mol Cell Biol 25:1200-12.
225. Willis, S. A., C. M. Zimmerman, L. I. Li, and L. S. Mathews. 1996. Formation and activation by phosphorylation of activin receptor complexes. Mol Endocrinol 10:367-79.
226. Wolfman, N. M., G. Hattersley, K. Cox, A. J. Celeste, R. Nelson, N. Yamaji, J. L. Dube, E. DiBlasio-Smith, J. Nove, J. J. Song, J. M. Wozney, and V. Rosen. 1997. Ectopic induction of tendon and ligament in rats by growth and differentiation factors 5, 6, and 7, members of the TGF-beta gene family. J Clin Invest 100:321-30.
227. Wozney, J. M. 1992. The bone morphogenetic protein family and osteogenesis. Mol Reprod Dev 32:160-7.
228. Wozney, J. M., and V. Rosen. 1998. Bone morphogenetic protein and bone morphogenetic protein gene family in bone formation and repair. Clin Orthop Relat Res:26-37.
229. Wozney, J. M., V. Rosen, M. Byrne, A. J. Celeste, I. Moutsatsos, and E. A. Wang. 1990. Growth factors influencing bone development. J Cell Sci Suppl 13:149-56.
230. Wozney, J. M., V. Rosen, A. J. Celeste, L. M. Mitsock, M. J. Whitters, R. W. Kriz, R. M. Hewick, and E. A. Wang. 1988. Novel regulators of bone formation: molecular clones and activities. Science 242:1528-34.
231. Wrana, J. L., L. Attisano, R. Wieser, F. Ventura, and J. Massague. 1994. Mechanism of activation of the TGF-beta receptor. Nature 370:341-7.
232. Wu, J. W., M. Hu, J. Chai, J. Seoane, M. Huse, C. Li, D. J. Rigotti, S. Kyin, T. W. Muir, R. Fairman, J. Massague, and Y. Shi. 2001. Crystal structure of a phosphorylated Smad2. Recognition of phosphoserine by the MH2 domain and insights on Smad function in TGF-beta signaling. Mol Cell 8:1277-89.
233. Xia, Z., and Y. Liu. 2001. Reliable and global measurement of fluorescence resonance energy transfer using fluorescence microscopes. Biophys J 81:2395-402.
234. Xiao, Z., A. M. Brownawell, I. G. Macara, and H. F. Lodish. 2003. A novel nuclear export signal in Smad1 is essential for its signaling activity. J Biol Chem 278:34245-52.
235. Xiao, Z., N. Watson, C. Rodriguez, and H. F. Lodish. 2001. Nucleocytoplasmic shuttling of Smad1 conferred by its nuclear localization and nuclear export signals. J Biol Chem 276:39404-10.
236. Xie, W., S. Bharathy, D. Kim, B. G. Haffty, D. L. Rimm, and M. Reiss. 2003. Frequent alterations of Smad signaling in human head and neck squamous cell carcinomas: a tissue microarray analysis. Oncol Res 14:61-73.

237. Xie, W., J. C. Mertens, D. J. Reiss, D. L. Rimm, R. L. Camp, B. G. Haffty, and M. Reiss. 2002. Alterations of Smad signaling in human breast carcinoma are associated with poor outcome: a tissue microarray study. Cancer Res 62:497-505.
238. Xu, L., Y. Kang, S. Col, and J. Massague. 2002. Smad2 nucleocytoplasmic shuttling by nucleoporins CAN/Nup214 and Nup153 feeds TGFbeta signaling complexes in the cytoplasm and nucleus. Mol Cell 10:271-82.
239. Yamaguchi, A., T. Ishizuya, N. Kintou, Y. Wada, T. Katagiri, J. M. Wozney, V. Rosen, and S. Yoshiki. 1996. Effects of BMP-2, BMP-4, and BMP-6 on osteoblastic differentiation of bone marrow-derived stromal cell lines, ST2 and MC3T3-G2/PA6. Biochem Biophys Res Commun 220:366-71.
240. Yamaguchi, A., T. Katagiri, T. Ikeda, J. M. Wozney, V. Rosen, E. A. Wang, A. J. Kahn, T. Suda, and S. Yoshiki. 1991. Recombinant human bone morphogenetic protein-2 stimulates osteoblastic maturation and inhibits myogenic differentiation in vitro. J Cell Biol 113:681-7.
241. Yamaji, N., A. J. Celeste, R. S. Thies, J. J. Song, S. M. Bernier, D. Goltzman, K. M. Lyons, J. Nove, V. Rosen, and J. M. Wozney. 1994. A mammalian serine/threonine kinase receptor specifically binds BMP-2 and BMP-4. Biochem Biophys Res Commun 205:1944-51.
242. Yamamoto, T. S., C. Takagi, and N. Ueno. 2000. Requirement of Xmsx-1 in the BMP-triggered ventralization of Xenopus embryos. Mech Dev 91:131-41.
243. Yamashita, H., P. ten Dijke, P. Franzen, K. Miyazono, and C. H. Heldin. 1994. Formation of hetero-oligomeric complexes of type I and type II receptors for transforming growth factor-beta. J Biol Chem 269:20172-8.
244. Yamashita, H., P. ten Dijke, D. Huylebroeck, T. K. Sampath, M. Andries, J. C. Smith, C. H. Heldin, and K. Miyazono. 1995. Osteogenic protein-1 binds to activin type II receptors and induces certain activin-like effects. J Cell Biol 130:217-26.
245. Yamato, K., S. Hashimoto, T. Imamura, H. Uchida, N. Okahashi, T. Koseki, A. Ishisaki, M. Kizaki, K. Miyazono, Y. Ikeda, and T. Nishihara. 2001. Activation of the p21(CIP1/WAF1) promoter by bone morphogenetic protein-2 in mouse B lineage cells. Oncogene 20:4383-92.
246. Yasko, A. W., J. M. Lane, E. J. Fellinger, V. Rosen, J. M. Wozney, and E. A. Wang. 1992. The healing of segmental bone defects, induced by recombinant human bone morphogenetic protein (rhBMP-2). A radiographic, histological, and biomechanical study in rats. J Bone Joint Surg Am 74:659-70.
247. Yoshikawa, H., W. J. Rettig, K. Takaoka, E. Alderman, B. Rup, V. Rosen, J. M. Wozney, J. M. Lane, A. G. Huvos, and P. Garin-Chesa. 1994. Expression of bone morphogenetic proteins in human osteosarcoma. Immunohistochemical detection with monoclonal antibody. Cancer 73:85-91.
248. Zaccolo, M. 2004. Use of chimeric fluorescent proteins and fluorescence resonance energy transfer to monitor cellular responses. Circ Res 94:866-73.
249. Zaccolo, M., F. De Giorgi, C. Y. Cho, L. Feng, T. Knapp, P. A. Negulescu, S. S. Taylor, R. Y. Tsien, and T. Pozzan. 2000. A genetically encoded, fluorescent indicator for cyclic AMP in living cells. Nat Cell Biol 2:25-9.

250. Zarrinpar, A., and W. A. Lim. 2000. Converging on proline: the mechanism of WW domain peptide recognition. Nat Struct Biol 7:611-3.
251. Zhang, J., R. E. Campbell, A. Y. Ting, and R. Y. Tsien. 2002. Creating new fluorescent probes for cell biology. Nat Rev Mol Cell Biol 3:906-18.
252. Zhang, J., Y. Ma, S. S. Taylor, and R. Y. Tsien. 2001. Genetically encoded reporters of protein kinase A activity reveal impact of substrate tethering. Proc Natl Acad Sci U S A 98:14997-5002.
253. Zhang, Y., X. Feng, R. We, and R. Derynck. 1996. Receptor-associated Mad homologues synergize as effectors of the TGF-beta response. Nature 383:168-72.
254. Zhang, Y., T. Musci, and R. Derynck. 1997. The tumor suppressor Smad4/DPC 4 as a central mediator of Smad function. Curr Biol 7:270-6.
255. Zhivov, A., O. Stachs, R. Kraak, J. Stave, and R. F. Guthoff. 2006. In vivo confocal microscopy of the ocular surface. Ocul Surf 4:81-93.

CURRICULUM VITAE

Personal

Name: Kira V. Gromova

Citizenship: Russian

Date of birth: 21.10.1980

Place of Birth: Samara, Russia

Education:

1998–2003 Student at the Samara State University, sub-faculty of Biochemistry of the Biological Faculty. Specialty – Biochemistry, specialization – Biochemistry and Molecular Biology. Degree: Graduate student.

2001-2004 Courses of lectures and practical work in molecular biology in Biology Educational Centre, Institute of Protein Research, Pushchino, Russia.

July–December 2000 Pre-diploma work at the Institute of Bioorganic Chemistry, Russian Academy of Sciences, Pushchino. Project: "Transformation of Ryska by tDNA of Agrobacterium tumefaciens".

July 2001 Practical work at the Center of Bioengineering, Russian Academy of Sciences. Moscow. Project: "RAPD-markers linked in Brassica rapa L".

2001–2002 Pre-diploma work at the Laboratory of Protein Biosynthesis Mechanisms, Institute of Protein Research, Russian Academy of Sciences. Project: "In vitro synthesis of the T-5 bacteriophage protein *SciA*". Advisor: Prof A.S. Spirin.

2002–2003 Diploma work at the Laboratory of Protein Biosynthesis Mechanisms, Institute of Protein Research, Russian Academy of Sciences. Project: "The role of mRNA untranslated regions in efficiency of cell-free translation system from wheat germs". Advisor: Prof A.S. Spirin.

2004–2007 PhD student at the Rudolf-Virchow-Zentrum für Experimentelle Biomedizin, Graduate College "Target Proteins", University of Würzburg,
Molecular Microscopy group (Prof. Gregory Harms).

***Publications and Patents*:**

Kira V. Gromova, Mike Friedrich, Andrey Noskov, Gregory S. Harms: "Visualizing Smad1/4 signaling response to bone morphogenetic protein-4 activation by FRET biosensors" (in press)

Gregory S. Harms, Kira V. Gromova, Andrey Noskov: "SMAD protein-based fluorescent biosensors for activation and intracellular signaling screening assays"; US Patent Application US11/490,307

Gelina S. Kopeina, Kira V. Gromova, Vladimir A. Shirokov,Victor D. Vasiliev and Alexander S. Spirin:"Step-wise formation of eukaryotic double-row polyribosomes and circular translation of polysomal mRNA in a long-term cell-free system" (submitted).

***Participation in scientific conferences**:*

IUPAB & 5. EBSA International Biophysics Congress, September 2005 Montpellier, France. Poster presentation.

SFB 488 International Symposium TGF-βs: Signaling and Roles in Neural Development, Maintenance, and Disese, September 2007 Heidelberg, Germany.

Helping in organization of the International Symposium: "From Bench to Bedside" October 23, 2006 at the Rudolf-Virchow-Zentrum für Experimentelle Biomedizin, University of Würzburg.

Participation in scientific workshops and courses:

The one-year lecture cycle "Clinical Medicine for Students of Natural Sciences" (as a part of the Graduate Program).

Workshop "Effective Scientific Writing" Rudolf Virchow Zentrum 24-26 October 2005.

Workshop "High Performance Presentation" Rudolf Virchow Zentrum 16/17 March 2006.

Helping in providing the Dynamic Microscopy workshops at the Rudolf Virchow Zentrum, as a member of the Molecular Microscopy group (organizer: Prof. Gregory Harms), December 9/10, 2004, and October 9/11, 2006.

Acknowledgments

The work presented here was carried out in the Molecular Microscopy Lab of Prof. Dr. Gregory Harms at the Rudolf Virchow Centre for Experimental Biomedicine, University of Würzburg.
Thanks to:
Prof. Dr. Gregory Harms for general supervision of my PhD work
Prof. Dr. Martin Lohse for critical reading and important suggestions
Prof. Dr. Thomas Müller, for critical reading of the thesis and supervision on behalf of the Faculty of Biology
Prof. Dr. Thorsten Stiewe for important suggestions
Prof. Dr. Wolfram Brune for reading and important suggestions

Through the years of the PhD work a number of people have been kindly helping and supporting me, and I would like to take this opportunity and express my sincere appreciation and gratitude:

Dear Prof. Dr. Greg Harms, dear boss, thank you for giving me an opportunity to work with you! It was very exciting experience. Thank you for helping me to learn a lot of techniques and become who I am now professionally. Working in your lab was a wonderful experience of an intensive and smart work! I enjoyed that, thank you.

To my colleagues: dear friends, this work would not be possible without the surrounding co-workers readily sharing experience and knowledge: Mike, Wiebke, Geoffrey, Isabell, Rezo, Ralf, Rasa and Slava! Thank you for your help! I really enjoy working with you and being your friend. Thanks to all my friends from Würzburg!

Prof. Dr. A. S. Spirin, dear Sir, thank you for your supervision and inspiring conversations, and for the school that I got from you. This work would not be possible without knowledge that I got in your laboratory.
Dr. Vladimir A. Shirokov, dear boss, dear friend who was very supportive and always ready to solve difficult problems and gave me a lot methodology and theoretical knowledge. Thank you for your supervision.
Thank you friends and colleagues from Institute of protein research, RAS, for school and support. Especially, all colleagues from laboratory of Protein Biosynthesis Mechanisms for help during my work. Elena Rafael'evna thanks for been so kind friend for me.

Thank you Dr. Marina Alexandrovna for supervision during my pre-diploma work.

Thanks to: Samara State University and Dr. G.L. Ritov, Prof. Dr. O.N. Makurina.
Dear Oxana Mihaylovna thank you for opening science for me.

Dearest Wolfram, thank you for being with me and help during my very difficult time…

Дорогие Мама и Папа, спасибо Вам за вашу поддержку, понимание и любовь …

Erklärung gemäβ §4 Abs. 3 der Promotionsordnung:

Hiermit erkläre ich ehrenwörtlich, dass ich die vorliegende Arbeit:

„Visualization of the Smad direct signaling response
to Bone Morphogenetic Protein 4 activation with FRET-based biosensors“

selbständig angefertigt und keine anderen als die angegebenen Hilfsmittel und Quellen verwendet habe.

Weiterhin erkläre ich, dass diese Dissertation weder in gleicher noch in ähnlicher Form in einem anderen Prüfungsverfahren vorgelegen hat.

Ich habe bisher außer dem mit dem Zulassungsbesuch urkundlich vorgelegten Graden keine weiteren akademischen Grade erworben oder zu erwerben versucht.

Kira Gromova

Würzburg, 2007.